VUF-3014
FINAL REPORT

Earth Vibrations from a Nuclear Explosion in a Salt Dome

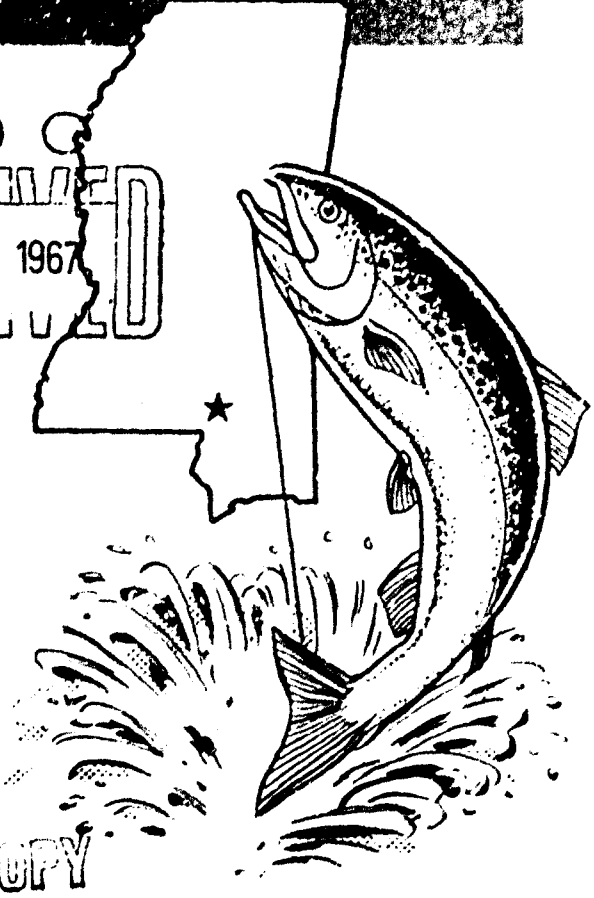

W. V. MICKEY / L. M. LOWRIE
T. R. SHUGART
U. S. COAST AND GEODETIC SURVEY

Issued: 17 March 1967

LEGAL NOTICE

This report has been reproduced directly from the best available copy.

Printed in USA. Price $3.00. Available from the Clearinghouse for Federal Scientific and Technical Information, National Bureau of Standards, U. S. Department of Commerce, Springfield, Virginia 22151.

VUF-3014

EARTH VIBRATIONS FROM A NUCLEAR EXPLOSION IN A SALT DOME

W. V. Mickey
Geophysicist

L. M. Lowrie
Geophysicist

T. R. Shugart
Geophysicist

U.S. DEPARTMENT OF COMMERCE
ENVIRONMENTAL SCIENCE SERVICES ADMINISTRATION
Coast and Geodetic Survey
Rockville, Maryland 20852

CONTENTS

CONTENTS (con.)

CONTENTS (con.)

CONTENTS (con.)

CONTENTS (con.)

ABSTRACT

Recorded earth particle motions in terms of displacements, velocities, and accelerations were near predictions in the distance range of 1.5 to 603 km for the 5 kt SALMON nuclear detonation in a Mississippi salt dome. These motions included measurements from nearby cities and industrial facilities. Scaled earth motions from HE detonations of 500 to 4000 lbs in the unconsolidated shallow sediments were consistently higher than the motions recorded from SALMON. Asymmetric seismic energy propagation was observed with more efficient propagation to the north and south. Apparent velocities of the first arrivals were: 1.458 to 6 km from ground zero, east 2.82 km/sec, south 2.67 km/sec; 6 to 100 km, 4.77 km/sec; and 100 to 603 km southwest, 8.5 km/sec. The maximum motions were propagated at near 1.9 km/sec. The horizontal resultant vector for first motion was anomalous for three stations with deviations from a radial path of 36.2° to 66°. Equivalent earthquake magnitude from calculated seismic energies was near 5.1 with a source-seismic energy ratio of 0.47 percent.

ACKNOWLEDGEMENTS

Grateful acknowledgements are due personnel of several agencies including the Atomic Energy Commission and Lawrence Radiation Laboratory. Special commendations are in order for P. L. Randolph, LRL; R. G. Preston, LRL; O. H. Roehlk, AEC; and R. A. Johnson, AEC.

The field work was conducted under the direction of T. H. Pearce. L. L. Davis of R. F. Beers, Inc. participated in the preliminary data analysis.

Particular recognition is due the administrative supervision of L. M. Murphy, Chief, Division of Seismology, USC&GS.

This research was sponsored by the Advanced Research Projects Agency, Department of Defense.

CHAPTER 1

INTRODUCTION

The principal purpose of the SALMON experiment was to provide a means for studying the mechanics of a tamped nuclear detonation in a salt dome in terms of the generated shock waves as they are propagated out of the dome and progressively through the crust and mantle of the earth.

The following is a summary of the event data:

Event	:	SALMON
Date	:	October 22, 1964
Time	:	16:00:00.0 GMT (10 a.m. CST)
Geographic Coordinates	:	31°08'31.57"N 89°34'11.78"W
Nominal Planned Yield	:	5 kt
Surface elevation from mean sea level	:	73.7 m (242 ft)
Shot depth from surface	:	828.1 m (2716 ft)

The Tatum salt dome top is relatively flat and has penetrated to within 1500 ft of the surface. Immediately above the salt is an anhydrite caprock about 450 ft thick

overlain by a calcite caprock about 100 ft thick. Undifferentiated surface deposits are above the caprocks. (Eargle,1963) Very complete geological surveys have been made of the area, and reported by the Geological Survey in the Technical Letter Series DRIBBLE 1 through 29.

1.1 OBJECTIVES

The Coast and Geodetic Survey Special Projects Field Party recorded transitory earth particle motions in the distance range of 1.458 to 603.2 km to accomplish the following objectives:

1. To determine the magnitude and attenuation with distance of the peak surface particle displacements, velocities, and accelerations.
2. To compare results obtained from studies of previous underground detonations.
3. To record earth motion in populated areas.
4. To describe the symmetry of maximum motion.

1.2 BACKGROUND

The Coast and Geodetic Survey started seismic monitoring of nuclear detonations with strong-motion

instruments during the CROSSROADS experiments in the Pacific in 1946. Participation in the Nevada Test Series starting September 15, 1961, has been summarized in a report (Mickey and Shugart, 1964).

Prior to SALMON only two other nuclear detonations of the contiguous United States detonation series were conducted outside of the Atomic Energy Commission's Nevada Test Site since 1961; GNOME near Carlsbad, New Mexico (Carder, et al., 1962), and SHOAL near Fallon, Nevada (Mickey and Lowrie, 1964; and Mickey, 1964 B).

Source media on the test site have been alluvium, tuff, basalt, granite, and dolomite. The SHOAL experiment was in granite, and GNOME was in bedded halite.

CHAPTER 2

PROCEDURE

2.1 PROJECT PARTICIPATION

There were essentially three seismic measurement projects fielded by the Coast Survey for SALMON:

1. On-site seismic measurements in the distance range of 1.458 to 6.263 km from surface zero.
2. Off-site seismic measurements in the distance range of 17.8 to 603.2 km.
3. Seismic safety measurements at 25 locations including six towns approximately equally spaced on a circle with a radius of 60 km and SALMON at its center.

For brevity the three projects are combined into one report.

2.2 STATIONS

The on-site stations are shown in Figure 4.20. The off-site stations are shown in Figure 2.1. Bearings and slant distances from the shot point are listed in Table 4.1.

Stations 1 through 6 East and 1 through 6 South were located in small wooden prefabricated shelters. Each seismograph was anchored to a concrete pad. The accelerographs contained three components each of Carder Displacement Meters and accelerometers as described in Section 2.3.

The Baxterville oil field station was in a one-story wood frame house and consisted of three components of Carder Displacement Meters and accelerometers.

The Purvis station with the accelerograph as above was in the National Guard Armory, a brick structure.

The Lumberton accelerograph station was also in a brick National Guard Armory.

The Mississippi-Gulf Oil Refinery Carder Vibration Meter station was in a one-story brick structure. Thirty-five geophones were located on and near large refinery structures to a height of 253 ft. The structural response from the geophone data was reported by John A. Blume and Associates.

The Columbia Coast Survey Vibration Meter station was in a brick National Guard Armory.

The Hattiesburg Coast Survey Vibration Meter station was in a two-story brick structure used by AEC as a warehouse.

Six stations were instrumented with Wood-Anderson seismograph systems as follows:

Bogalusa, Louisiana-------High school boiler room
Tylertown, Mississippi----High school boiler room
Prentiss, Mississippi-----High school boiler room
Ellisville, Mississippi---Junior College darkroom
Perkinston, Mississippi---Junior College storeroom in gymnasium
Beaumont, Mississippi-----High school women's washroom

The five mobile stations were located as follows:

10 Miles South
20 Miles South
Ville Platte, Louisiana
Silsbee, Texas
Hockley, Texas

Structures at Stations 3E, 4E, and 5E were instrumented with Statham strain gauges. Structural analysis from this data was reported by John A. Blume and Associates.

A station at McIntosh, Alabama, was occupied with twelve 19L geophones.

Eleven seismoscopes were in the following locations:

Purvis city water tank
Baxterville oil field derrick
Baxterville oil field tank base
Purvis Court House
Purvis High School
Baxterville School
Fire tower, State Highway, 13.5 miles north of Baxterville
Purvis Baptist Church
Union Gas hydrating plant
Fire tower
Station 4E

The seismoscope data have been transmitted to John A. Blume and Associates for analysis.

Wiss, Janney, Elstner and Associates occupied the following stations:

Tatums Camp: 31°11'11"N, 89°32'24"W; M-B velocity gauges, three components; Sprengnether blast vibration seismograph displacement meter, three components.

Forest Lookout Tower, U.S. Highway 98, 15 miles west of Hattiesburg: 31°17'43"N, 89°34'26"W; Shure Brothers accelerometers, three components; Sprengnether blast vibration seismograph displacement meter, three components.

Sumrall, Lamar County Branch Public Health Center: 31°24'56"N, 89°32'52"W; Sprengnether blast vibration seismograph displacement meter, three components.

The Waterways Experiment Station operated a seismograph station at Vicksburg, Mississippi, consisting of one vertical and one radial horizontal geophone.

Seismic information from the long period and short period systems operated for AFTAC at the following stations was also used:

Eutaw, Alabama
Jena, Louisiana
Cumberland Plateau Observatory, Tennessee
Grapevine, Texas
Wichita Mountains Observatory, Oklahoma
Beckley, West Virginia
Vinton, Iowa

Worldwide seismograph stations regularly reporting to the Coast Survey recorded signals from SALMON out to Nurmijarvi, Finland, a distance of about 8240 km.

The Geotechnical Corporation coordinated a Volunteer Team Program composed of oil companies, universities, research organizations and other scientists who made seismic measurements of the SALMON experiment at distances of

9.2 to 3208.6 km. Sixty-two teams participated with thirty-eight monitoring the event (Weisbrich, 1965).

2.3 INSTRUMENTS

The three basic parameters measured by the instruments listed below are earth particle displacements, velocities, and accelerations.

2.3.1 Strong-Motion seismographs.--Stations 1E to 6E, 1S to 6S, Baxterville Oil Field, Purvis, and Lumberton were instrumented with the strong-motion seismograph systems used by the Coast and Geodetic Survey to record nearby earthquakes.

Each seismograph consisted of a camera, dynamic elements, timing devices and remote control circuitry. Torsional or compound pendulums comprised the dynamic elements with their motion, relative to the earth, recorded on photographic paper through a system of optical levers. Calibration of the individual instruments was by tilt and free period tests prior to installation and by period and damping tests after installation.

Internal timing was imposed on each seismograph with backup time control (1 pulse/sec) simultaneously supplied by EG&G by means of a "tone barrel" receiver.

The instruments were actuated by a -2 or -1 sec closure of EG&G relays. Closure of an EG&G zero time relay was used to reference firing time on each record. Each recorder was stopped by the opening of a mechanical circuit breaker after approximately two minutes operation. Recording paper speeds were 10 cm/sec.

2.3.1.1 Carder Displacement Meters (CDM).--The horizontal Carder Displacement Meter consisted of a compound pendulum which recorded the horizontal components of earth motion by means of optical-mechanical recording on photographic paper. The natural periods varied from less than 1 to over 3 sec. The magnification ranged from less than 1 to over 8. Vertical displacement components of earth motion were recorded by dynamic components consisting of small disks mounted on pivot and jewel spindles. The effective pendulum length was governed by offset weights on the rim of the disk with coiled springs supplying the balance and

restoring force. Magnification for the vertical displacement meters was near unity with normal instrument periods of about 2.5 sec.

2.3.1.2 Accelerometers (ACCEL).--The horizontal accelerometer was essentially a torsion seismometer with an inertia mass suspended eccentrically on a vertical fiber so that it virtually acted as a horizontal pendulum, the period of which was controlled by the torsional reaction in the fiber and a small gravity component. The vertical seismometer had a horizontal fiber element. Damping was provided for both vertical and horizontal components by permanent magnets. The seismic information was recorded on photographic paper by an optical-mechanical system. Instrumental periods of 0.03 to 0.17 sec were used with static magnification of about 120, sensitivities of 2.3 to 70 cm/g, and damping about 60 percent critical.

2.3.1.3 Coast Survey Vibration Meters (CSVM).--The CSVM was a torsion seismometer operating under the same principle as the accelerometers, but with longer natural periods so that the instrument responded to displacement

within the designed range of operation. For the event covered by this report the CSVM seismometers operated with a natural period of about 4 sec, magnification near 100 and damping at 60 percent critical.

2.3.1.4 Carder Vibration Meters (CVM).--The CVM was a direct-recording seismometer consisting of a pendulum damped by permanent magnets. These instruments were used with operating periods of about 4 sec, magnification near 25 and a damping coefficient of 0.60. Shake table tests for the CDM, ACCEL, CSVM and CVM instruments give results closely approximating theoretical response for sustained simple harmonic motion.

2.3.1.5 Background on the Strong-Motion Instruments. --The need for a strong-motion seismic program became apparent during the 1929 World Engineering Congress in Tokyo, where American engineers were able to see the results of research conducted at the Japanese Earthquake Research Institute. Continued interest and work made available Federal aid with Congress allocating funds in 1931 to the Coast and Geodetic Survey for a strong-motion program (Cloud and Carder, 1956).

The accelerometers used in the present accelerograph system were developed in 1931 by Frank Wenner of the National Bureau of Standards, with modifications by the Coast and Geodetic Survey (Wenner, 1932; McComb, 1936; U.S. Department of Commerce, 1936; and McComb, 1933). Other organizations active in the development of prototype instruments were the Massachusetts Institute of Technology and the University of Virginia. The complete strong-motion accelerograph presently in use is practically the same as the one developed in 1931 under the direction of H.E. McComb and D. L. Parkhurst of the Coast and Geodetic Survey, and Frank Wenner of the National Bureau of Standards, except for some modifications including the addition of displacement meters (U.S. Department of Commerce, 1965).

The horizontal displacement meters used in the accelerograph (Figure 3.1) were designed by D. S. Carder of the Coast and Geodetic Survey. A compound pendulum is suspended by X hinges and stablized by a torsion wire located in line with the axis of rotation. Static

magnification up to 10 can be obtained by varying the size of the torsion wire and adjusting the position of the upper mass.

Figure 3.2 shows an accelerograph with the various components. The pendulum starter is not used in the nuclear monitoring program since remote start signals activate the system as discussed in Section 2.3.1. The vertical Carder Displacement Meter is not shown, but is installed in the center near the terminal board end of the container.

The Coast and Geodetic Survey Vibration Meter was originally designed to measure the periods of structures. Static magnification up to 1200 can be obtained by changing from a loop-type to a rod-type mass and by changing focal lengths of mirrors attached to the steady mass. Periods up to 10 sec can be obtained by changing the size of torsion wire and tilting the instrument. Figure 3.3 shows a C&GS vibration meter. The C&GS vibration meters used for the shot program are adjusted to have magnification near 125.

Figure 3.4 is a typical seismograph station with three components of Carder Vibration Meters. The recorder, light source, and control circuitry are in the background with the three seismographs in the foreground. The camera opening faces ground zero.

Torsion seismometers are susceptible to vibrations within the suspension systems which can adversely affect the recorded data. The so-called "bowstring vibration" has been observed on shaking table tests and it was shown that the response was not affected, if the natural period of the forcing motion was greater than four times the bowstring period (Carder, 1940). The first mode of vibration of the suspension had periods of 0.093 and 0.0731 sec parallel and normal to the vane supported by the torsion wire suspension. The natural period of the seismometer was 2.5 sec; therefore, recorded motions of periods less than about 0.38 sec, or conversely, frequencies greater than 2.6 cps were questionable. The second mode of vibration was also observed and found to be 0.0278 and 0.0212 sec.

Care must be taken in the installation of the C&GS vibration meters to insure that the suspension ribbon is centered in the damping oil cups. Erratic performance has been observed when the suspension is allowed to touch the oil cup. If the suspension is clamped into place with static torsion, the seismometer becomes unstable. Field procedures have been developed to minimize these and other problems. Table 3.1 is a summary of the instrument constants for the strong-motion seismograph operated for SALMON.

2.3.2 National Geophysical Company Type 21 Seismometer (NGC-21).--Stations 10 MS, 20 MS, Ville Platte, Silsbee, and Hockley had six each NGC-21 geophones. Three components, vertical, radial, and transverse were located in a cluster with three verticals in a linear array on a radial line from ground zero at 1000 ft spacing, resulting in a total surface coverage of 3000 ft.

The NGC-21 seismometer was a velocity sensitive, moving coil instrument with a 1.0 cps natural frequency. Seismometer signals were electronically amplified and recorded simultaneously on a photographic oscillograph and

a magnetic tape recorder. The gain of the amplifier was adjustable from 0 db to 120 db in 6 db steps. At maximum amplifier gain, the velocity sensitivity for the seismograph was 1.88×10^5 cm/cm/sec with sensitivity down 3 db at about 0.9 cps and 32 cps. Seismometer damping was adjusted to 0.57 critical. Oscillograph paper speed was 8.5 cm/sec, tape speed 1.875 in/sec. Programmed time marks and WWV timing signals were recorded on both systems.

Additional information on the NGC system is contained in reference (Lowrie, 1965).

2.3.3 Wood-Anderson Seismograph (W-A).--The Wood-Anderson was a torsion seismometer consisting of a small mass suspended on a fine vertical fiber so that it acted as a horizontal pendulum. Magnetic damping was maintained at 0.8 critical and seismometer natural period at 0.8 sec. At forcing periods of 0.8 sec or less the seismometer response was flat to displacement. (Anderson and Wood, 1925)

The Wood-Anderson seismograph stations recorded north-south and east-west oriented components on a continuous 24-hour-a-day basis. The seismometers were recorded on 12-inch photographic paper by Sprengnether Autocorders,

which allowed up to 30 days of continuous recording without a change of paper.

2.3.4 Wiss, Janney, Elstner and Associates Instruments.--The three stations occupied recorded displacement, velocities, and accelerations.

2.3.4.1 Sprengnether Blast Vibration Seismograph (SBVS).--The SBVS system consisted of two inverted pendulums which responded to perpendicular components of horizontal ground motion and a vertical motion spring-supported pendulum to register vertical ground motion. Eddy-current damping was accomplished by a vane in a magnetic field. Earth motion was recorded photographically through a mechanical-optical lever system. The unit was self-contained with the recording motor, timing system and recording lights operated by batteries.

2.3.4.2 Velocity Gauges (M-B).--The three component M-B (Type 124) velocity system was recorded on a four-channel Edin oscillograph through associated amplifiers. The fourth channel recorded the time signals of the countdown broadcast.

2.3.4.3 Shure Brothers Accelerometers (S-B).--Three components of acceleration from the Model 61B accelerometers were recorded by an Esterline Angus Recorder Model 0-293 with amplification.

2.3.5 John A. Blume and Associates Station.--Two Sprengnether Blast Vibration seismographs were operated at the Women's Dormitory of the University of Southern Mississippi. They were located at the top and bottom of the center section of the building. A complete description and analysis are included in the referenced report (Blume, 1965).

2.3.6 Seismoscopes.--The seismoscope consisted of a magnetically damped conical pendulum which was free to move in any horizontal direction. Relative motion between the pendulum mass and the instrument frame was recorded by a scriber on a smoked spherical watchglass. The operation and response of this instrument are fully described elsewhere (Cloud and Hudson, 1961).

The following instrument systems as noted in Section 2.2 are described in the indicated reference:

Station	Instrument Description Reference
Mississippi-Gulf Oil Refinery geophones	John A. Blume and Associates SALMON report
3E, 4E, and 5E Statham strain gauges	John A. Blume and Associates SALMON report
McIntosh, Alabama	R. F. Beers, Inc., SALMON report
AFTAC stations	Air Force Technical Applications Center, Long Range Seismic Measurements, Project 8.4, SALMON
WES, Vicksburg	Waterways Experiment Station, Vicksburg, Mississippi
Spring Hill and Oxford	Handbook: World-Wide Standard Seismograph Network, U.S. Coast and Geodetic Survey

CHAPTER 3

RESULTS

Stations 1E and 1S each had two sets of strong-motion accelerographs with one as a backup in the event the yield was different from planned. In each case, the measurements were made from the higher gain recording.

Seismologists have long been plagued with the problems of constructing a strong-motion seismograph able to record vertical displacements. The recording of vertical motion in terms of particle velocities and acceleration is less of a problem.

The vertical displacements at the following stations were less than optimum and were not used: 1E, 1S, 3S, 6S, Purvis and Lumberton. Vertical accelerations were recorded at these stations, and displacements can be determined by double integration of the digitized acceleration data.

Transverse displacements at 3S and radial displacements at Purvis were not usable.

There were no vertical displacement meters at Columbia, Hattiesburg, and the six Wood-Anderson instrumented stations.

Maximum particle velocities from the Pre-DRIBBLE experiments are shown in Figures 4.1, 4.2, 4.3, and 4.4. Figure 4.5 is a graph of the velocities versus scaled distance as recorded and as computed from accelerations and displacements for the SALMON Event, with the scaling functions as derived from the shots in unconsolidated sediments and the salt dome superimposed on the graph.

Figures 4.6, 4.8, and 4.9 are maximum displacements, velocities and accelerations versus distance for SALMON.

Figure 4.7 shows the amplitude of first motion relative to distance for SALMON.

The relationship of the period of maximum motion to distance range is shown in Figures 4.10 and 4.11.

Figures 4.12, 4.13, 4.14, and 4.15 are contoured maximum displacements and velocities showing the symmetry of motion.

The propagation velocities are shown in Figures 4.16, 4.17, 4.18, and 4.19.

Figures 4.20 and 4.21 are location plots of the stations showing the horizontal resultant vector direction.

Table 4.1 is a summary of recorded earth motions also showing distance and azimuth for each station.

Copies of selected seismograms are included as Appendix A of this report. Reproduction of any of the SALMON strong-motion records are available from the Coast and Geodetic Survey, Washington Science Center, Rockville, Maryland 20852.

CHAPTER 4

DISCUSSION

4.1 PRE-DRIBBLE COMPARISONS

During April, May, and June 1963, there were a large number of high explosive detonations in and above the Tatum Dome, and near the Mississippi towns of Ansley, McNeill, Collins, and Raleigh (Mickey, 1963 A). Charge sizes were 500, 1000, 2000, and 4000 lbs.

The purposes of the Pre-DRIBBLE HE series were as follows:

1. They were to serve as seismic sources for determination by the U.S. Geological Survey of the crustal structures of the Mississippi Basin. Derived information was to be applied in the theoretical calculations of decoupling.

2. The two 1000 lb explosions in salt, which were located with similar geometrical symmetry to the originally planned 100 ton coupled and decoupled nuclear explosions, were to serve both as sources with signal strength comparable to that expected from the decoupled

nuclear explosion and also as a test of the possible asymmetries to be expected for the two 100 ton experiments.

Theoretical hydrodynamics relies upon cube root scaling and there is some empirical evidence that it can be applied outside the hydrodynamic region (DASA, 1964). Since the convenience of such scaling is apparent, it is often extended to ranges which it does not necessarily apply.

If it can be assumed that cube root scaling applies to peak particle velocities recorded at all distances from ground zero, the following formula applies:

$$v = k_v \left(\frac{R}{W^{1/3}} \right)^{-n} \qquad (4.1)$$

where:

v = peak particle velocities in cm/sec

R = source to detector distance in km

W = charge size in lbs

k_v = a constant characteristic of the shot medium relative to particle velocity

n = attenuation with distance exponent assuming inverse power decay

Figure 4.1 is the maximum earth motion on the seismogram from all the shots using cube root scaling for distance. The upper group of data were shots in sediments. Most of the data are within a factor of three from an average line of the form:

$$v_{cm/sec} = 9.2 \times 10^{-3} W_{lbs}^{0.693} R_{km}^{-2.08} \qquad (4.2)$$

within the scaled ranges of

$$7.7 \times 10^{-2} < \left(\frac{R}{W^{1/3}} \right) < 12.0$$

One station at a scaled range of 0.24 km/$W^{1/3}$ and one at 1.7 km/$W^{1/3}$ for shots above the dome exceeded the limits. Two stations, 7.7 km/$W^{1/3}$ and 9.5 km/$W^{1/3}$ for the Raleigh shots also exceeded the limits, but in general the data fit is acceptable.

The lower set of data are from one 500 lb and three 1000 lb shots detonated in the salt. It is immediately apparent that the shots in the sedimentary section are much larger at the same scaled distance than those in salt and that the attenuation with distance is less. Here again the data varies from the regression line within a factor of 3, except for selected instances.

Also shown on the bottom of the graph are the 1000 lb shots in the Winnfield, Louisiana, salt mine during Operation COWBOY (Carder and Mickey, 1960). All but one of the values are above the envelope for the Tatum salt particle velocities.

To check the cube root scaling equation for the sedimentary shots, Figures 4.2, 4.3, and 4.4 are presented. The upper limit is used and the data for the 500, 2000, and 4000 lb shots substantiate the scaling equation.

In summary, the cube root scaling for particle velocity was observed for sedimentary shots of 500, 1000, 2000, and 4000 lbs:

$$v = \begin{pmatrix} 27.6 \\ 9.2 \\ 3.07 \end{pmatrix} \times 10^{-3} W_{lbs}^{0.693} R_{km}^{-2.08} \qquad (4.3)$$

for scaled ranges of

$$7.7 \times 10^{-2} < \left(\frac{R}{W^{1/3}} \right) < 12.0 \text{ km}$$

For the 500 and 1000 lb shots in the salt dome, cube root scaling gave:

$$v = \begin{pmatrix} 7.05 \\ 2.35 \\ 0.783 \end{pmatrix} \times 10^{-4} W_{lbs}^{0.76} R_{km}^{-2.27} \qquad (4.4)$$

for scaled ranges of

$$6.2\text{x}10^{-2} < \left(\frac{R}{W^{1/3}}\right) < 2.6 \text{ km}$$

Figure 4.5 shows that cube root scaling for the 500 and 1000 lb shots in salt cannot be used for the SALMON 5 kt detonation in salt. This figure is a composite of velocity data derived from accelerations and displacements.

4.2 EARTH PARTICLE AMPLITUDES

Earth motion was derived from the Coast Survey data, AFTAC report, Waterways Experimental Station, and Wiss, Janney, Elstner and Associates' seismograms at distances of 1.5 to over 1000 km. Table 4.1 lists the data.

4.2.1 Displacements.--Maximum peak displacements are shown in Figure 4.6 for stations out to 1251 km. A least squares solution for the data out to 34 km was computed based upon the assumption of a power decay function of the type

$$d = kR^{-n}$$

where

d = displacement in cm

R = source to detector distance in km

k,n = constants determined by least squares analysis

The resulting equation is $d = 1.21R^{-1.15}$ with a standard error of 1.74. The function is plotted in Figure 4.6 with dashed lines indicating plus and minus one standard error. A prediction function for Nevada Test Site detonations in alluvium is also shown (Mickey, 1963 B). This equation represents the upper limits of the NTS data and agrees closely with the upper limits of the SALMON displacements out to 34 km. Excess attenuation is indicated for greater distances.

The data from stations at distances greater than 70 km may not represent the maximum motion since the systems have a narrow band-pass.

If a simple inverse power function can define the attenuation with distance then two equations are required, one from 1.5 to 35 km, and another from 35 to 1250 km. Changes in the distance attenuation exponent were noted by Kuz'mina, et al., (1963) for closer ranges for maximum displacements. The present example differs from his with the greater ranges showing faster attenuation for SALMON.

4.2.2 Acceleration.--The acceleration data are shown on Figure 4.6. The least squares equation describing the data out to 20 km is $a = 1.56R^{-1.48}$ where the acceleration, a, is in units of gravity, and the distance, R, is in kilometers. The standard error is 2.11. The accelerations from the SALMON Event exceed by almost an order of magnitude those for Nevada Test Site explosions (Mickey, 1963 B). Preshot predictions for adjusting acceleration sensitivities were based upon results of the GNOME explosion scaled to 5 kt for SALMON (Carder, et al., 1962). The scaling factor was $(5/3.1)^{0.75}$. The GNOME data provided adequate predictions although it is apparent from Figure 4.6 that attenuation of maximum accelerations with distance was much less for SALMON.

The east line averages are slightly higher than the south line. The 0.1 g line is near 10 km, if it can be assumed that the random maximums are two times predictions.

Earthquake intensity scales refer to the degree of shaking at a particular location. The Modified Mercalli Scale of 1931 defines Intensity I as "Not felt. Marginal and long-period effects of large earthquakes," and Intensity

II as "Felt by persons at rest, on upper floors, or favorably placed." The perception threshold would be somewhere between these two values and could be placed arbitrarily at Intensity 1-1/2. Various seismologists have related the Intensity Scale to ground motion. Richter (1958) related intensity to acceleration with Intensity 1-1/2 at 1 gal (1 cm/sec^2 or 0.001 g). For SALMON the 0.001 g line or perception limit is near 78 km.

Figure 4.7 is a graph of the first motion amplitudes for displacements and accelerations versus distance. Also shown on the graph is the regression line for maximum motion as a comparison. As would be expected, the higher frequency first motion attenuates faster than the maximum. The displacement first motion shows excess attenuation beyond 18 km. This break is not reflected in the travel time curve.

4.2.3 Velocity.--Table 4.2 lists maximum earth particle velocities both directly recorded and derived from measured displacements and accelerations. The recorded motions were converted to velocity by assuming

simple harmonic motion and correcting for the measured angular frequency. The horizontal displacement records for stations 1 East through 6 East, Columbia, and Hattiesburg were digitized, corrected for instrument response and differentiated on an IBM 1620 computer. The vertical and horizontal components were differentiated for the Mississippi Gulf Oil Refinery.

Least squares regression equations were computed for two different groups of data, one using velocity derived from acceleration, the other using velocity from displacement. Directly recorded velocity data were used where available. Computer determined velocities from displacement were used in preference to simple harmonic motion calculations. Each station-component was represented by only one data point in the least squares analyses. No data from beyond 34 km were used. Velocity information could not be obtained from the slow speed Wood-Anderson recordings at 54 to 62.5 km, and data was scarce at greater distances.

Figure 4.8 shows peak maximum earth particle velocities. The data from Wiss No. 1, 10 M South, 20 M South and the stations beyond 62.5 km were recorded directly in terms of

velocity. All other data were derived from displacements. The least squares regression equation is $v = 26.2R^{-1.23}$ where v is particle velocity in cm/sec and R is distance in km. The standard error of estimate is 2.13. In Figure 4.9 the directly recorded earth particle velocities are augmented by velocity derived from acceleration. The least squares equation is $v = 17.1R^{-1.13}$ with a standard error of 2.09. The difference in slope between the two equations is not significant since the standard errors of the regression coefficients for the data in Figures 4.8 and 4.9 are respectively 0.27 and 0.29.

In Figures 4.8 and 4.9 two prediction functions are shown which represent experience prior to SALMON. One is the Coast and Geodetic Survey scaling function for NTS events in granite from the Third Plowshare Symposium report (Mickey, 1964 A). The equation denoted DASA 1285 Salt was derived from the peak radial velocity pulse out to a scaled distance of 22,000 ft/kt$^{1/3}$ (DASA, 1964). The R. F. Beers, Inc., SALMON report contains a complete tabulation of particle velocities derived from both displacement and acceleration by digital computer (Beers, 1965).

4.2.4 Period of Maximum Motion.--Since it is normal for high frequency signal to attenuate faster than lower frequency, graphs were plotted of the period of maximum motion in the particle displacements, velocities, and acceleration versus distance in Figures 4.10 and 4.11. Vertical, radial, and transverse components are included.

Figure 4.10 shows that there was no systematic increase of period with distance out to 63 km. If the AFTAC data as shown in Figure 4.6 were plotted, the increase with distance could be more apparent with the average Rayleigh phase period for the seven stations at over 13 sec.

The maximum motions for accelerations, velocities and displacements occur in progressively longer periods as would be expected. They also normally occur at different times during the time history with the accelerations first, velocities second, and the displacements last. For this reason, the long period surface wave displacement frequencies of the AFTAC stations cannot be compared with the frequencies of the maximum velocities, since they are different measurements. It is interesting

to note that the frequencies of the maximum velocities of the narrow band-pass short period Benioff system are near those on the broad band-pass geophone systems at comparable distances. The Benioff response was designed to reach an optimum of signal reception, while rejecting unwanted seismic noise.

4.2.5 Asymmetry.--The maximum motions in terms of particle displacements and velocities were plotted on maps for the stations. An average regression line was drawn through the graphical data of Figures 4.6 and 4.7 to determine the average attenuation of the signal with distance for the observed ranges. Contour intervals were selected based upon this, so that for symmetric propagation and attenuation according to the regression line the contours would be equally spaced concentric circles.

The data points represent measurements at one point. Each value is affected by local or regional geological structure as well as instrument characteristics. Similar instruments were uniformly calibrated and coupled to the ground through concrete piers. Stations in existing permanent buildings were affected to an undetermined degree

by the response of the building, which would tend to increase rather than decrease the maximum motions. While the data are one point measurements, the contours infer a constant value which is not necessarily so, since large deviation can be observed between closely spaced stations. This is due to several conditions, one of which is the material underlying the station. The figures are presented to show general conditions.

4.2.5.1 Displacement.--The maximum displacements for the 13 close-in stations were contoured at 1 km intervals based upon $R^{-1.34}$ distance attenuation. Figure 4.12 shows that the east line of stations was slightly higher than the south line. The component, vertical, radial, or transverse, recording the maximum motion is also shown. Station 3E is anomalously high as compared to 2E. This could be contributed to either a station condition or the configuration of the salt dome.

The stations from 10 to 63 km as shown in Figure 4.13 were contoured at 5 km intervals with the same attenuation exponent. The component recording the maximum motion is indicated on the figure. The data from Stations 1, 2, and

3 Sumrall indicated slightly more efficient energy propagation to the north, as does Lumberton to the southeast. The Purvis station should possibly be disregarded since only one component, transverse, recorded maximum displacements. At practically all stations the transverse component recorded the least motion.

4.2.5.2 Velocity.--The maximum particle velocities for the 13 close-in stations were also contoured at 1 km intervals based upon a $R^{-1.37}$ distance attenuation. The velocities shown in Figure 4 4 are averages of four numbers, which are the vertical and radial components derived from both displacement and acceleration. Figure 4.14 shows more efficient energy propagation on the east line with Station 3E still high. Station 4S is also high.

The 10 to 63 km stations show a definite north-south contour elongation (Figure 4.15). The Wood-Anderson seismograph stations are represented by the average of the north-south and east-west velocities. Columbia and Hattiesburg data are the averages of the radial and transverse components. The plotted value for the Mississippi Gulf Oil Refinery is the average of three components of

velocity derived from displacement and three components of directly measured velocity. The directly recorded velocities were obtained as parts of the refinery structural response measurements program. They were ground level measurements as follows: vertical component -0.339 cm/sec, radial component -0.248 cm/sec, transverse component 0.207 cm/sec. All other data in Figure 4.15 represent the largest motion from any component, and the component recording the largest motion is indicated. The contour interval is 5 km with $R^{-1.87}$ attenuation.

4.3 TRAVEL TIMES

The propagation velocities derived from the travel times at the various seismic stations are apparent velocities, since the profile was not reversed. Downdip profiles would yield apparent velocities lower than the true velocity with updip profiles resulting in higher apparent velocities. Arrival times for the stations possibly out to 15 km should be predominantly downdip due to the sedimentary drape around the dome. The travel time segments representing different apparent velocities are grouped

into four segments based upon ground range: 0 to 6 km, 2.82 km/sec to the east and 2.67 km/sec toward the south; 6 to 100 km, 4.77 km/sec; 100 and beyond, 8.5 km/sec; and for the velocity of the maximum motions from 0 to the Wood-Anderson safety stations 1.9 km/sec.

4.3.1 Ground Range 0 to 6 km.--Figure 4.16 is a least squares fit to the first arrival data from the on-site strong-motion stations at recording ranges of 1.5 to 6.3 km. The arrival times were picked from the vertical accelerogram.

It will be noted that the time intercepts are negative, -0.28 for the east line and -0.37 for the south. Under normal sedimentary layering and velocity increase with depth, this would indicate that the recorded phase originated before shot time, but such is not the case. The seismic velocities within the salt dome were much higher than velocities outside in the sediments.

The east line of six stations has a slightly higher apparent velocity which could indicate steeper dips along the south line within the observation zone.

4.3.2 Ground Range 6 to 100 km.--Figure 4.17 shows the travel time-distance curves for the stations out to 63 km. The apparent velocity of 4.77 km/sec does not differ significantly from that of the Geological Survey findings from controlled reversed profiles during Pre-DRIBBLE which were near 5 km/sec. The near zone to 6 km had two radial lines from ground zero, therefore, a representative profile was obtained. In this second range, the stations were located completely around SALMON, resulting in a spatial sampling rather than a profile.

The noticeable data scatter for the Wood-Anderson stations is to be expected. The stations out to 34 km had WWV time control and paper speeds of about 10 cm/sec, while the Wood-Anderson safety stations had chronometer time at 60 s·c intervals with paper speeds of 1 mm/sec.

4.3.3 Ground Range Beyond 100 km.--The apparent velocity of 8.5 km/sec as shown on Figure 4.18 was obtained on the southwest radial line to the station near Houston, Texas. This indicates a dipping refractor and crustal thinning toward the southwest. Velocities of 8.4 km were observed by the Geological Survey during

Pre-DRIBBLE with crustal thickening toward the south. Cram (1961) interpreted the Mohorovicic to be at a depth of 33 km in the vicinity of Houston with a velocity of 8.18 km/sec. He also observed velocities of 2.3, 3.94, 5.38, and 6.92 km/sec above the 8.18 refractor.

4.3.4 Maximum Motion Propagation Velocity.--Figure 4.19 shows the travel times versus distance for the maximum earth motions observed on the seismograms. All travel times are for maximum displacements, except for 10 M South and 20 M South which are represented by maximum particle velocity travel times. This indicates that the maximum motions were generally in the surface wave group with the surface waves generated at or near the ground surface above the detonation point.

The data of Figure 4.18 are supplemented by arrival times from the University of Mississippi's station at Oxford, three AFTAC stations, and a station at the U.S. Army Waterways Experimental Station at Vicksburg, Mississippi.

In summary, the arrival times conformed to the following equations:

$t = \frac{km}{2.82} - 0.28$	East line	1.5 to	6 km
$t = \frac{km}{2.67} - 0.37$	South line	1.5 to	6 km
$t = \frac{km}{4.77} + 0.6$		6 to	100 km
$t = \frac{km}{8.5} + 10.0$	Southwest line	100 to	600 km

The maximum earth motion travel times were: $t = \frac{km}{1.9}$

4.4 RESULTANT VECTOR FROM FIRST ARRIVALS

In a homogeneous medium with a point source, first arrivals on a free surface should be up and away. The apparent emergence angle would be determined from the ratio of the vertical and radial earth motion. There should be no transverse or shear first motions. Such is not the case in the heterogeneous stratified earth.

The apparent emergence angle is also a function of the velocity of the medium in which the first motion is propagated and the velocity of the shallow sediments.

First motion data were used from particle displacements and accelerations to determine the apparent emergence angles. The resultant horizontal vector was also determined from the first motion on the transverse and radial instruments. Table 4.3 summarizes the data.

It will be noted from the table that in all instances the apparent angle of emergence is less when computed from displacements than from accelerations. This is to be expected since the frequencies are higher for the accelerations and, therefore, are affected by smaller order discontinuities in the propagation path.

The apparent emergence angles for accelerations varied from 66.9 to 85.3 degrees and for displacements 30.4 to 73.2 degrees. The lowest angle from acceleration was also the lowest angle for displacement. The apparent angle rather thar the true angle is used because the true angle can only be derived from an accurate knowledge of the compressional and shear velocities.

Apparent angle of emergence:

$$\bar{e} = \tan^{-1} \frac{A_v}{A_h} \qquad (4.5)$$

True angle of emergence:

$$2\cos^2 e = \frac{\alpha^2}{\beta^2}\,(1\text{-sine }\bar{e}) \qquad (4.6)$$

where:

A_v and A_h are the vertical and horizontal ground displacements

α is compressional velocity

β is shear velocity

The geometry of the ray path for stations in the vicinity of the salt dome is complicated by the fact that the energy is released in a high velocity zone, but is propagated along a refractor with a slower velocity than the source medium.

Based upon the apparent emergence angle, the apparent refractor velocity and assuming iso-layering of sediments, approximate velocities can be derived for the shallow surface compressional velocities.

The computed velocities are shown in the table. The velocities are larger as computed from the displacement data, as is to be expected since the period

is longer and, therefore, the longer wave lengths penetrate to the higher velocities at depth. The propagation velocities from accelerations vary from 0.22 to 1.11 km/sec and from displacements, 0.82 to 2.43 km/sec. The least variation is observed on the south line with mean velocities of 0.45 and 1.06 with standard deviations of $\pm$0.16 and $\pm$0.19.

The horizontal resultant vectors were computed from the radial and transverse first motion and are shown in Table 4.3. The horizontal vector with a large transverse component can be interpreted as the effect of a refractor with a normal plane deviating from the vertical. The table shows that the horizontal vector differed from the radial by -66.0 to +36.8 degrees measured clockwise from a radial line through surface zero.

Figures 4.20 and 4.21 show that there is no systematic vector orientation. The stations with the largest deviations are 2S, Ellisville, and Hattiesburg. The travel time curve indicates that a portion of the travel

path was through the same refractor, yet the horizontal vectors at Hattiesburg and Ellisville are in opposite quadrants. Ellisville has an additional anomaly with the maximum motion arriving about 8 sec early based upon the average travel time of 1.9 km/sec.

4.5 GEOLOGY

The Physical Division Map of the United States shows the Tatum Dome area to be in the Atlantic Plain major division, the Coast Plain Province, and the East Gulf Coastal Plain section with the characteristics of a young to mature belted coastal plain. The U.S. Geological Survey's Geologic Map of the United States defines the surface deposits as the Citronelle formation, Continental deposit of the Pliocene age in the Tertiary system.

The Tectonic Map of the United States by the U.S. Geological Survey and the American Association of Petroleum Geologists shows the top of the Cretaceous at about -1.92 km (-6300 ft) dipping toward the southwest. Also shown on this map are 23 known salt domes within 80 km of the Tatum Dome. This is within the radius of the so-called threshold of feeling zone of 0.001 g for

the SALMON experiment. The average surface elevations are near 76 m (250 ft), therefore, the total depth of the top of the Cretaceous would be near 2 km.

Very little is known of the basement rocks because of their great depths. A map in preparation shows the top of the pre-Mesozoic at about -7.93 km (-26,000 ft) dipping toward the south.

Referring back to the travel time curves in Figures 4.17 and 4.18, it will be noted that for distances as far as 32 km (Hattiesburg) a propagation velocity of 4.77 km/sec is indicated. This velocity can possibly be extended to a crossover distance of almost 100 km when the apparent crustal velocity of 8.5 predominates. Using the velocities and zero intercept times the 4.77 km/sec refractor should be near 1 km which is above both the Cretaceous and pre-Mesozoic. With more dense coverage and time control, both the Cretaceous and pre-Mesozoic should provide a refraction surface of increasingly higher velocities.

From this it can be deduced that the first arrivals out to at least 32 km did not penetrate to the Cretaceous beds. The 8.5 refractor was computed to be at a depth of 30.4 km based upon the apparent velocities out to Houston, Texas. This compares with 35 km as determined by the U.S. Geological Survey from Pre-DRIBBLE high explosive work with much more data.

It is interesting to note that Rawson and Hansen (1965) observed Moho reflections at 11 sec. With pre-shot salt velocities of 4.55 km/sec and assuming a vertical reflection with constant salt velocity to the Moho, a depth of 25 km is indicated. The velocities between the salt and the Moho discontinuity are undoubtedly higher than the 4.55 km/sec and the true depth would be greater than the 25 km. A 3.3 sec reflection was also obtained from the bottom of the salt and with a constant salt velocity would be at about 7.5 km. The information obtained from the basement map and the 3.3 sec reflection suggests that the salt extends to the basement rocks.

Figure 4.21 shows the 23 salt domes within an 80 km radius of the Tatum Dome. The numbers identify the known

domes as shown on the U.S.G.S. Oil and Gas Investigations Map OM200. The horizontal resultant vector is also shown. There does not seem to be a correlation between this vector and the salt dome. The tectonic map shows that the Ellisville station is located in an area of major fractures of the Gilbertown fault zone on the Ouachita Tectonic Belt. This, in part, could explain the horizontal resultant deviation from the radial. The map does not show similar tectonic disturbances near Hattiesburg as a possible explanation of the large deviation from the radial. Table 4.4 identifies the 23 salt domes within 80 km of Tatum Dome.

4.6 SEISMIC ENERGY

The source seismic energy of an explosion may be calculated for a measured phase on the seismogram if several assumptions are accepted (Berg, et al., 1961; Carder, et al., 1958, 1961, 1962; and Howell and Budenstein, 1955). Among the factors which must be assumed are seismic energy propagation characteristics and energy distribution or partitioning. If the wave fronts are hemispherical, and

if surface motions are twice those within the earth the following formula could relate transitory earth particle displacements to the source seismic energy:

$$E = \rho \pi^3 R^2 f d^2 V Q 10^{2kR} \qquad (4.7)$$

where:

E = total source seismic energy in ergs

ρ = density in gm/cm^3 with 2,5 assumed

f = frequency in cps of measured phase

V = propagation velocity of the measured phase in cm/sec with 1.9×10^5 assumed

d = transitory peak maximum displacement in cm

Q = factor for energy loss at seismic interfaces and assumed unity for the present example

k = absorption coefficient/km with 0.013 assumed

R = distance from source to detector in cm

This formula was applied to 23 seismograph stations at distance ranges of 1.458 to 63 km.

An explosion of 1 kt TNT results in the prompt release of 10^{12} calories of energy or 4.2×10^{19} ergs. The seismic source energy for SALMON was calculated to be about 9.9×10^{17} ergs. The total available energy based

upon 5 kt TNT equivalence is 2.1×10^{20} ergs. The percentage of total source energy converted to seismic energy would, therefore, be about 0.47 percent. This compares with 0.30 percent for the SHOAL granite detonation (Mickey and Lowrie, 1964) and 0.15 for the HARDHAT granite experiment. Seismic efficiences for the GNOME explosion in salt were reported by Carder, et al., (1962) as 0.78 to 2.48 percent. Seven stations were used for the 2.48 value and one station for the 0.78 percent calculation.

4.7 EQUIVALENT EARTHQUAKE MAGNITUDES

The AFTAC SALMON (1964) report observed larger magnitudes out to 16 degrees (1780 km) than at greater distances. The magnitudes with their standard deviations were:

For distances $\leqq$ 16° 5.37 ± 0.30

For distances $>$ 16° 4.15 ± 0.41

The method for determining the magnitudes is explained in the referenced report. In brief, the values

are determined by compressional arrivals as follows:

Unified magnitude:

$$m = \log_{10}\left(\frac{A}{T}\right) + B \qquad (4.8)$$

where:

A = zero to peak ground motion in millimicrons

T = period of signal in sec

B = distance factor as determined by Richter (1958) and extrapolated to closer distances by AFTAC

The overall magnitude as reported by AFTAC was 4.58 $\pm$ 0.73, based upon a distance range of 242 to 5,704 km using 37 stations.

Using the energy calculations for the Coast Survey stations equivalent magnitudes were calculated. Richter (1958) reported a relationship of energy to magnitude as follows:

$$\log_{10}E = 5.8 + 2.4\ m \qquad (4.9)$$

Using the formula a magnitude was determined for each of the 23 stations. Magnitude was also calculated using the average energy for all stations.

Individual station magnitude from seismic energy:

$$m = 5.08^{+0.09}_{-0.16}$$

Overall magnitude averages with each station assigned a magnitude:

$$m = 5.05 \pm 0.11$$

The five seismic safety stations at Tylertown, Perkinston, Prentiss, Beaumont, and Ellisville also provided an independent method for determining magnitudes. The Richter (1958) method of magnitude calculations for the Wood-Anderson seismograph system is:

$$M_L = \log_{10}A - \log_{10}A_o \qquad (4.10)$$

where:

M_L = magnitude determined from seismograms at less than 600 km distance

A = peak maximum motion in mm from a torsion seismometer with magnification of 2800, natural period of 0.8 sec and damping 0.8 critical

A_o = peak maximum motion in mm for a "magnitude zero" earthquake recorded by a torsion seismometer with constants as above

It must be noted that this determination is from the maximum motion on a horizontal seismograph as compared to the "m" magnitude from compressional energy.

The five stations gave the following magnitude:

$$M_L = 5.04 \pm 0.36$$

Richter (1958) relates M_L to m as follows:

$$m = 1.7 + 0.8M_L - 0.01M_L^2$$

which would yield

$$m = 5.48$$

This is abnormally high. Shallow earthquakes generate larger surface waves than explosions, and since M_L is normally based on surface waves of earthquakes, the m to M_L relationship would not hold.

4.8 SOUND FROM AN UNDERGROUND EXPLOSION

There have been numerous reports of people hearing rumbling sounds during an earthquake. There were reports that the SALMON detonation was heard.

It is possible for sounds to be generated by ground vibrations, as reported by W. L. Donn and Postmentier (1964) and Cook and Young (1962). The equation from Beranek (1954) relates the radiated sound pressure to atmospheric density and particle velocity.

$$P = \rho c v \qquad (4.11)$$

where:

P = sound pressure

ρ = atmospheric density

c = seismic velocity

v = particle velocity of the vibrating medium

Weart (1963) reported that the surface particle velocity above the 3.1 kt GNOME Event was 5.6×10^{2} cm/sec. With normal density of 1.19×10^{-3} g/cm^3 and velocity of 3.3×10^{4} cm/sec, the sound pressure generated at GNOME surface zero was 2.2×10^{4} dynes/cm^2 or 161 db.

Preliminary reports from SALMON indicated that the surface accelerations were 25 g and displacements were 25.4 cm. Assuming that the motions were of the same frequency and time of occurrence (which they were not,

but direct frequency measurements were not available), the two may be combined to arrive at a particle velocity. Based upon these tenuous assumptions the sound pressure on the earth's surface above SALMON was 1.53×10^5 dynes/cm^2 or 177 db.

The International Organization for Standardization (I.S.O.) in I.S.O. Recommendation R.226 placed the normal binaural minimum audible field for 20 cps at about 74 db and for the most efficient frequency of 4000 cps at -3 db. Wood (1940) reported that some kind of auditory sensation is experienced for frequencies down to 2 or 3 cps, but that the tonal character is established at about 25 cps. The calculated frequency for the peak acceleration and displacement was near 25 cps.

Based upon the computed particle velocities at the observers site (5.63 km) the sound pressure generated at the site was about 126 db, but at frequencies near 5 cps which would be sub-audible. Assuming a small source and normal acoustic attenuation with distance, the sound from surface zero would have been less than the sound pressures generated by ground motions at the observer's site.

Richter (1958) wrote of instances where audible sounds were generated by vibrations near the observer originating from distant earthquakes. Based upon the sound radiation formula, it is quite easy to experience ground vibrations and associated high sound pressure levels, but the problem seems to be complicated by sub-audible frequencies usually associated with the seismic waves. It is a common occurrence for earthquakes to be recorded on low frequency microbarograph and infrasonic microphone systems with two sources, one at the earthquake epicenter with atmospheric propagation and the other from ground motions at some intermediate point normally close to the detector. Unusually large earthquakes are needed for source generation and atmospheric propagation to occur.

4.9 APPENDIXES

Appendix A contains a sample strong-motion seismogram and an oscillograph record from one of the mobile seismograph stations. Appendix B describes a detailed analysis of the anomalous seismograms recorded at Hattiesburg and Columbia.

CHAPTER 5

CONCLUSIONS AND RECOMMENDATIONS

5.1 CONCLUSIONS

Cube root scaling for particle velocities were compatible for HE detonations of 500 to 4000 lbs in the unconsolidated near-surface sediments and for 500 to 1000 lbs HE shots in the salt dome. The sedimentary shots scaled higher by more than a factor of 10. Velocity cube root scaling for SALMON was less consistent, but was lower than the sedimentary shots.

Asymmetric seismic energy propagation was observed with major axes oriented north and south at distances of 10 to 63 km. From 1.458 to 6.263 km more efficient propagation was in an easterly direction.

Apparent velocities conformed to the following time-distance equations:

$t = \frac{km}{2.82} - 0.28$	East line	1.5	to	6	km
$t = \frac{km}{2.67} - 0.37$	South line	1.5	to	6	km
$t = \frac{km}{4.77} + 0.6$		6	to	100	km
$t = \frac{km}{8.5} + 10.0$	Southwest line	100	to	600	km

The maximum displacements propagated at:

$$t = \frac{km}{1.9}$$

Apparent emergence angles for the first arrivals varied from 66.9 to 85.3 degrees measured from the horizontal, based upon recorded accelerations and 30.4 to 73.2 degrees for the lower frequency displacements.

The horizontal resultant vector from first motion was greater than 36 degrees from a radial line passing through ground zero and the recording station for three stations: Station 2S, +36.8 degrees with plus in a clockwise direction; Hattiesburg, -66.0 degrees; and Ellisville, +36.2 degrees.

There are 23 known salt domes within a radius of 80 km from SALMON. These are within the extrapolated 0.001 g acceleration limits defining the threshold of feeling for vibrations.

Based upon seismic energy calculations about 0.47 percent of the total source energy was converted into seismic energy. Equivalent earthquake magnitude as derived from seismic energy was near 5.1.

Calculations of sound pressure levels as generated by the earth vibrations in the vicinity of ground zero were about 177 db and were in the lower frequencies of the audible range.

5.2 RECOMMENDATIONS

It is suggested that more work be assigned to determining the threshold of feeling, especially in places where the actual ground motion is measured.

The generation of seiches in confined basins or streams has often been observed in earthquake studies. The mechanics for describing the response of a body of water subjected to vibrations has been fairly well

defined. In an area such as Mississippi there are many natural water basins such as streams, reservoirs, swimming pools, ponds, etc., where the seiche actions can be observed and recorded as an adjunct to vibration measurements.

The National Bureau of Standards (Cook, 1962) has developed an infrasonic acoustic system which can be used to measure the sound pressure levels generated by earth vibrations. It is recommended that studies be made to determine if such a system could be used in vibration experiments. This system responds to earth vibrations over a large area, while a seismometer measures vibrations in an area proportional to the size of its base.

Studies should be made on the effects of geology as related to earth vibrations. It has often been observed that earthquakes produce larger vibrations in deep unconsolidated sediments. Greater damages from earth vibrations are experienced by structures located on deep alluvium and artificial areas. Methods need to be developed to determine to what extent the seismic signal is intensified by local geological conditions.

REFERENCES

1. Air Force Technical Applications Center, Project 8.4; "SALMON"; December 7, 1964.

2. Anderson, J. A., and H. O. Wood; "Description and Theory of the Torsion Seismometer"; Bulletin of the Seismological Society of America, Vol 15, No. 1, 1925.

3. Beers, Roland F., Inc.; "Investigation of Salmon Ground Motions and Effects"; Final Report AEC-NVO-1163-51, 1965.

4. Beranek, Lec L.; "Acoustics"; McGraw-Hill Electric and Electronic Engineering Series; 1954.

5. Berg, J. W., Jr., and K. L. Cook; "Energies, Magnitudes, and Amplitudes of Seismic Waves from Quarry Blasts at Promontory and Lakeside, Utah"; Bulletin of the Seismological Society of America, Vol 41, No. 3, 1961.

6. Blume, John A., and Associates, Research Division; "Structural Response of Tall Industrial and Residential Structures to an Underground Detonation"; Submitted to AEC for publication, February 19, 1965.

7. Carder, D. S.; "Response of a Torsion Seismometer to Sustained Vibrations"; Bulletin of the Seismological Society of America, Vol 30, No. 4, 1940.

8. Carder, D. S., W. K. Cloud, L. M. Murphy, and J. Hershberger; "Operation PLUMBBOB, Surface Motions from an Underground Explosion"; WT-1530, AEC Category, Physics and Mathematics; June 1958.

9. Carder, D. S., and W. V. Mickey; "Project COWBOY, Seismic Effects from Coupled and Decoupled Shots in Salt"; U.S. Department of Commerce, Coast and Geodetic Survey; December 1960.

10. Carder, D. S., L. M. Murphy, T. H. Pearce, W. V. Mickey, and W. K. Cloud; "Operation HARDTACK Phase II, Surface Motions from Underground Explosions"; WT-1741; March 1961.

11. Carder, D. S., W. V. Mickey, L. M. Murphy, W. K. Cloud, J. N. Jordan, and D. W. Gordon; "Project GNOME, Seismic Waves from an Underground Explosion in a Salt Bed"; AEC PNE-110P; April 1962.

12. Cloud, W. K., and D. S. Carder; "The Strong-Motion Program of the Coast and Geodetic Survey"; Proceedings of the World Conference on Earthquake Engineering; 1956.

13. Cloud, W. K., and D. E. Hudson; "A Simplified Instrument for Recording Strong-Motion Earthquakes"; Bulletin of the Seismological Society of America, Vol 51, No. 2; April 1961.

14. Cook, Richard K., and Jessie M. Young; "Strange Sounds in the Atmosphere, Part II"; Sound, Vol 1, No. 3; May-June 1962.

15. Cram, Ira H., Jr.; "A Crustal Structure Refraction Survey in South Texas"; Geophysics, Vol XXVI, No. 5; October 1961.

16. Defense Atomic Support Agency; "Nuclear Geoplosics, Part IV, Empirical Analysis of Ground Motion and Cratering"; Editor-in-Chief, F. M. Saure, SRI; DASA-1285 (IV); 1964.

17. Donn, William L., and Eric S. Postmentier; "Ground Coupled Air Waves from the Great Alaskan Earthquake"; Journal of Geophysical Research; Vol 69, No. 24; December 15, 1964.

18. Eargle, D. H.; "Southwest-Northeast Cross Section, Tatum Salt Dome, Lamar County, Mississippi"; U.S. Geological Survey, Technical Letter, DRIBBLE 29; April 3, 1963.

19. Howell, B. F., Jr., and D. Budenstein; "Energy Distribution in Explosion-Generated Seismic Pulses"; Geophysics, Vol XX, No. 1, January 1955.

20. Kuz'mina, N. V., and A. N. Romashev, B. G. Ruler, D. A. Kharin, and E. D. Shemyakin; "Seismic Effect of Eruptive Explosions in Nonrock Coherent Ground"; Problems of Engineering Seismology, Translation from the Russian, Consultants Bureau, New York; 1963.

21. Lowrie, L. M.; "Seismograph System Calibration"; U.S. Coast and Geodetic Survey; 1965.

22. McComb, H. E.; "Strong-Motion Seismograph Equipment and Installations"; Transactions of the American Geophysical Union, 14th Meeting; 1933.

23. McComb, H. E.; "Selection, Installation, and Operation of Seismographs"; U.S. Department of Commerce, Coast and Geodetic Survey, Special Publication No. 206; 1936.

24. Mickey, W. V.; "Operation Pre-DRIBBLE, Seismic Effects of 1000 lb HE Detonations in Salt and Sedimentary Deposits"; U.S. Coast and Geodetic Survey; 1963 A.

25. Mickey, W. V.; "Operation PLOWSHARE, Project SEDAN, Seismic Effects from a High Yield Nuclear Cratering Experiment in Desert Alluvium"; AEC PNE-213F; February 1963 B.

26. Mickey, W. V., and T. R. Shugart; "Seismic Data Summary, Nuclear Detonation Program, 1961 through 1963"; U.S. Coast and Geodetic Survey; 1964.

27. Mickey, W. V., and L. M. Lowrie; "Seismic Safety Net, Project SHOAL"; AEC VUF-1011; August 1964.

28. Mickey, W. V.; "Seismic Wave Propagation"; Proceedings of Third Plowshare Symposium; AEC TID-7695; 1964 A.

29. Mickey, W. V.; "Microearthquake Monitoring a at the SHOAL Site"; U.S. Department of Commerce, Coast and Geodetic Survey; April 1964 B.

30. Rawson, D. E., and S. M. Hansen; "The Post-Explosion Environment Resulting from the SALMON Event"; from Abstract of paper to be delivered at Americal Geophysical Union Meeting; April 1965.

31. Richter, C. F.; "Elementary Seismology"; W. H. Freeman and Company; San Francisco, California; 1958.

32. U.S. Department of Commerce, Coast and Geodetic Survey; "Earthquake Investigation in California, 1934-1935"; Special Publication 201; 1936.

33. U.S. Department of Commerce, Coast and Geodetic Survey; "Earthquake Investigation in the Western United States, 1931-1964"; Publication 41-2; 1965.

34. Weart, W. D; "Particle Motion near a Nuclear Detonation in Halite"; AEC-PNE-108F; September 5, 1963.

35. Weisbrich, R. A.; "Technical Report No. 65-17, Project DRIBBLE-SALMON Event Volunteer Program"; The Geotechnical Corporation; Dallas, Texas; 1965.

36. Wenner, F.; "Development of Seismological Instruments at the Bureau of Standards"; Bulletin of the Seismological Society of America, Vol 22, No. 1, 1932.

37. Wood, A., "Acoustics"; Interscience Publishers, Inc.; New York, N. Y.; 1940.

TABLE 3.1 INSTRUMENT CONSTANTS

Station	Pend.	T_o	ϵ	Sens.	Mag.	T_g	Serial Number Accel.	CDM	L
		sec		cm/g		sec			
				Coast Survey Accelerographs					
1 East	up	0.0211	8	1.27			1052 V		0.92
	away	.0197	9	1.16			1053 R		.92
	left	.0204	8	1.21			1054 T		.92
	down	1.64	10		1.26	2.29		116 V	130.1
	away	3.86	10		0.976	2.47		121 R	151.3
	right	4.00	10		0.95	2.46		120 T	150.1
1 East	up	.0322	8	3.1			218 V		.92
	away	.0304	10	2.80			219 R		.92
	left	.0301	10	2.74			220 T		.92
	down	1.75	10		1.06	2.44		19 V	147.6
	away	3.90	10		2.58	1.52		112 R	57.3
	right	4.01	10		2.45	1.52		111 T	57.3
1 South	up	.0315	10	2.78			1058 V		.92
	away	.0315	10	3.02			1059 R		.92
	left	.0299	10	2.81			1060 T		.92
	down	1.88	10		1.17	2.25		25 V	125.6
	away	3.92	10		2.44	1.54		108 R	58.8
	right	3.94	10		2.52	1.54		109 T	58.8

TABLE 3.1 INSTRUMENT CONSTANTS (con.)

Station	Pend.	T_o	ϵ	Sens.	Mag.	T_g	Serial Number Accel.	Serial Number CDM	L
		sec		cm/g		sec			
1 South	up	0.0178	10	0.88			1064 V		0.92
	away	.0196	10	1.15			1065 R		.92
	left	.0202	9	1.21			1066 T		.92
	down	1.76	10		1.26	2.20		none	120.0
	away	3.98	10		0.99	2.46		127 R	150.1
	right	4.06	10		0.96	2.46		126 T	150.1
2 East	up	.0278	10	2.15			3016 V		.92
	away	.0275	9	2.24			3017 R		.92
	left	.0276	10	2.36			3018 T		.92
	down	1.40	10		1.22	2.30		110 V	131.2
	away	4.10	10		1.97	1.74		133 R	75.1
	right	4.07	10		1.83	1.76		132 T	76.8
2 South	up	.0275	9	2.16			2008 V		.92
	away	.0286	8	2.37			2026 R		.92
	left	.0283	8	2.52			2027 T		.92
	down	1.65	10		1.26	2.21		16 V	121.1
	away	3.92	10		1.97	1.74		103 R	75.1
	right	3.85	10		1.89	1.74		102 T	75.1

TABLE 3.1 INSTRUMENT CONSTANTS (con.)

Station	Pend.	T_o	ϵ	Sens.	Mag.	T_g	Serial Number Accel.	Serial Number CDM	L
		sec		cm/g		sec			
3 East	up	0.0295	8	2.56			3007 V		0.92
	away	.0287	9	2.42			3008 R		.92
	left	.0307	9	2.86			3009 T		.92
	down	1.66	10		0.94	2.62		5 V	170.2
	away	4.04	10		3.04	1.40		118 R	48.6
	right	3.89	10		2.92	1.40		117 T	48.6
3 South	up	.0332	10	3.19			3010 V		.92
	away	.0318	10	3.09			3011 R		.92
	left	.0334	8	3.47			3012 T		.92
	down	1.67	10		0.99	2.46		119 V	150.1
	away	3.90	10		3.20	1.40		124 R	48.6
	right	4.00	10		2.94	1.40		123 T	48.6
4 East	up	.0431	10	5.40			1016 V		.92
	away	.0435	9	5.65			1017 R		.92
	left	.0431	8	5.59			1018 T		.92
	down	2.00	10		2.30	1.70		none	71.7
	away	3.88	10		4.80	1.10		72 R	30.0
	right	3.80	10		4.86	1.10		73 T	30.0

TABLE 3.1 INSTRUMENT CONSTANTS (con.)

Station	Pend.	T_o	ϵ	Sens.	Mag.	T_g	Serial Number Accel.	Serial Number CDM	L
		sec		cm/g		sec			
4 South	up	0.0457	10	6.26			1061 V		0.92
	away	.0461	11	6.45			1062 R		.92
	left	.0438	10	5.64			1063 T		.92
	down	1.65	10		1.67	1.90		12 V	89.5
	away	3.85	10		4.80	1.10		63 R	30.0
	right	3.80	10		4.86	1.10		64 T	30.0
5 East	up	.0568	9	9.44			1028 V		.92
	away	.0586	9	10.3			1029 R		.92
	left	.0566	9	9.20			1030 T		.92
	down	1.40	10		1.69	1.90		21 V	89.5
	away	3.75	10		8.54	0.82		40 R	16.7
	right	3.80	10		8.56	0.82		41 T	16.7
5 South	up	.0612	10	11.35			2006 V		.92
	away	.0586	9	9.85			2022 R		.92
	left	.0618	10	11.58			2023 T		.92
	down	1.82	10		1.15	2.26		15 V	126.7
	away	3.85	10		8.90	0.82		67 R	16.7
	right	4.00	10		9.0	0.82		68 T	16.7

TABLE 3.1 INSTRUMENT CONSTANTS (con.)

Station	Pend.	T_o	ϵ	Sens.	Mag.	T_g	Serial Number Accel.	CDM	L
		sec		cm/g		sec			
6 East	up	0.0895	10	22.9			1034 V		0.92
	away	.0942	9	27.1			1035 R		.92
	left	.0921	9	24.4			1036 T		.92
	down	1.75	10		1.06	2.40		8 V	142.8
	away	3.85	8		8.78	0.83		1B R	17.1
	right	3.93	10		8.68	0.815		1A T	16.5
6 South	up	.0942	10	26.7			2000 V		.92
	away	.0946	9	26.6			2010 R		.92
	left	.0946	9	27.8			2011 T		.92
	down	1.70	10		1.30	2.40		14 V	142.8
	away	3.75	10		8.70	0.82		106 R	16.7
	right	3.81	10		8.64	0.82		105 T	16.7
Baxter-ville Oil Field	up	.1469	8	60.0			1013 V		.92
	away	.1426	8	60.0			1014 R		.92
	left	.1418	10	60.5			1015 T		.92
	down	1.65	10		1.2	2.20		29 V	120.0
	away	3.60	10		8.85	0.825		38 R	16.9
	right	3.75	10		8.60	0.825		39 T	16.9

TABLE 3.1 INSTRUMENT CONSTANTS (con.)

Station	Pend.	T_o	ϵ	Sens.	Mag.	T_g	Serial Number Accel.	Serial Number CDM	L
		sec		cm/g		sec			
Purvis	up	0.1453	9	58.0			1049 V		0.92
Nat'l	away	.1488	10	68.2			1050 R		.92
Guard	left	.1480	9	63.0			1051 T		.92
Armory	down	1.62	10		0.99	2.54		122 V	160.0
	away	3.69	10		8.60	0.83		17 R	17.1
	right	3.83	10		8.50	0.82		16 T	16.7
Lumberton	up	.1526	8	64.6			1037 V		.92
Nat'l	away	.1527	8	62.1			1038 R		.92
Guard	left	.1527	9	65.8			1039 T		.92
Armory	down	1.65	10		1.09	2.40		22 V	142.8
	away	3.90	10		8.54	0.82		27 R	16.7
	right	3.88	10		8.22	0.825		26 T	16.9
				Carder Vibration Meters					
Gulf Oil	down	4.00	10		23.2	0.65		C V	10.5
Refinery	away	4.25	10		21.8	0.67		B R	11.1
	left	4.20	10		21.3	0.67		A T	11.1

TABLE 3.1 INSTRUMENT CONSTANTS (con.)

Station	Pend.	T_o	ϵ	Sens.	Mag.	T_g	Serial Number Accel.	Serial Number CDM	L
		sec		cm/g		sec			
Coast Survey Vibration Meters									
Columbia	away	4.50	10	126.0				5 R	0.92
	left	4.55	10	114.7				M-8 T	.92
Hatties-burg	away	4.55	10	128.9				M-3 R	92
	left	4.75	10	129.7				M-2 T	.92

Pend. - Pendulum displacement for trace up
T_o - Natural period of pendulum
ϵ - Damping ratio
Sens. - Sensitivity
Mag. - Magnification
T_g - Gravity period
Accel. - Accelerometer
CDM - Carder Displacement Meter
L - Effective pendulum length
V - Vertical
R - Radial
T - Transverse

TABLE 4.1 EARTH MOTIONS

Station Slant Distance and Direction from WP	Instrument and Component		Maximum Acceleration	Maximum Velocity	Maximum Displacement	Period	Travel Time
			10^{-1}g	10^{-2}cm/sec	10^{-2}cm	sec	sec
1 East	Accel	V	28.4			0.05	0.23
1.458 km		R	7.6			.13	
S74.6°E		T	3.4			.03	
	CDM	V			--	--	
		R			118	.45	
		T			32	.58	
1 South	Accel	V	41.0			.04	.19
1.463 km		R	11.6			.12	
S14.9°W		T	5.99			.03	
	CDM	V			--	--	
		R			121	.27	
		T			63.1	.41	
2 East	Accel	V	10.6			.07	.37
1.804 km		R	5.41			.11	
N88.9°E		T	1.69			.15	
	CDM	V			74.6	.18	
		R			73.6	.18	
		T			29.0	.90	

TABLE 4.1 EARTH MOTIONS (con.)

Station Slant Distance and Direction from WP	Instrument and Component		Maximum Acceleration	Maximum Velocity	Maximum Displacement	Period	Travel Time
			10^{-1}g	10^{-2}cm/sec	10^{-2}cm	sec	sec
2 South	Accel	V	9.16			0.05	0.28
1.805 km		R	4.22			.12	
S14.2°W		T	2.58			.15	
	CDM	V			74.5	.24	
		R			91.4	.25	
		T			54.5	.41	
3 East	Accel	V	15.6			.15	.49
2.118 km		R	7.11			.15	
S62°E		T	1.4			.13	
	CDM	V			70.2	.16	
		R			111	.33	
		T			20.6	.17	
3 South	Accel	V	4.76			.04	.44
2.169 km		R	6.15			.10	
S32.4°W		T	2.88			.09	
	CDM	V			--	--	
		R			59.5	.22	
		T			--	--	

TABLE 4.1 EARTH MOTIONS (con.)

Station Slant Distance and Direction from WP	Instrument and Component		Maximum Acceleration	Maximum Velocity	Maximum Displacement	Period	Travel Time
			10^{-1}g	10^{-2}cm/sec	10^{-2}cm	sec	sec
4 East	Accel	V	3.80			0.09	0.78
3.067 km		R	9.48			.17	
S81.2°E		T	1.48			.15	
	CDM	V			10.9	.12	
		R			75.2	.39	
		T			16.7	.71	
4 South	Accel	V	5.25			.13	.95
3.398 km		R	3.64			.15	
S10.7°W		T	1.15			.13	
	CDM	V			41.9	.16	
		R			59.5	.38	
		T			17.9	.21	
5 East	Accel	V	4.29			.11	1.20
4.140 km		R	3.35			.14	
S72.5°E		T	0.63			.16	
	CDM	V			42.0	.20	
		R			54.4	.25	
		T			11.0	1.32	

TABLE 4.1 EARTH MOTIONS (con.)

Station Slant Distance and Direction from WP	Instrument and Component		Maximum Acceleration	Maximum Velocity	Maximum Displacement	Period	Travel Time
			10^{-1}g	10^{-2}cm/sec	10^{-2}cm	sec	sec
5 South	Accel	V	2.65			0.10	1.19
4.195 km		R	2.16			.17	
S23.6°W		T	0.863			.15	
	CDM	V			30.4	.32	
		R			36.1	.22	
		T			12.3	.51	
6 East	Accel	V	2.88			.17	1.83
5.945 km		R	1.71			.19	
S70.9°E		T	0.717			.14	
	CDM	V			47.2	.23	
		R			21.7	.21	
		T			6.59	.15	
6 South	Accel	V	2.38			.15	1.97
6.263 km		R	1.08			.13	
S22.4°W		T	0.417			.15	
	CDM	V			--	--	
		R			17.1	.23	
		T			7.99	.32	

TABLE 4.1 EARTH MOTIONS (con.)

Station Slant Distance and Direction from WP	Instrument and Component		Maximum Acceler-ation	Maximum Velocity	Maximum Displace-ment	Period	Travel Time
			10^{-1}g	10^{-2}cm/sec	10^{-2}cm	sec	sec
Baxterville	Accel	V	0.439			0.17	2.58
Oil Field		R	.225			.15	
10.104 km		T	.489			.15	
S36.3°W	CDM	V			10.0	.21	
		R			3.06	.31	
		T			9.30	.20	
Purvis,	Accel	V	.317			.17	3.97
Mississippi		R	.156			.28	
14.9 km		T	.0587			.15	
East	CDM	V			--	--	
		R			--	--	
		T			2.12	.37	
Gulf Oil	CVM	V			8.19	.18	4.40
Refinery		R			5.73	.12	
18.1 km		T			3.19	.56	
N59°E							

TABLE 4.1 EARTH MOTIONS (con.)

Station Slant Distance and Direction from WP	Instrument and Component		Maximum Acceleration	Maximum Velocity	Maximum Displacement	Period	Travel Time
			10^{-1}g	10^{-2}cm/sec	10^{-2}cm	sec	sec
Lumberton, Mississippi 19.6 km S36.5°E	Accel	V	0.242			0.21	4.81
		R	.274			.25	
		T	.157			.26	
	CDM	V			--	--	
		R			6.33	.29	
		T			5.73	.30	
Columbia, Mississippi 25.9 km N63°W	CSVM	R			1.98	.52	5.78
		T			1.40	.36	
Hattiesburg, Mississippi 33.7 km N54°E	CSVM	R			1.67	.49	7.7
		T			3.51	.45	
Bogalusa, Louisiana 49.5 km S34°W	W-A	N-S			--	--	11.5
		E-W			--	--	

TABLE 4.1 EARTH MOTIONS (con.)

Station Slant Distance and Direction from WP	Instrument and Component		Maximum Acceleration	Maximum Velocity	Maximum Displacement	Period	Travel Time
			$10^{-1}g$	10^{-2}cm/sec	10^{-2}cm	sec	sec
Tylertown, Mississippi 54.4 km S87°W	W-A	N-S			0.34	(0.5)	12
		E-W			.57	(.5)	
Perkinston, Mississippi 58 km S45°E	W-A	N-S			.67	(.5)	10.5
		E-W			.76	(.5)	
Prentiss, Mississippi 58 km N29°W	W-A	N-S			.46	(.5)	11
		E-W			.29	(.5)	
Beaumont, Mississippi 62.5 km N87°E	W-A	N-S			.22	(.5)	12
		E-W			.38	(.5)	

TABLE 4.1 EARTH MOTIONS (cont.)

Station Slant Distance and Direction from WP	Instrument and Component		Maximum Acceleration	Maximum Velocity	Maximum Displacement	Period	Travel Time
			10^{-1}g	10^{-2}cm/sec	10^{-2}cm	sec	sec
Ellisville, Mississippi 61.5 km N35°E	W-A	N-S			0.47	(0.5)	11.5
		E-W			.54	(.5)	
10 Miles South 17.8 km S9.8°W	NGC-21	V		130		.23	4.46
		R		70.7		.24	
		T		48.0		.25	
20 Miles South 31.7 km S24.6°W	NGC-21	V		56.0		.30	7.41
		R		18.4		.30	
		T		16.7		.30	
Ville Platte, Louisiana 273 km S81°W	NGC-21	V		0.186		.31	42.02
		R		.372		.35	
		T		.224		.38	
Silsbee, Texas 451 km S79.7°W	NGC-21	V		.064		.25	62.0
		R		.125		.45	
		T		.0833		.34	

TABLE 4.1 EARTH MOTIONS (con.)

Station Slant Distance and Direction from WP	Instrument and Component		Maximum Acceleration	Maximum Velocity	Maximum Displacement	Period	Travel Time
			10^{-1}g	10^{-2}cm/sec	10^{-2}cm	sec	sec
Hockley, Texas 603.2 km S78.8°W	NGC-21	V		0.0234		0.36	80.3
		R		.0236		.40	
		T		.016		.37	
Wiss, Janney, Elstner & Associates Stations							
Wiss-1 8.84 km N23°E	MB	V		106.7		.12	--
		R		186.2		.15	
		T		52.6		.10	
	SBVS-d	V			11.3	.44	
		R			10.4	.28	
		T			5.44	.28	
Wiss-2 16.61 km N5°W	SB-a	V	0.63			.14	--
		R	.37			.15	
		T	.40			.15	
	SBVS-d	V			7.24	.22	
		R			3.05	.44	
		T			3.30	.44	

TABLE 4.1 EARTH MOTIONS (con.)

Station Slant Distance and Direction from WP	Instrument and Component		Maximum Acceleration	Maximum Velocity	Maximum Displacement	Period	Travel Time
			10^{-1}g	10^{-2}cm/sec	10^{-2}cm	sec	sec
Wiss-3 30.26 km N7°E	SBVS-d	V			4.75	0.32	--
		R			3.81	.29	
		T			1.45	.29	
Air Force Technical Applications Center Stations							
EU-AL 242 km N41°E	LPZ-LR	V			0.0226	11.5	36.5
JE-LA 243 km N72°W	LPZ-LR	V			.0366	10.0	37.4
CPSO 618 km N36°E	LPZ-LR	V			.00721	14.0	82.4
GV-TX 728 km N73°W	LPZ-LR	V			.0024	14.0	94.6

TABLE 4.1 EARTH MOTIONS (con.)

Station Slant Distance and Direction from WP	Instrument and Component		Maximum Acceleration	Maximum Velocity	Maximum Displacement	Period	Travel Time
			10^{-1}g	10^{-2}cm/sec	10^{-2}cm	sec	sec
WMSO 931 km N62°W	LPZ-LR	V			0.00126	17.0	120.8
BL-WV 1058 km N44°E	LPZ-LR	V			.00605	12.0	138.5
VO-IO 1251 km N10°W	LPZ-LR	V			.0037	14.5	(140.6)
Waterways Experiment Station							
WES 168 km N47°W	HS	V R		1.76 2.92		0.14 .36	(30.0)

TABLE 4.1 EARTH MOTIONS (con.)

Station Slant Distance and Direction from WP	Instrument and Component		Maximum Acceleration	Maximum Velocity	Maximum Displacement	Period	Travel Time
			10^{-1}g	10^{-2}cm/sec	10^{-2}cm	sec	sec
Worldwide Standardized Seismograph Network							
SHA 145 km S70.4°E	SPZ	V			0.35	0.30	--
OX 453 km N2.24°E	SPZ	V			.025	.30	(26.0)

WP	-	Working Point
V	-	Vertical
R	-	Radial
T	-	Transverse
Accel	-	Accelerometer
CVM	-	Carder Vibration Meter
CDM	-	Carder Displacement Meter
CSVM	-	Coast Survey Vibration Meter
W-A	-	Wood-Anderson Seismograph
NGC-21	-	National Geophysical Company Model 21 Velocity Geophone
MB	-	M-B Velocity Gauge
SBVS	-	Sprengnether Blast Vibration Seismograph
SB	-	Shure Brothers Model 61B Accelerometer
SPZ	-	Benioff Short Period Vertical
LPZ	-	Sprengnether Long Period Vertical Seismograph
HS	-	Hall-Sears Velocity Geophone
EU-AL	-	Eutaw, Alabama
JE-LA	-	Jena, Louisiana
CPSO	-	Cumberland Plateau Observatory, Tennessee
GV-TX	-	Grapevine, Texas
WMSO	-	Wichita Mountains Observatory, Oklahoma
BL-WV	-	Beckley, West Virginia
VO-IO	-	Vinton, Iowa
SHA	-	Spring Hill, Alabama
OX	-	Oxford, Mississippi

TABLE 4.2 MAXIMUM EARTH PARTICLE VELOCITIES

Station Slant Distance and Direction from WP		Recorded Directly	From Displacement*	From Acceleration*	From Digital Computer**
		cm/sec	cm/sec	cm/sec	cm/sec
1 East	V		--	22.2	--
1.458 km	R		16.4	15.4	16.8
S74.6°E	T		3.46	1.59	3.78
1 South	V		--	25.6	
1.463 km	R		28.2	21.7	
S14.9°W	T		9.68	2.8	
2 East	V		26.0	11.6	--
1.804 km	R		25.7	9.3	11.5
N88.9°E	T		2.02	3.95	3.70
2 South	V		19.5	7.15	
1.805 km	R		22.9	7.90	
S14.2°W	T		8.35	6.04	
3 East	V		27.6	36.5	--
2.118 km	R		21.1	16.6	11.2
S62°E	T		7.60	2.84	2.89
3 South	V		--	2.94	
2.169 km	R		17.0	9.59	
S32.4°W	T		--	4.04	
4 East	V		5.70	5.34	--
3.067 km	R		12.1	25.2	16.6
S81.2°E	T		1.48	3.46	2.58
4 South	V		16.4	10.6	
3.398 km	R		9.68	8.52	
S10.7°W	T		5.35	2.34	

TABLE 4.2 MAXIMUM EARTH PARTICLE VELOCITIES (con.)

Station Slant Distance and Direction from WP		Recorded Directly	From Displacement*	From Acceleration*	From Digital Computer**
		cm/sec	cm/sec	cm/sec	cm/sec
5 East	V		13.2	7.35	--
4.140 km	R		13.6	7.31	10.7
S72.5°E	T		0.524	1.57	2.57
5 South	V		5.96	4.14	
4.195 km	R		10.3	5.73	
S23.6°W	T		1.51	2.02	
6 East	V		12.9	7.64	--
5.945 km	R		6.49	5.23	4.84
S70.9°E	T		2.76	1.57	1.59
6 South	V		--	5.56	
6.263 km	R		4.66	2.16	
S22.4°W	T		1.56	0.975	
Wiss No. 1	V	1.07			
8.84 km	R	1.86			
N23°E	T	0.526			
Baxter-ville Oil Field	V		2.99	1.16	
	R		0.620	0.526	
10.104 km	T		2.92	1.14	
S36.3°W					
Purvis	V		--	0.841	
14.9 km	R		--	0.681	
East	T		0.360	0.137	
Wiss No. 2	V	2.08		1.40	
16.61 km	R	0.441		0.863	
N5°W	T	0.476		0.931	

TABLE 4.2 MAXIMUM EARTH PARTICLE VELOCITIES (con.)

Station Slant Distance and Direction from WP		Recorded Directly	From Displacement*	From Acceleration*	From Digital Computer**
		cm/sec	cm/sec	cm/sec	cm/sec
10 Miles South	V	1.20			
17.8 km	R	0.727			
S9.8°W	T	0.480			
Gulf Oil Refinery	V		2.85		2.10
18.1 km	R		2.99		0.999
N59°E	T		0.358		0.657
Lumberton	V		--	0.792	
19.6 km	R		1.37	1.07	
S36.5°E	T		1.20	0.636	
Columbia	R		0.240		0.220
25.9 km	T		0.244		0.154
N63°W					
Wiss No. 3	V	0.925			
30.26 km	R	0.838			
N7°E	T	0.310			
20 Miles South	V	0.560			
31.7 km	R	0.184			
S24.6°W	T	0.167			
Hattiesburg	R		0.214		0.166
33.7 km	T		0.489		0.420
N54°E					
Tylertown	N-S		0.0426		
54.4 km	E-W		0.0715		
S87°W					

TABLE 4.2 MAXIMUM EARTH PARTICLE VELOCITIES (con.)

Station Slant Distance and Direction from WP		Recorded Directly	From Displacement*	From Acceleration*	From Digital Computer**
		cm/sec	cm/sec	cm/sec	cm/sec
Perkinston 58 km S45°E	N-S E-W		0.0841 0.0954		
Prentiss 58 km N29°W	N-S E-W		0.0578 0.0364		
Beaumont 62.5 km N87°E	N-S E-W		0.0276 0.0477		
Ellisville 61.5 km N35°E	N-S E-W		0.0590 0.0679		
WES 168 km N47°W	V R	0.0176 0.0292			
Ville Platte, La. 273 km S81°W	V R T	0.00186 0.00372 0.00224			
Silsbee, Texas 451 km S79.7°W	V R T	0.000640 0.00125 0.000833			

TABLE 4.2 MAXIMUM EARTH PARTICLE VELOCITIES (con.)

Station Slant Distance and Direction from WP		Recorded Directly	From Displacement*	From Acceleration*	From Digital Computer**
		cm/sec	cm/sec	cm/sec	cm/sec
Hockley, Texas 603.2 km S78.8°W	V	0.000234			
	R	0.000236			
	T	0.000160			

* Computation based on the assumption of simple harmonic motion.

** Computer differentiation using simple differences.

TABLE 4.3 APPARENT EMERGENCE ANGLES AND HORIZONTAL RESULTANT VECTORS

Station and Distance	Bearing from Ground Zero	Horizontal Resultant Vector	Differences Clockwise Positive		Apparent Emergence Angle		Approximate Surface Velocity
km			degrees		degrees		km/sec
1 East 1.458	S74.6°E	S86°E	+11.4	d	84.9 68.5	a d	0.25 1.03
1 South 1.463	S14.9°W	S5.4°W	- 9.5	a	81.6 --	a	0.39 --
2 East 1.804	N88.9°E	N75.8°E	-13.1	d	83.5 73.2	a d	.32 .82
2 South 1.805	S14.25°W	S51.05°W S26.45°W	+36.8 +12.2	a d	85.3 71.9	a d	.22 .83
3 East 2.118	S62.0°E	S57.8°E	- 4.2	a	71.3 71.2	a d	.90 .91
3 South 2.169	S32.4°W	--	--		81.8 61.1	a d	.38 1.29
4 East 3.067	S81.25°E	--	--		66.9 30.4	a d	1.11 2.43

TABLE 4.3 APPARENT EMERGENCE ANGLES AND HORIZONTAL RESULTANT VECTORS (con.)

Station and Distance	Bearing from Ground Zero	Horizontal Resultant Vector	Differences Clockwise Positive	Apparent Emergence Angle	Approximate Surface Velocity
km			degrees	degrees	km/sec
4 South 3.398	S10.7°W	--	--	76.4 a 66.5 d	0.63 1.07
5 East 4.140	S72.5°E	--	--	--	--
5 South 4.195	S23.6°W	--	--	--	--
6 East 5.945	S70.9°E	S61.8°E	+ 9.1 d	81.5 a 67.0 d	0.42 1.10
6 South 6.263	S22.4°W	--	--	76.3 a	0.63
Baxterville Oil Field 10.104	S36.25°W	--	--	--	--
Purvis 14.9	East	--	--	80.0 a	0.49

TABLE 4.3 APPARENT EMERGENCE ANGLES AND HORIZONTAL RESULTANT VECTORS (con.)

Station and Distance	Bearing from Ground Zero	Horizontal Resultant Vector	Differences Clockwise Positive	Apparent Emergence Angle	Approximate Surface Velocity
km			degrees	degrees	km/sec
Gulf Oil Refinery 18.1	N59°E	--	--	79.9 d	0.62
Lumberton 19.6	S36.5°E	--	--	--	--
Columbia 25.9	N63°W	--	--	--	--
Hattiesburg 33.7	N54°E	N12.0°W	-66.0 d	--	--
Bogalusa 49.5	S34°W	S43.7°W	- 9.3 d	--	--
Tylertown 54.5	S87°W	N80.3°W	+12.7 d	--	--
Perkinston 58.0	S45°E	S26.1°E	-18.9 d	--	--

TABLE 4.3 APPARENT EMERGENCE ANGLES AND HORIZONTAL RESULTANT VECTORS (con.)

Station and Distance	Bearing from Ground Zero	Horizontal Resultant Vector	Differences Clockwise Positive	Apparent Emergence Angle	Approximate Surface Velocity
km			degrees	degrees	km/sec
Prentiss 58.0	N29°W	N28.8°W	- 0.2 d	--	--
Ellisville 61.5	N35°E	N71.2°E	+36.2 d	--	--
Beaumont 62.5	N87°E	--	--	--	--

a - acceleration
d - displacement

TABLE 4.4 KNOWN SALT DOMES WITHIN 80 KM OF TATUM DOME

Identification Number	Name
2	Arm
5	Byrd
7	Carson
9	Centerville
12	Dont
13	Dry Creek
16	Eminence
19	Glazier
25	Kola
26	Lampton
30	McLaurin
31	Midway
32	Monticello
33	Moselle
38	Oak Vale
39	Ovett
40	Petal
41	Prentiss
42	Richmond
43	Richton
44	Ruth
46	Sunrise
47	Tatum

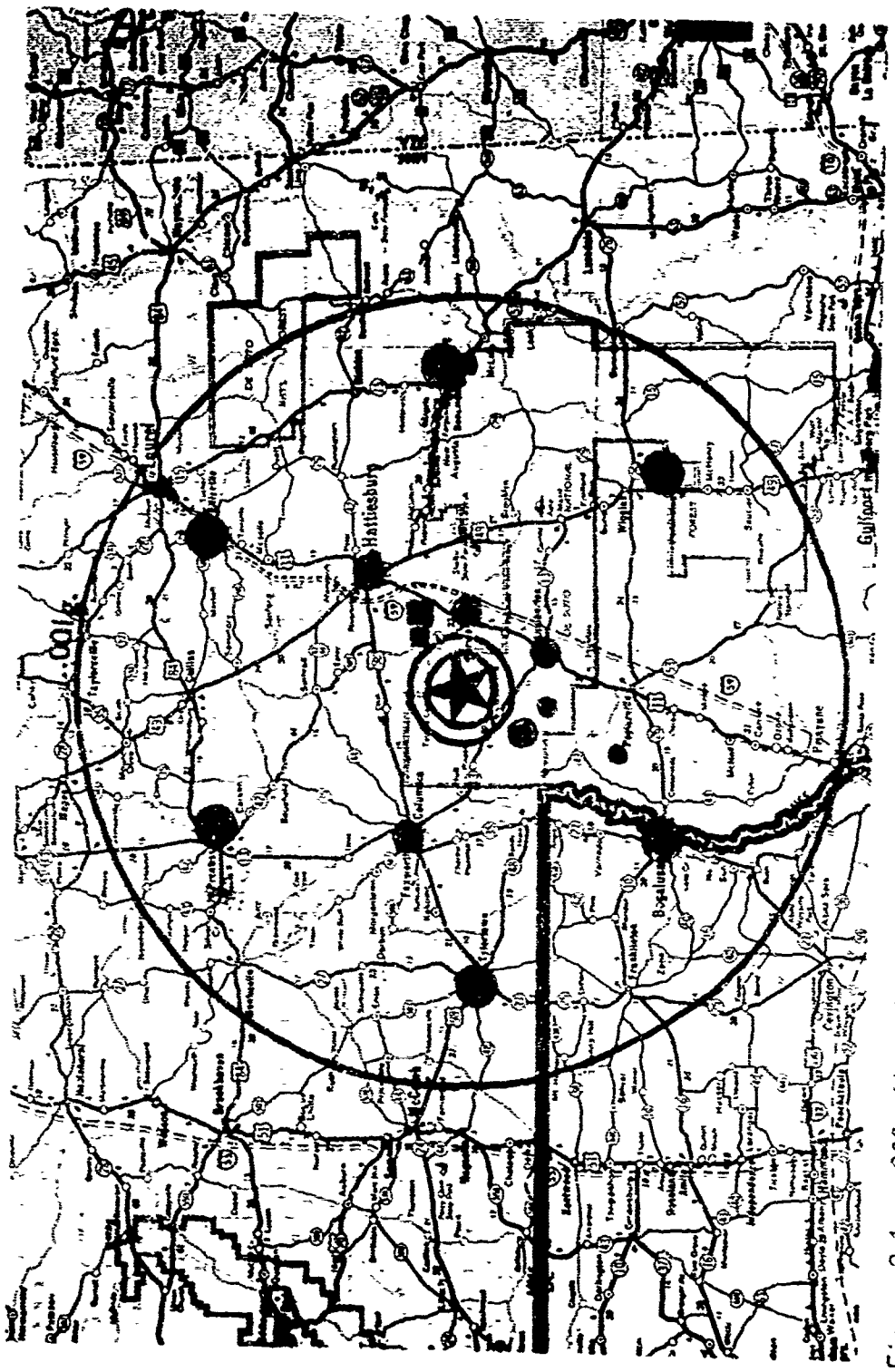

Figure 2.1 Off-site seismograph stations. Small circle around SALMON shows 10 cm/sec region, second circle 0.1 g and large circle the so-called feeling threshold of 0.001 g.

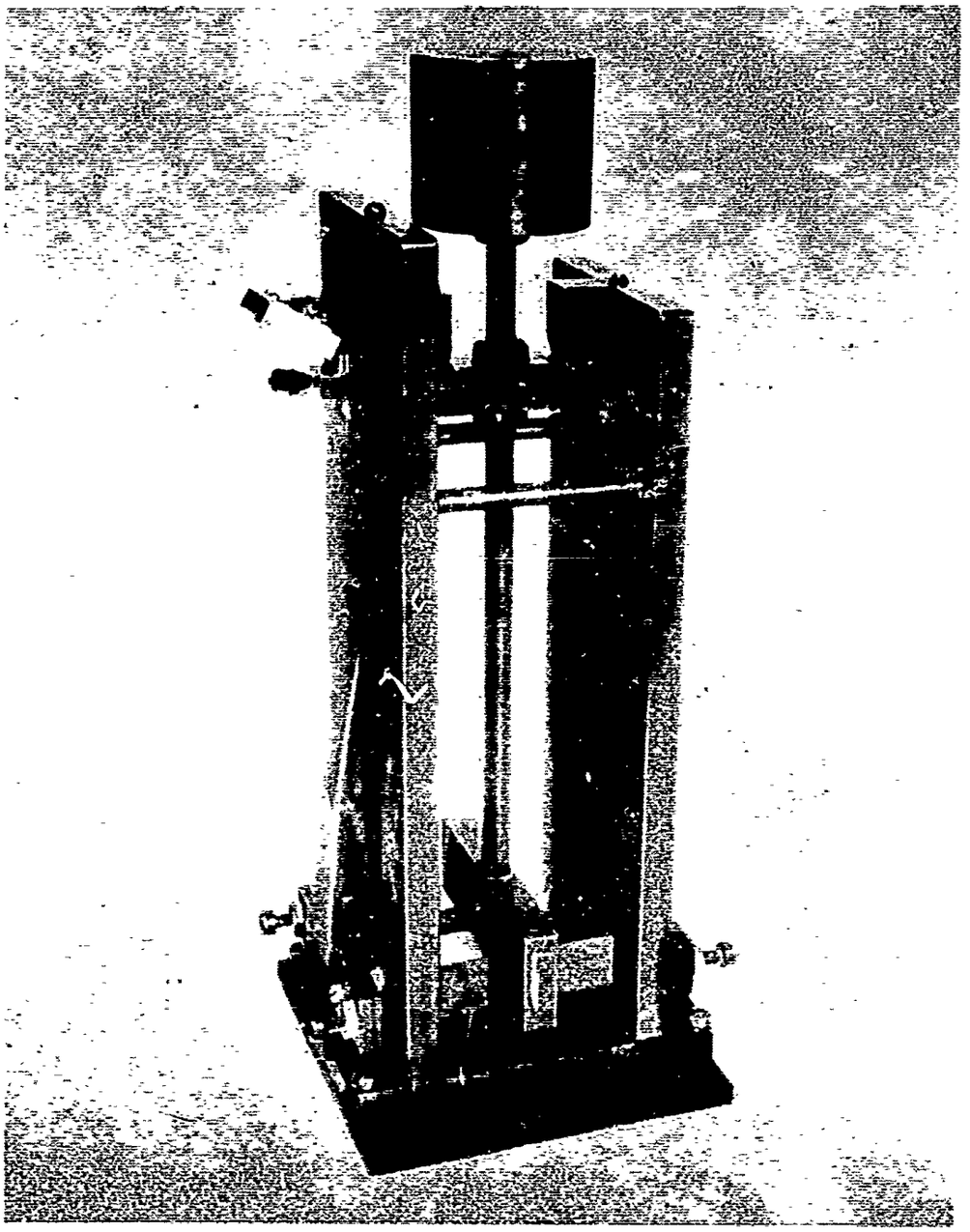

Figure 3.1 Horizontal Carder Displacement Meter.

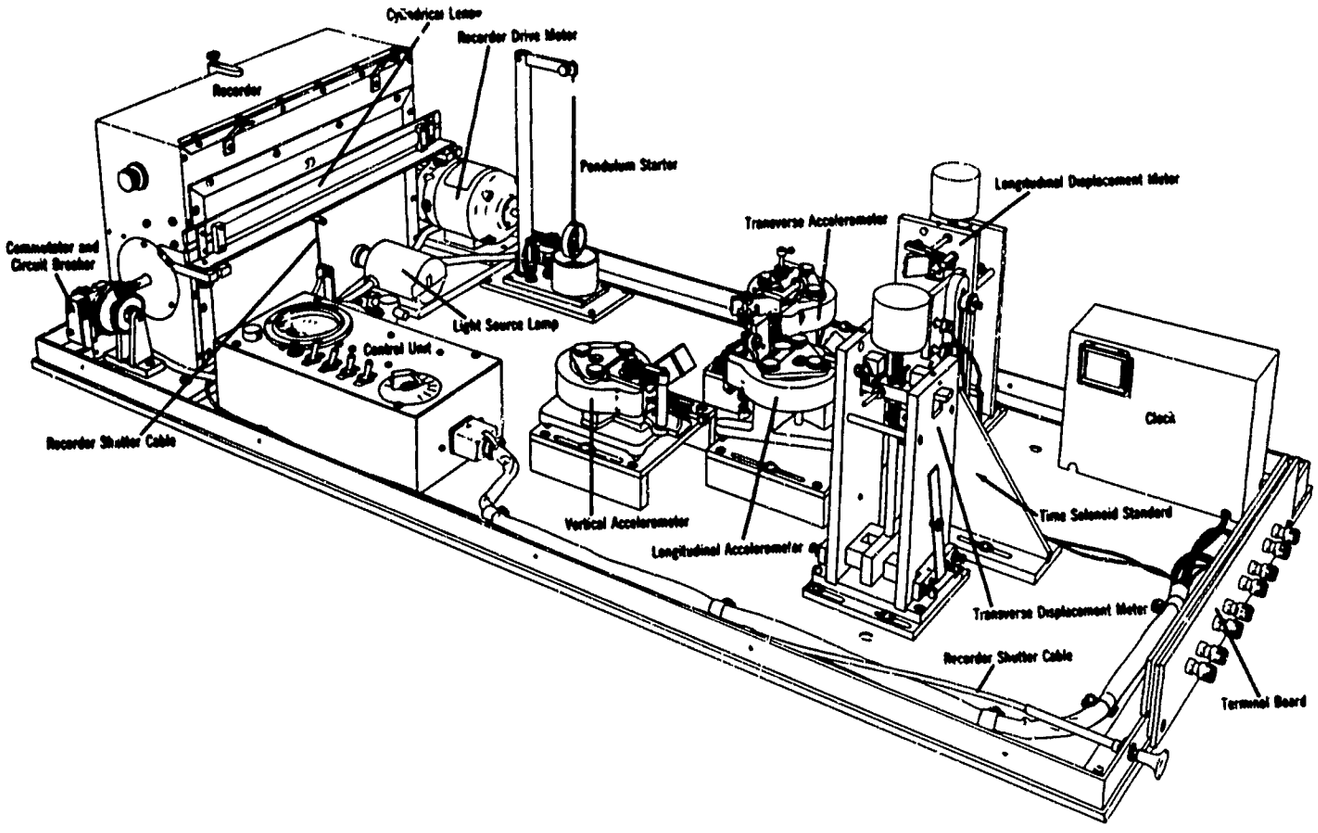

Figure 3.2 Coast and Geodetic Survey Accelerograph showing three components of accelerometers and two horizontal Carder Displacement Meters.

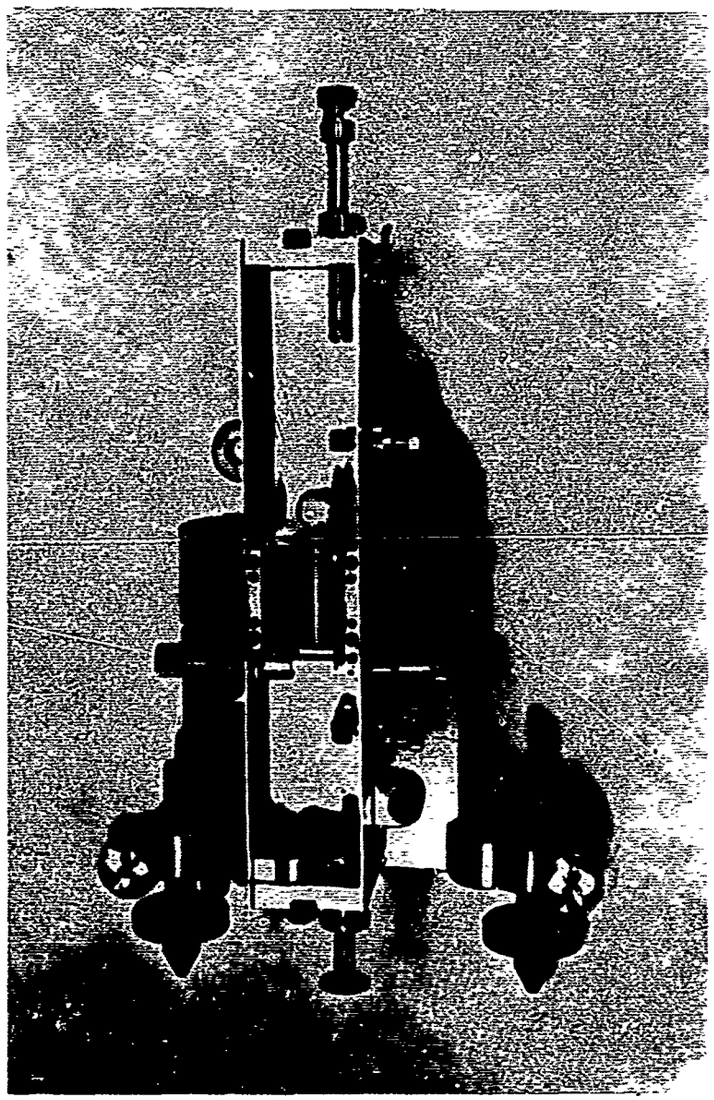

Figure 3.3 Coast Survey Vibration Meter with front cover removed to show torsion fiber suspension system.

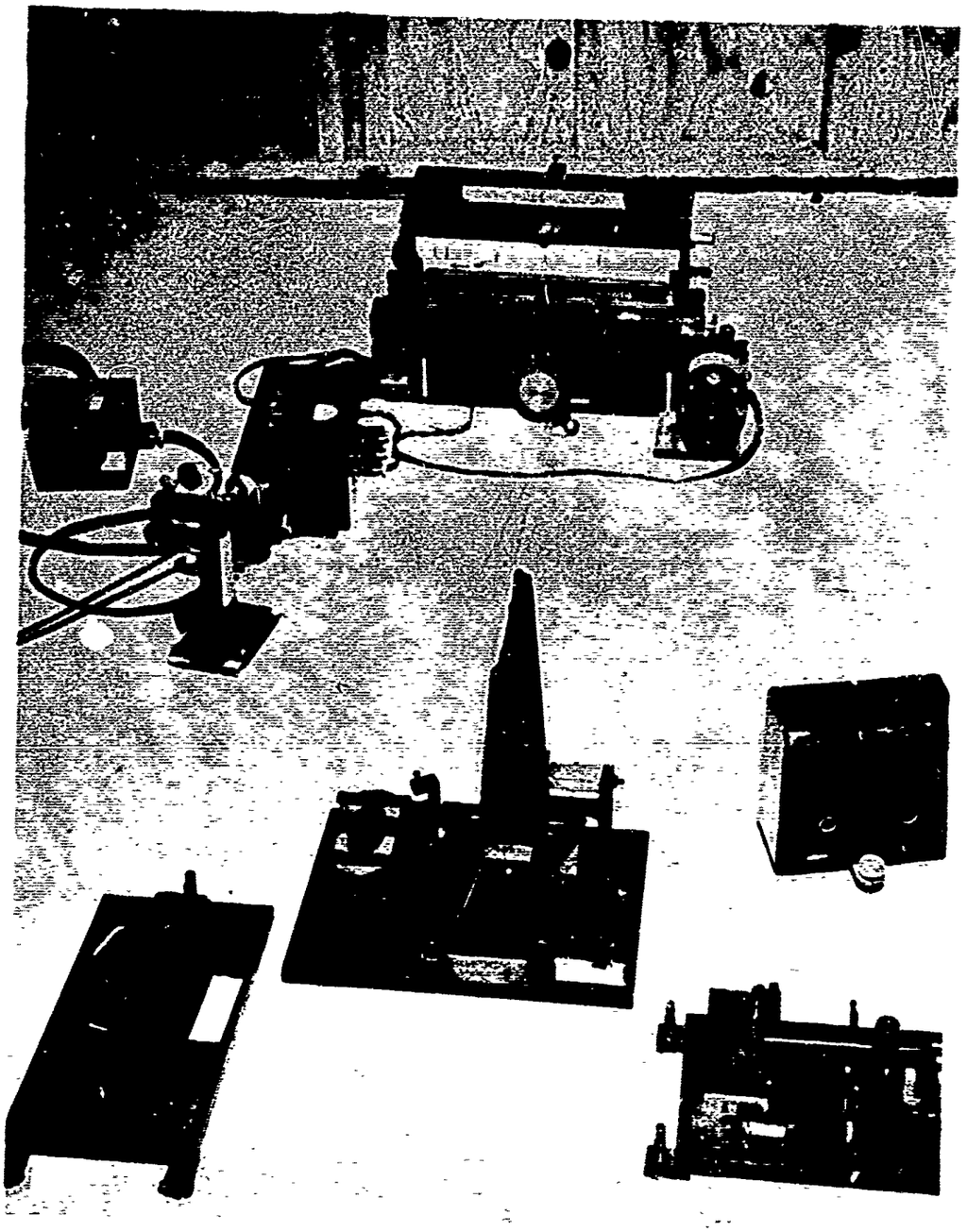

Figure 3.4 Typical Strong-Motion Station with three components of Carder Vibration Meters. Recorder in background with radial, vertical and transverse seismometers in foreground from left to right.

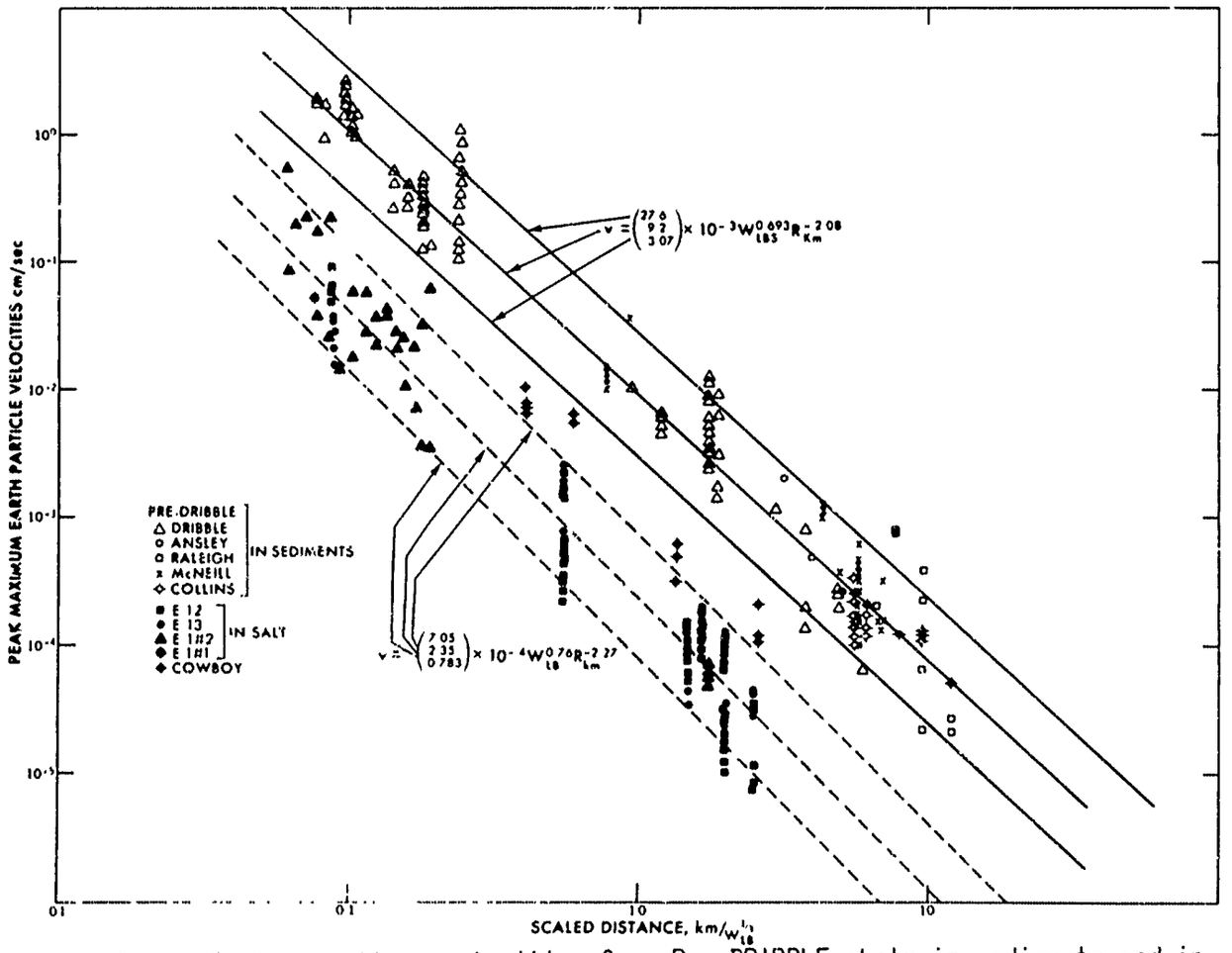

Figure 4.1 Scaled particle velocities from Pre-DRIBBLE shots in sediments and in the Tatum Salt Dome, vertical components.

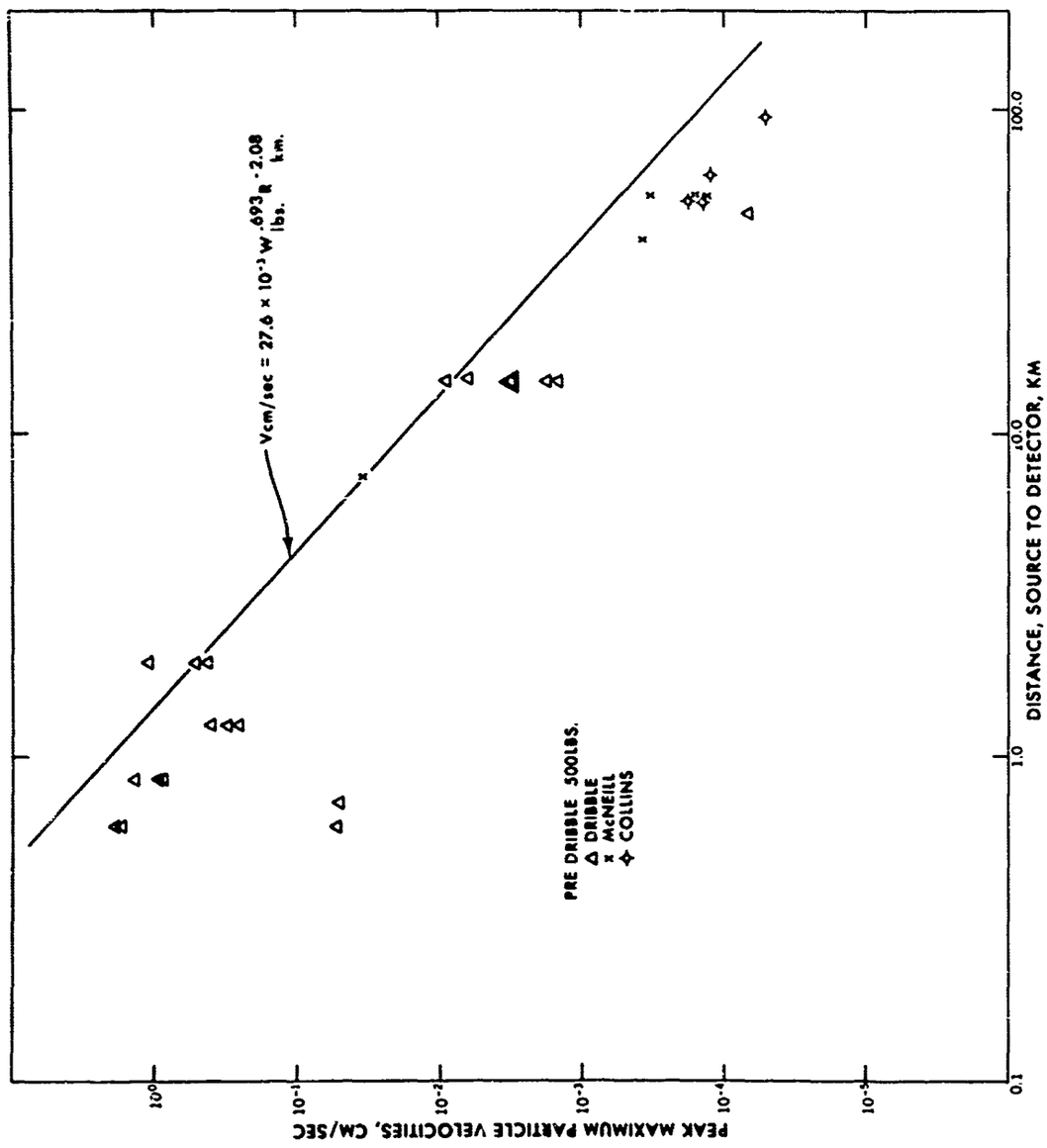

Figure 4.2 Pre-DRIBBLE.particle velocities versus distance for 500 lb TNT shots in sediments at DRIBBLE, McNeill, and Collins, Mississippi, vertical comoonents.

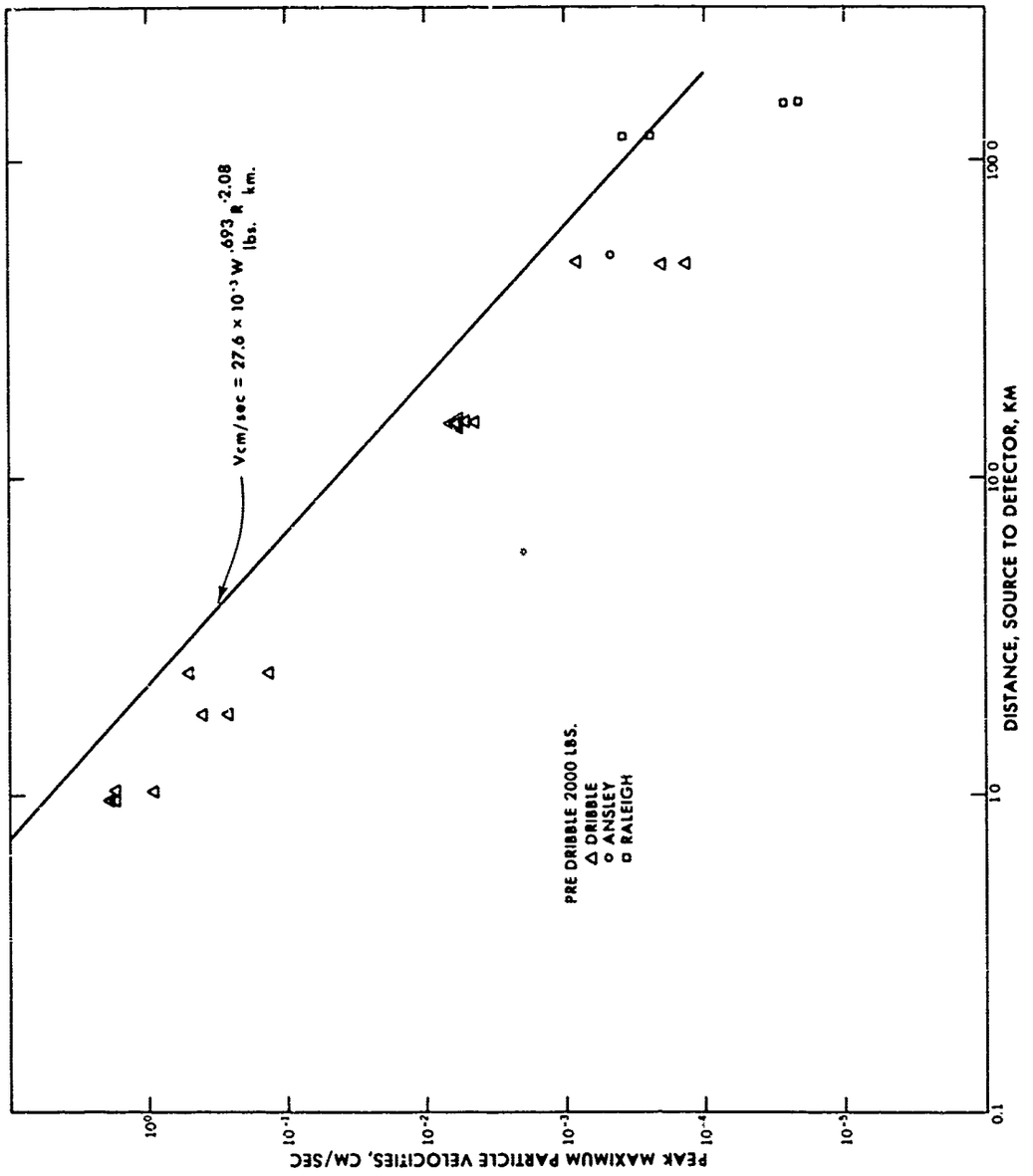

Figure 4.3 Pre-DRIBBLE particle velocities versus distance for 2000 lb TNT shots in sediments at DRIBBLE, Ansley, and Raleigh, Mississippi, vertical components.

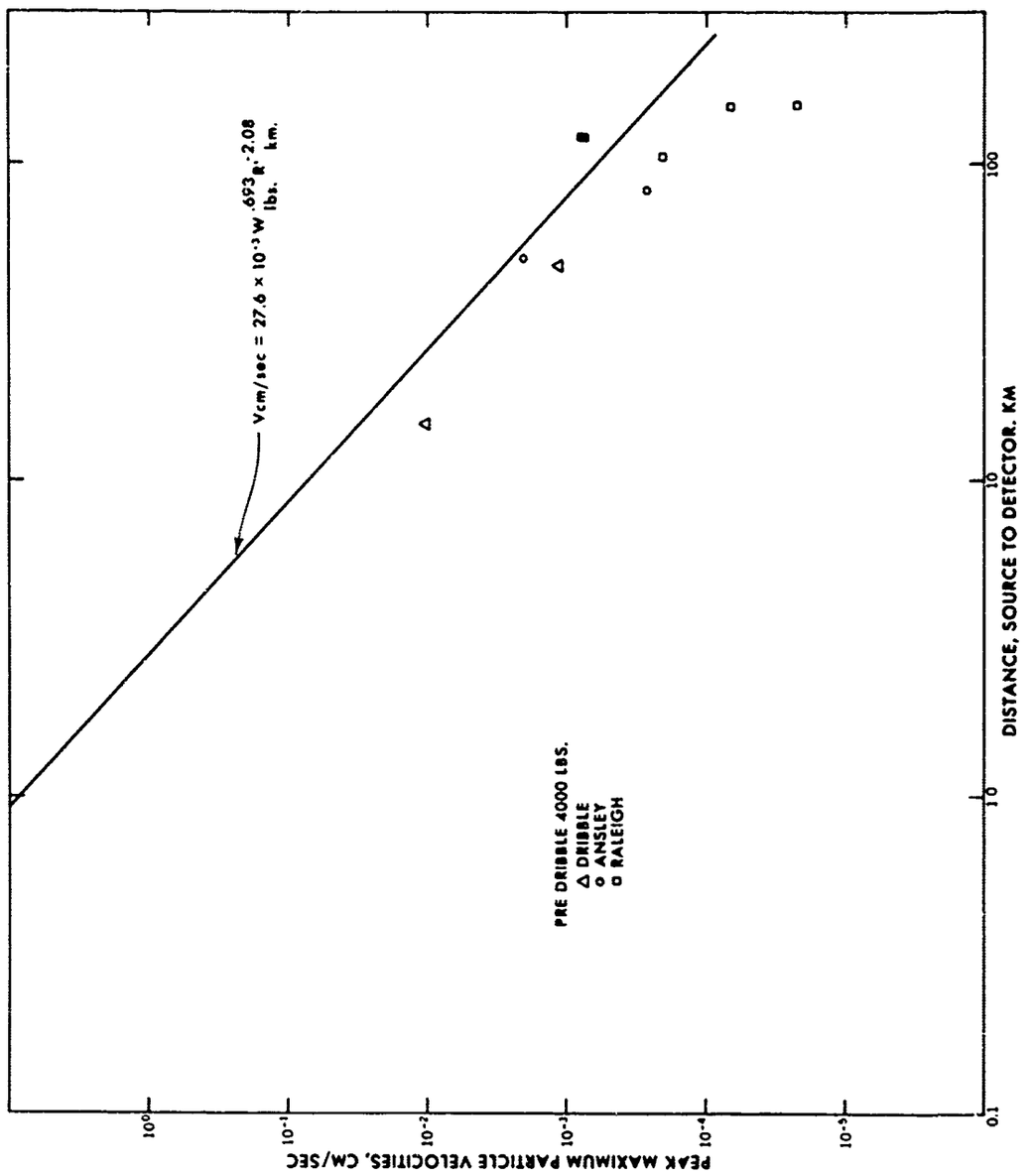

Figure 4.4 Pre-DRIBBLE particle velocity versus distance for 4000 lb TNT shots in sediments at DRIBBLE, Ansley, and Raleigh, Mississipoi, vertical comoonents.

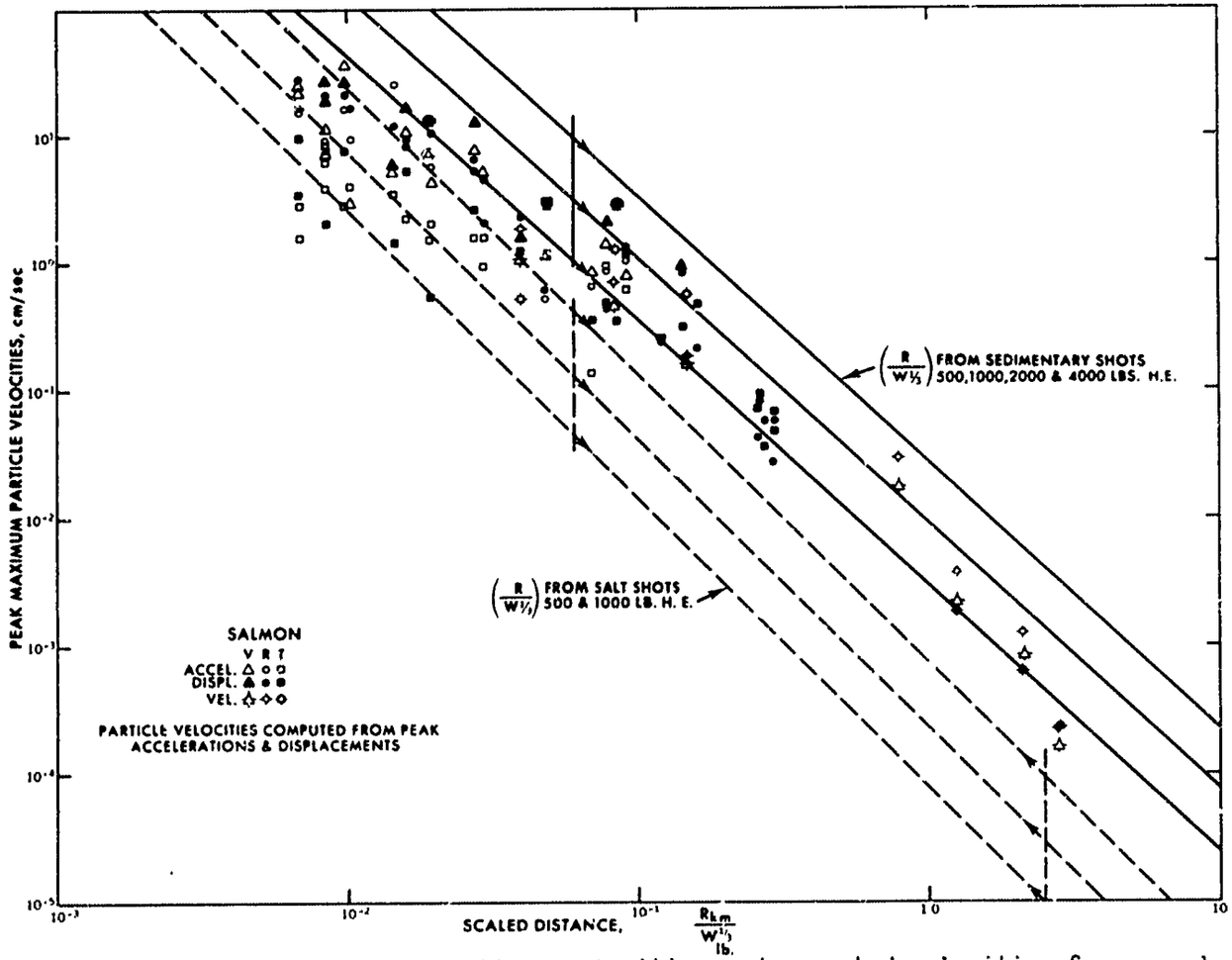

Figure 4.5 SALMON measured particle velocities and computed velocities from accelerations and displacements versus cube root scaled distance. The upper group of three lines are the mean and envelope of the Pre-DRIBBLE sedimentary shots. The lower group of three lines are the mean and envelope of the Pre-DRIBBLE salt dome shots.

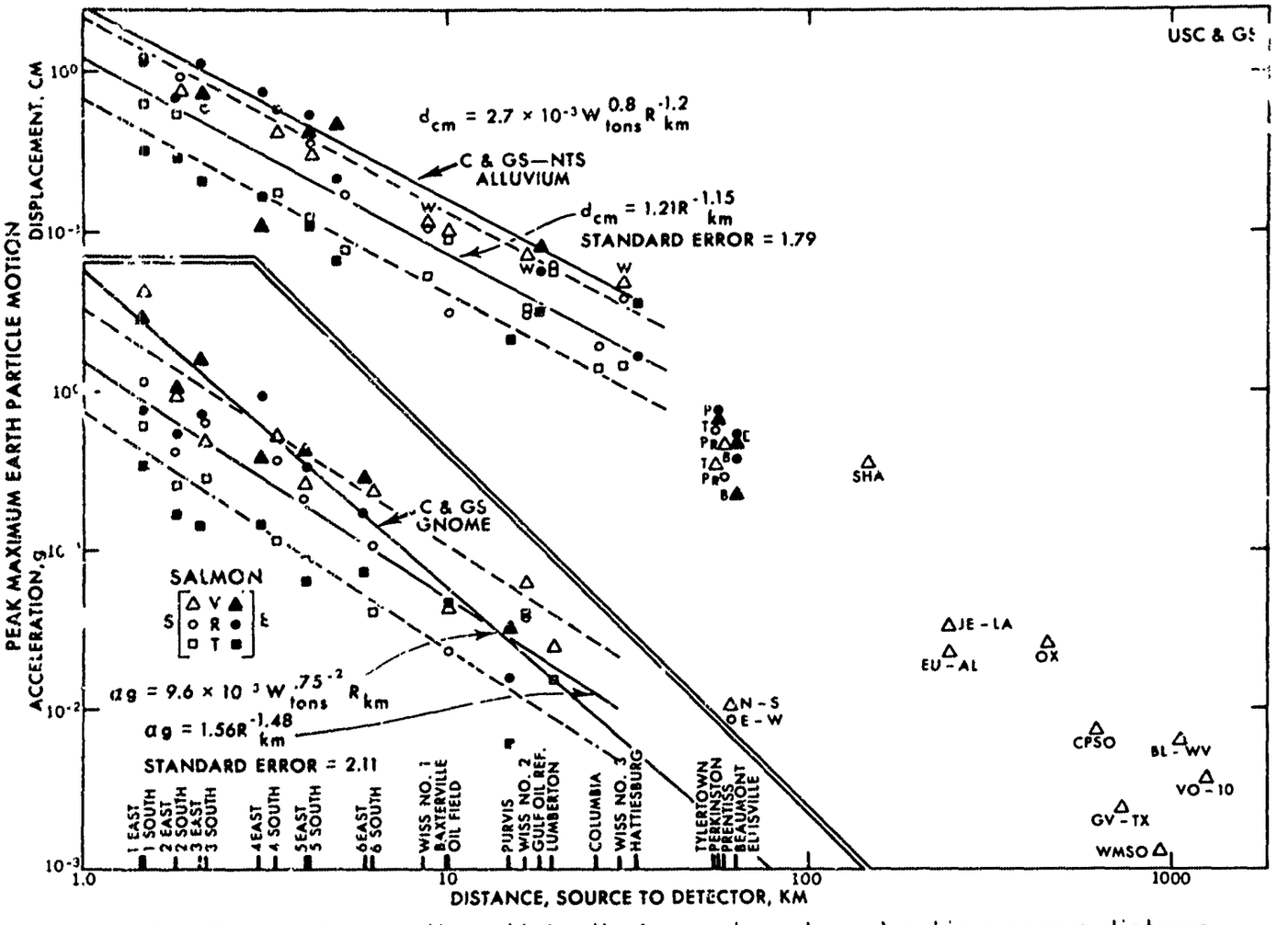

Figure 4.6 Peak maximum earth particle displacements and accelerations versus distance for SALMON.

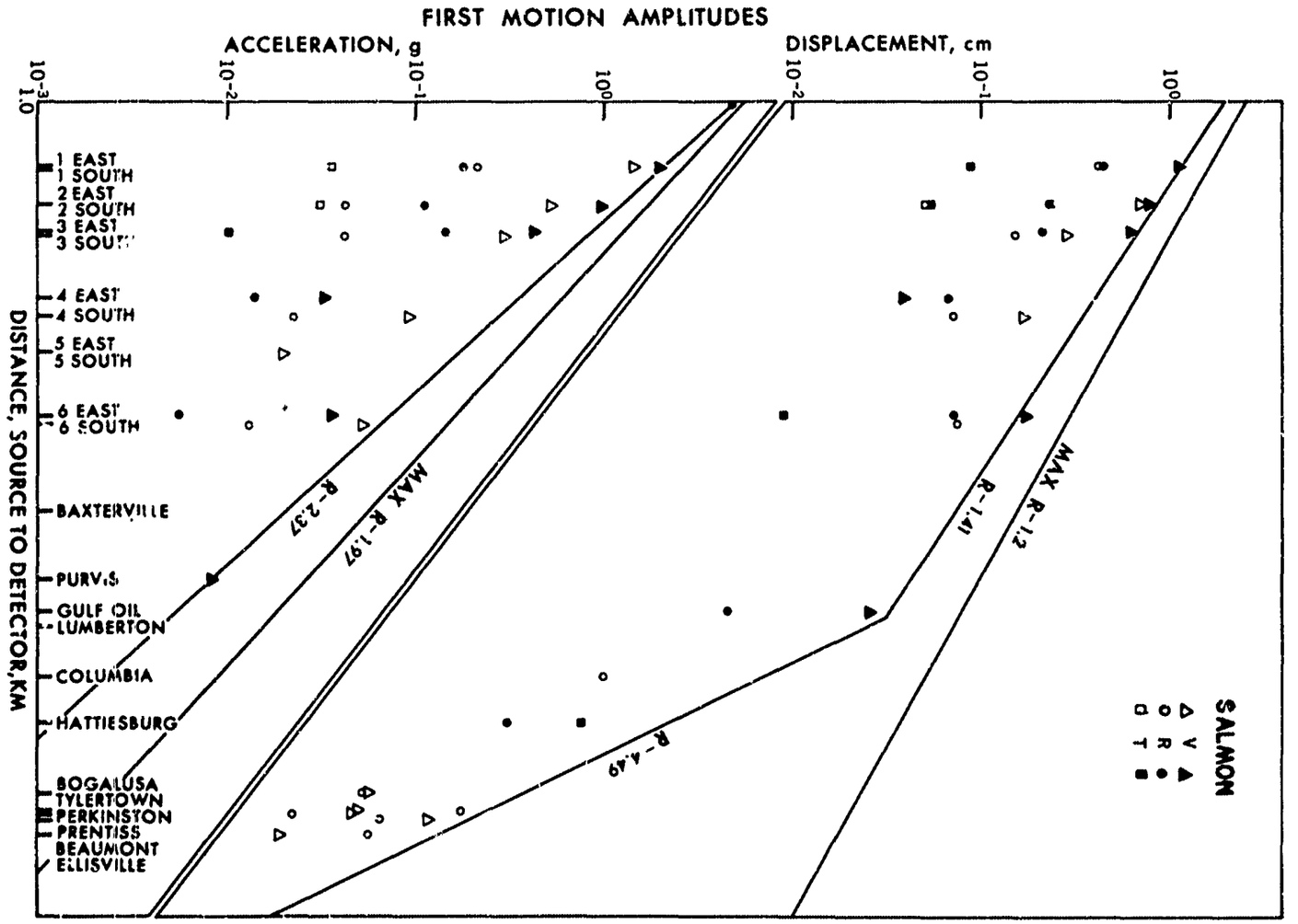

Figure 4.7 First motion amplitudes for displacements and accelerations versus distance.

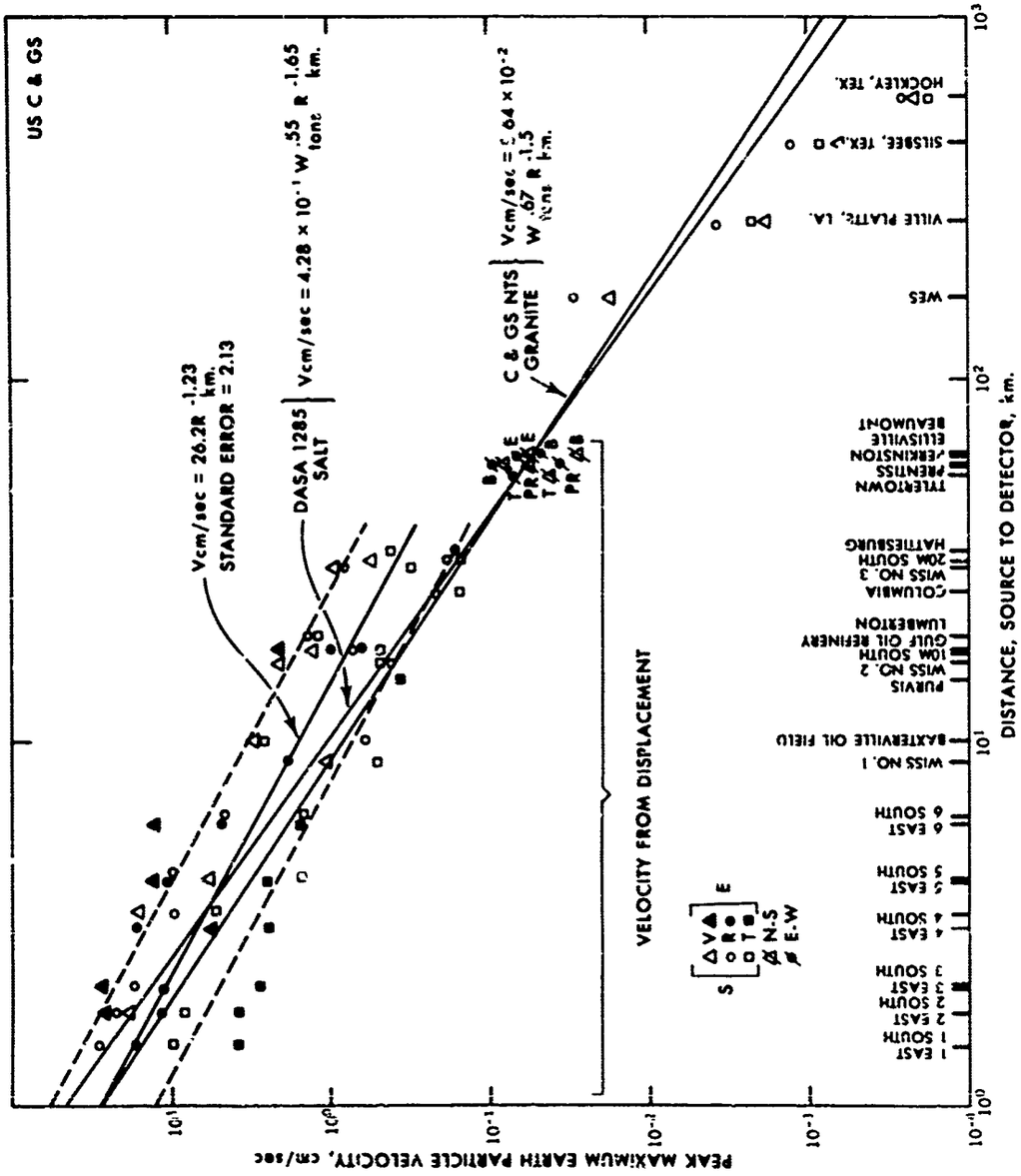

Figure 4.8 Peak maximum recorded velocities and computed velocities from displacement versus distance.

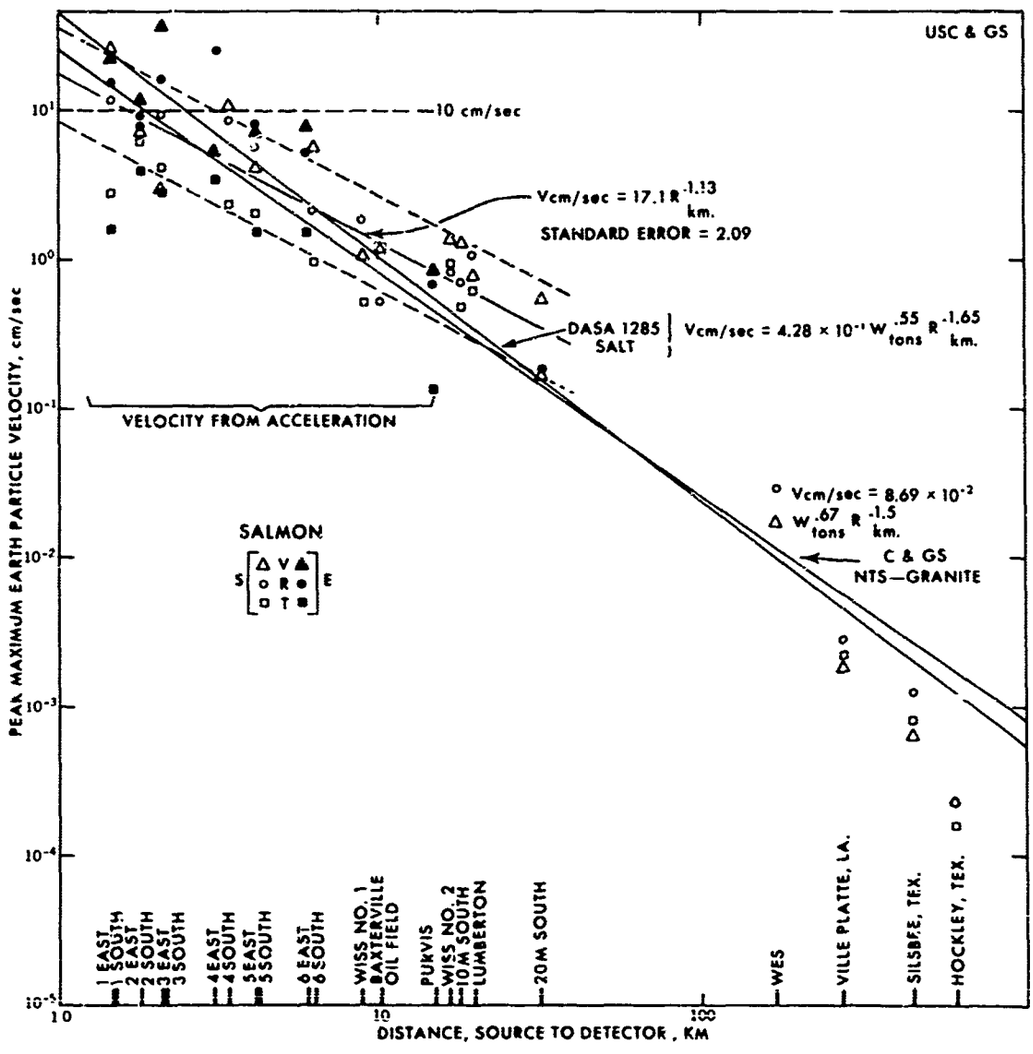

Figure 4.9 Peak maximum recorded velocities and computed velocities from acceleration versus distance.

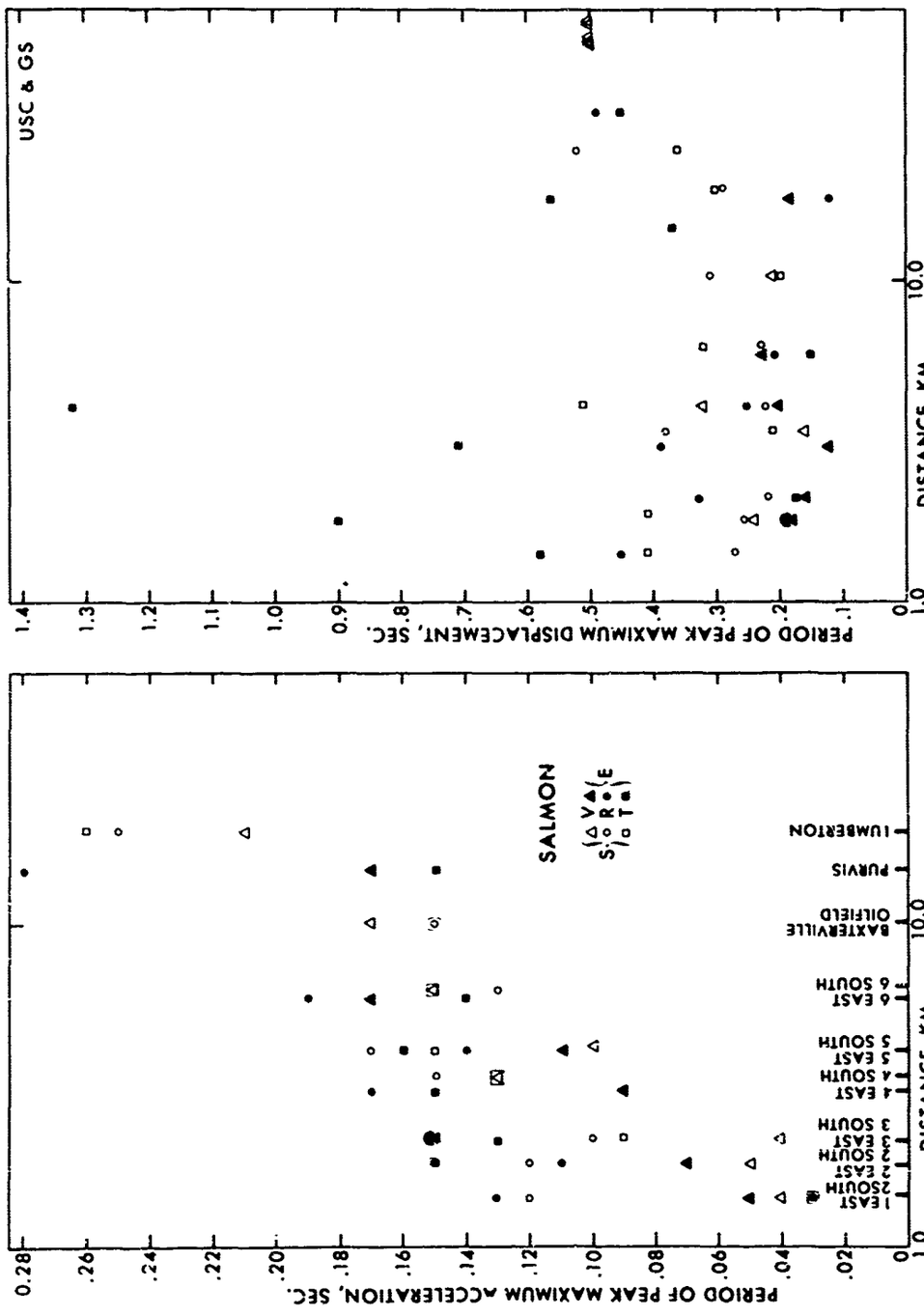

Figure 4.10 Period of peak maximum accelerations and displacements versus distance.

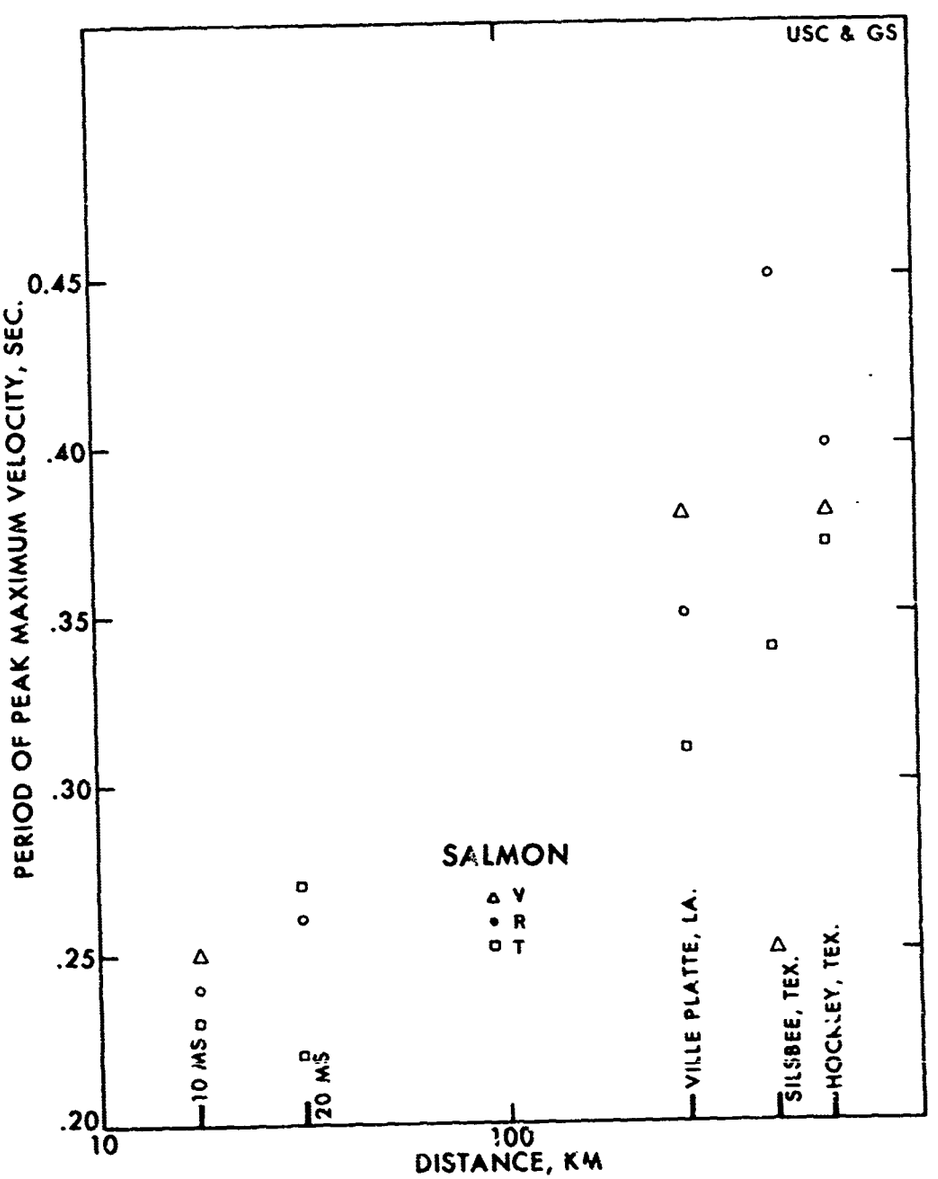

Figure 4.11 Period of peak maximum velocities versus distance.

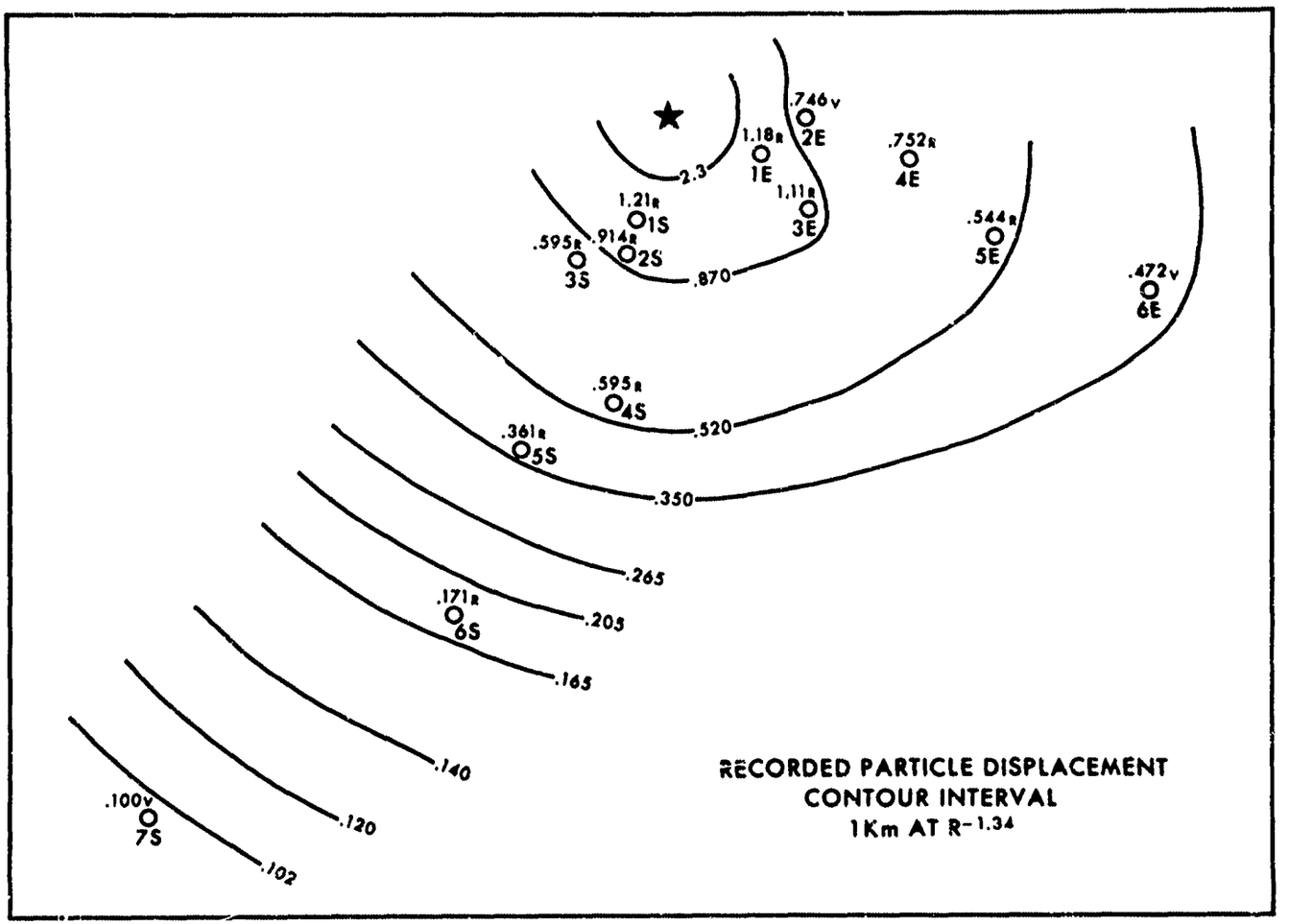

Figure 4.12 Contoured maximum displacements from surface zero to 10 km with 1 km contour interval assuming attenuation of $R^{-1.34}$.

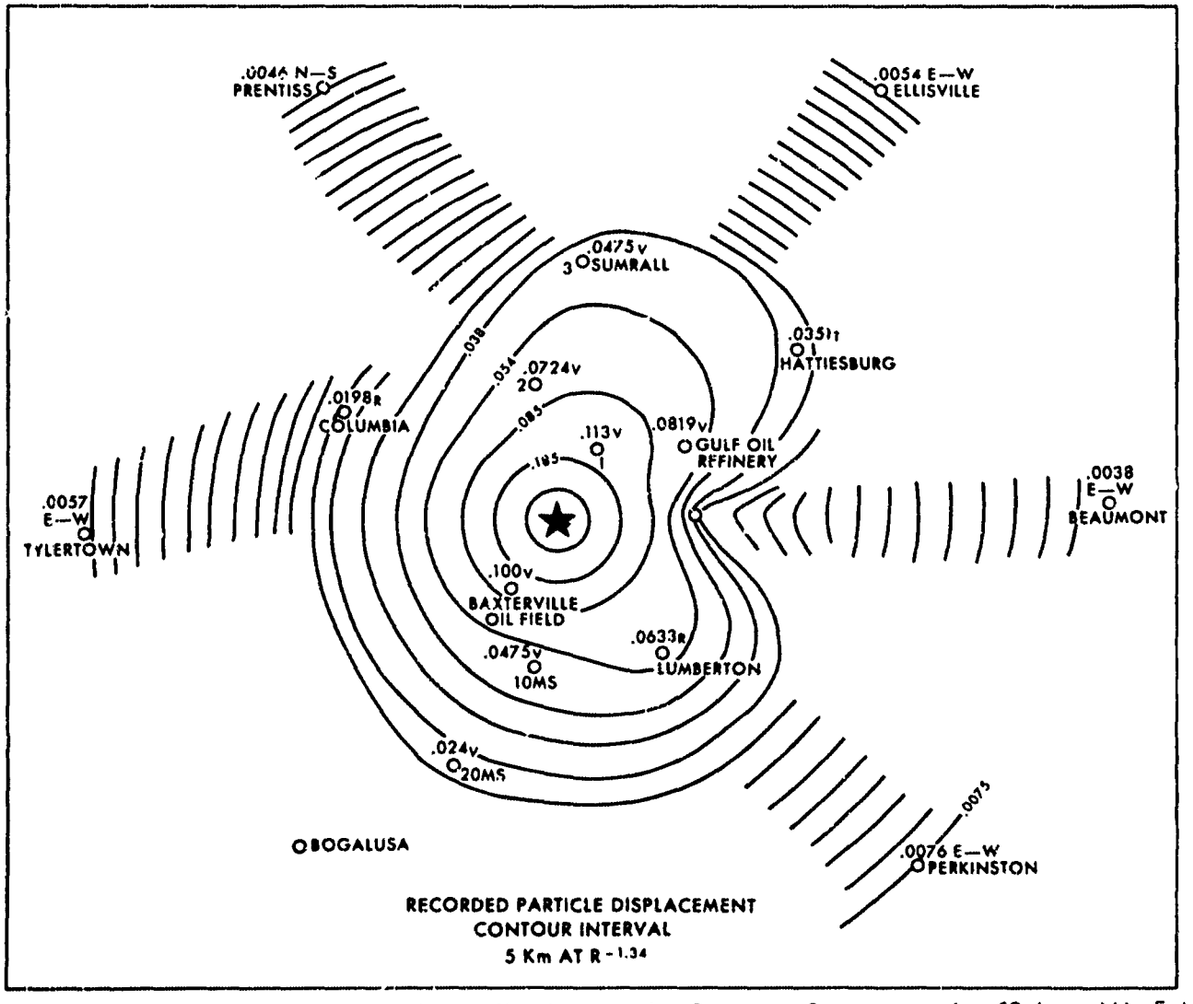

Figure 4.13 Contoured maximum displacements from surface zero to 63 km with 5 km contour interval assuming attenuation of $R^{-1.34}$.

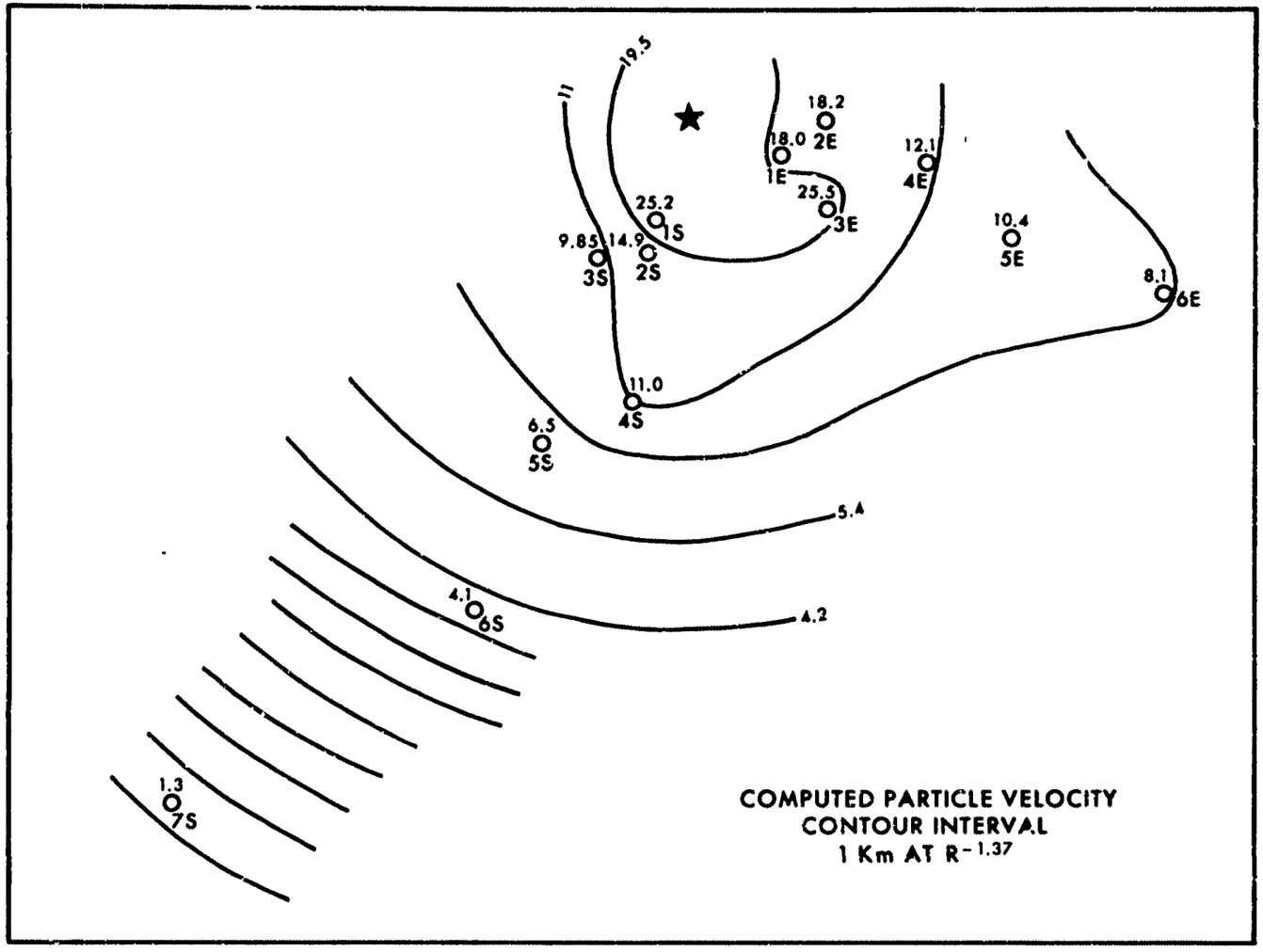

Figure 4.14 Contoured maximum velocities from surface zero to 10 km with 1 km contour interval assuming attenuation of $R^{-1.37}$. Plotted values are the averages of the vertical and radial components of computed particle velocity.

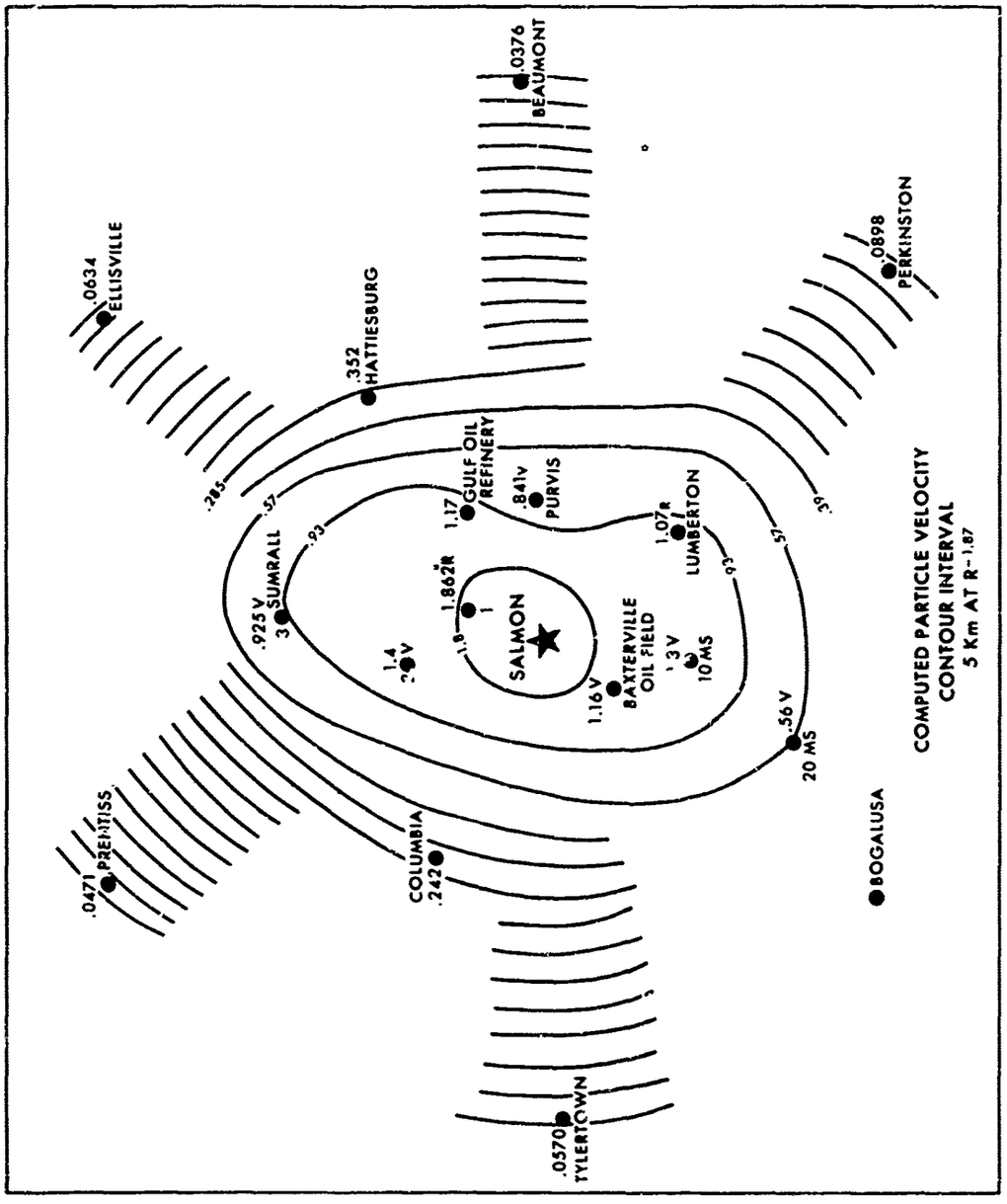

Figure 4.15 Contoured maximum velocities from surface zero to 63 km with 5 km contour interval assuming attenuation of $R^{-1.87}$. See text for identification of components plotted.

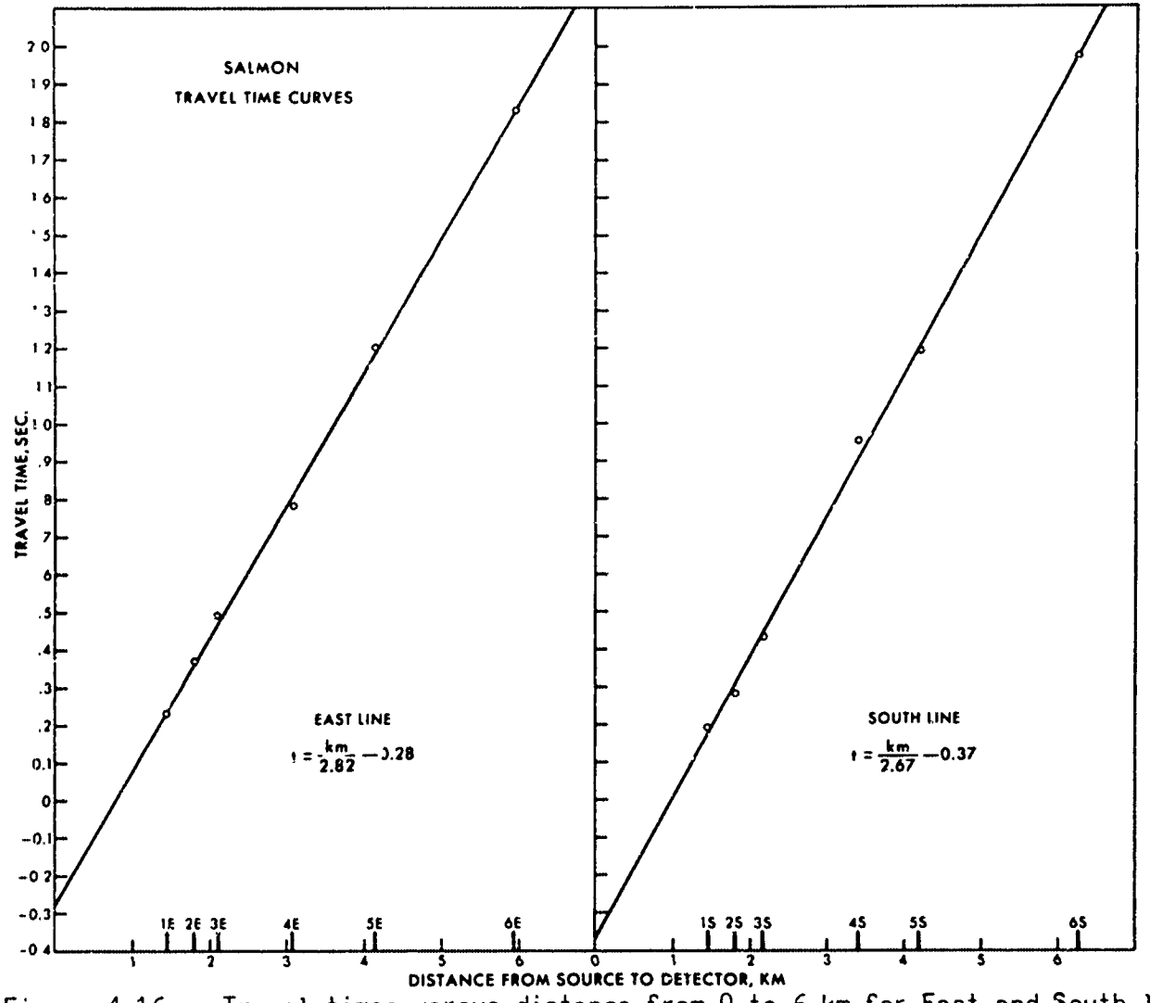

Figure 4.16 Travel times versus distance from 0 to 6 km for East and South lines.

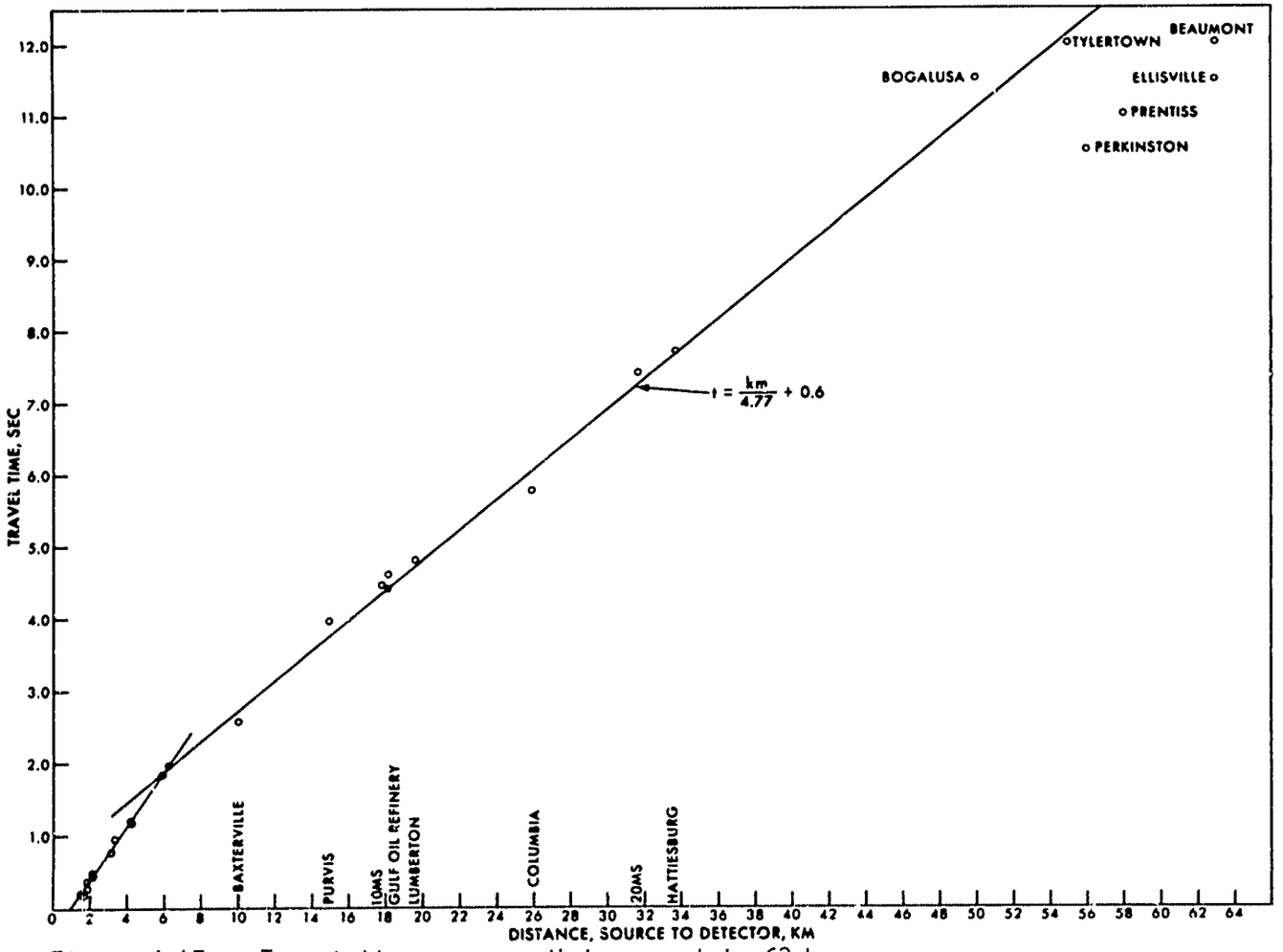

Figure 4.17 Travel times versus distance out to 63 km.

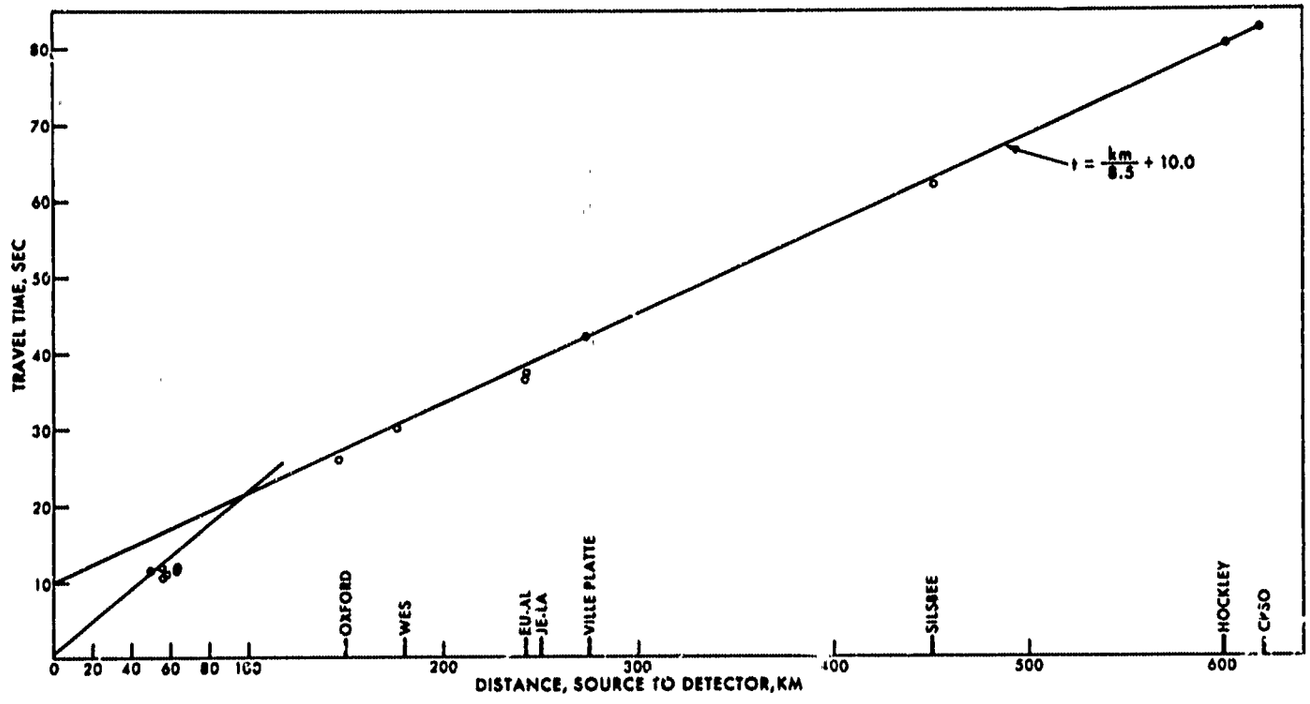

Figure 4.18 Travel times versus distance out to 610 km.

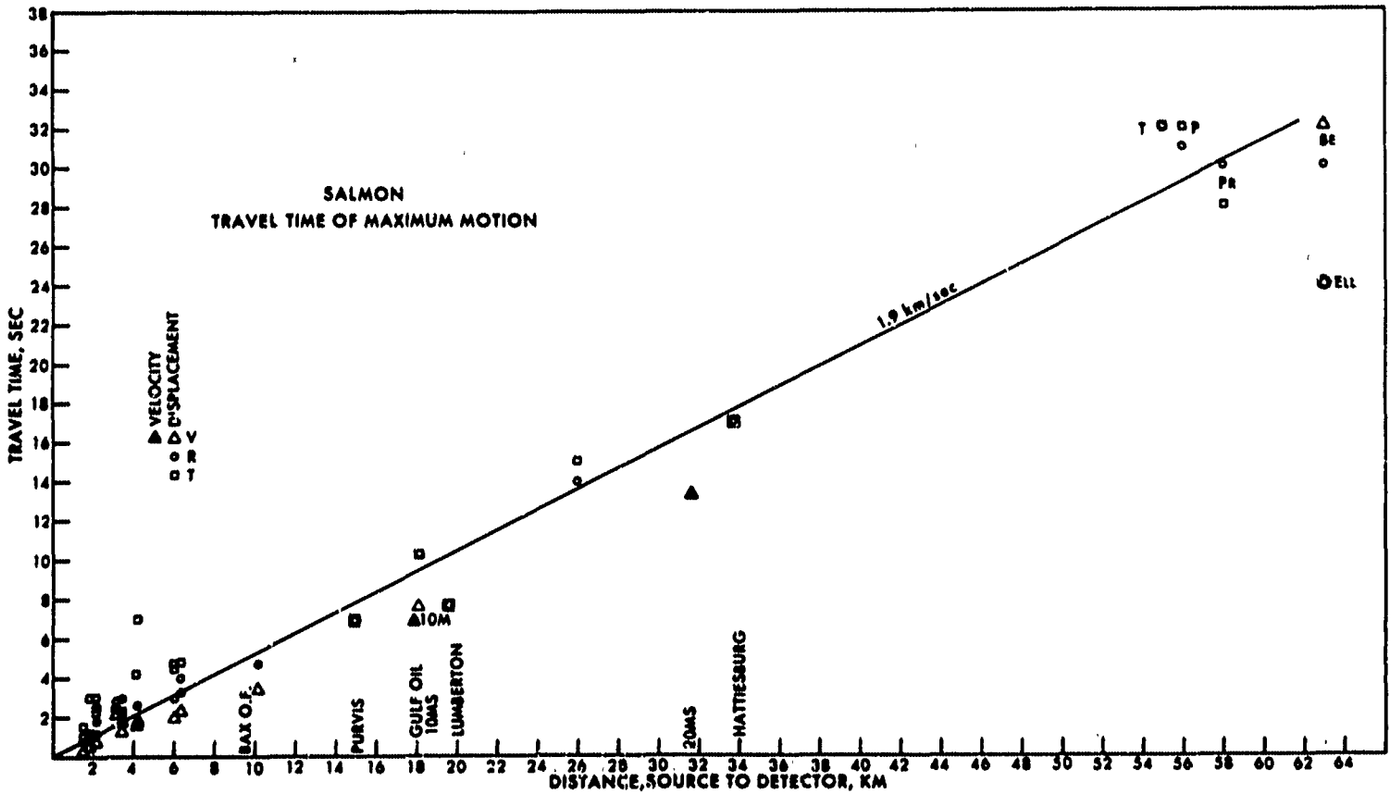

Figure 4.19 Travel times of maximum motion versus distance out to 63 km.

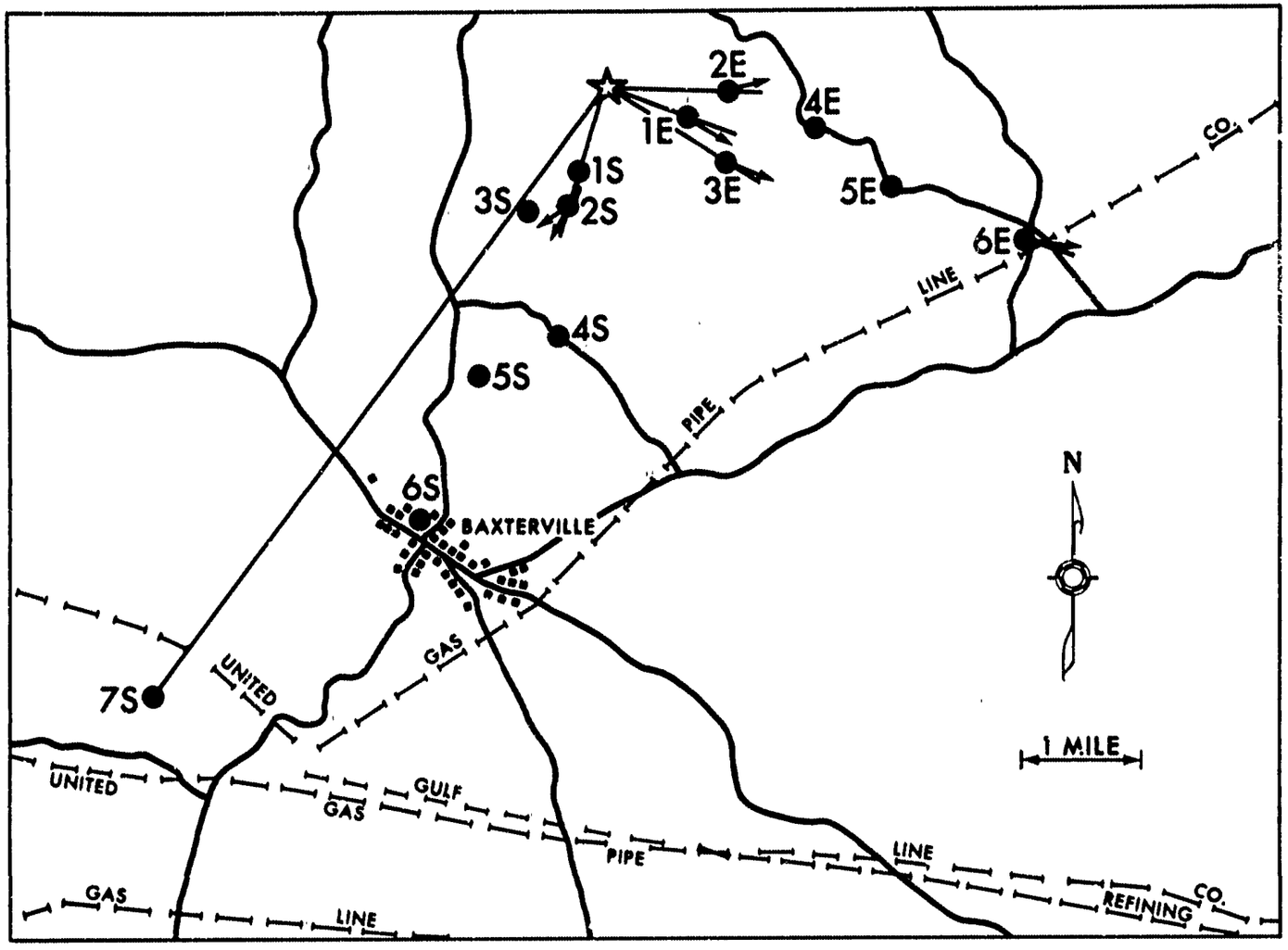

Figure 4.20 Strong-motion station location map showing horizontal resultant vectors.

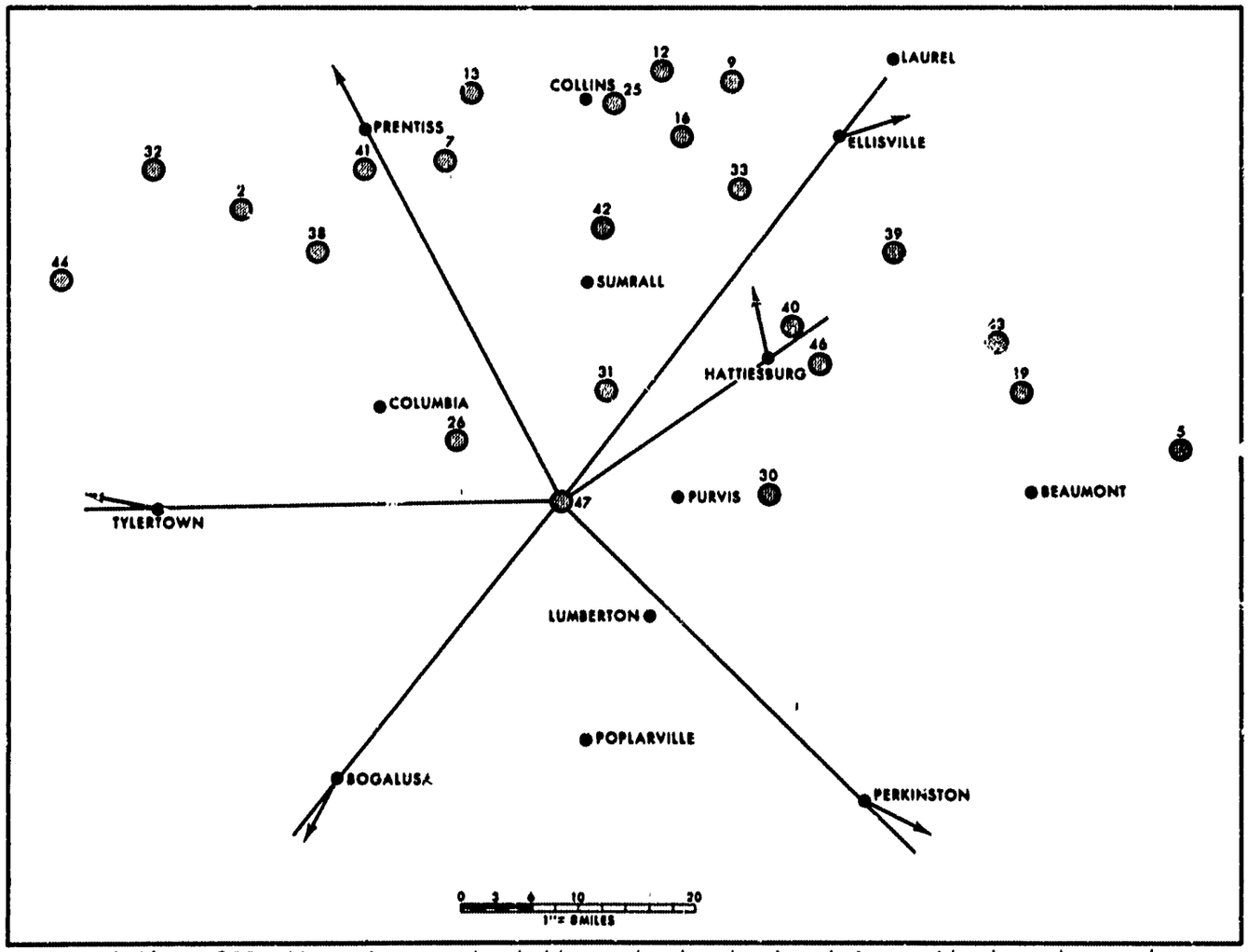

Figure 4.21 Off-site seismograph stations showing horizontal resultant vectors. Large circles are known salt domes with index numbers as explained in Table 4.3.

APPENDIX A

SELECTED SEISMOGRAMS

SALMON EVENT

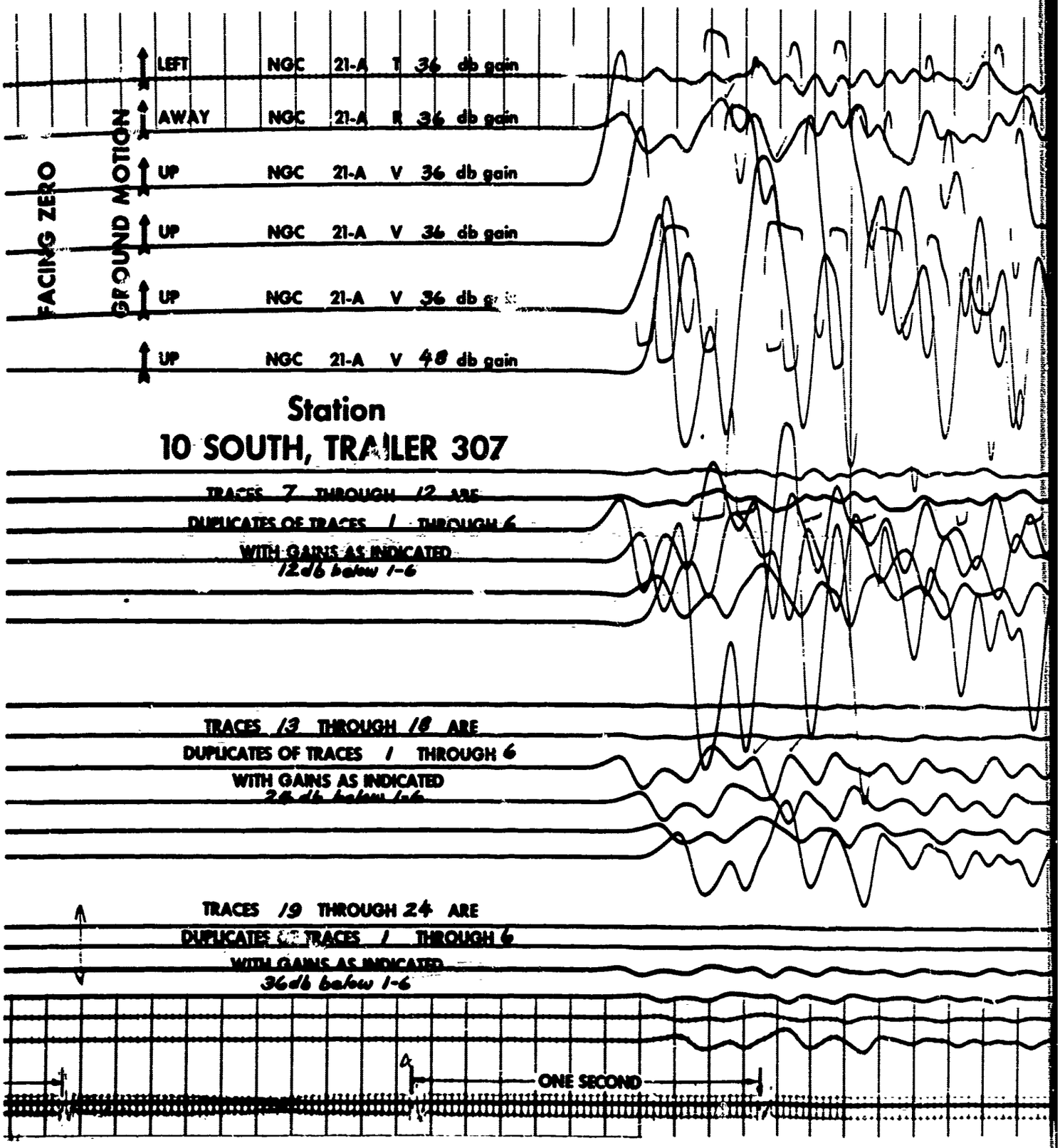
FACING ZERO
GROUND MOTION
LEFT NGC 21-A T 36 db gain
AWAY NGC 21-A R 36 db gain
UP NGC 21-A V 36 db gain
UP NGC 21-A V 36 db gain
UP NGC 21-A V 36 db gain
UP NGC 21-A V 48 db gain
Station
10 SOUTH, TRAILER 307
TRACES 7 THROUGH 12 ARE
DUPLICATES OF TRACES 1 THROUGH 6
WITH GAINS AS INDICATED
12db below 1-6
TRACES 13 THROUGH 18 ARE
DUPLICATES OF TRACES 1 THROUGH 6
WITH GAINS AS INDICATED
24 db below 1-6
TRACES 19 THROUGH 24 ARE
DUPLICATES OF TRACES 1 THROUGH 6
WITH GAINS AS INDICATED
36db below 1-6
ONE SECOND

A

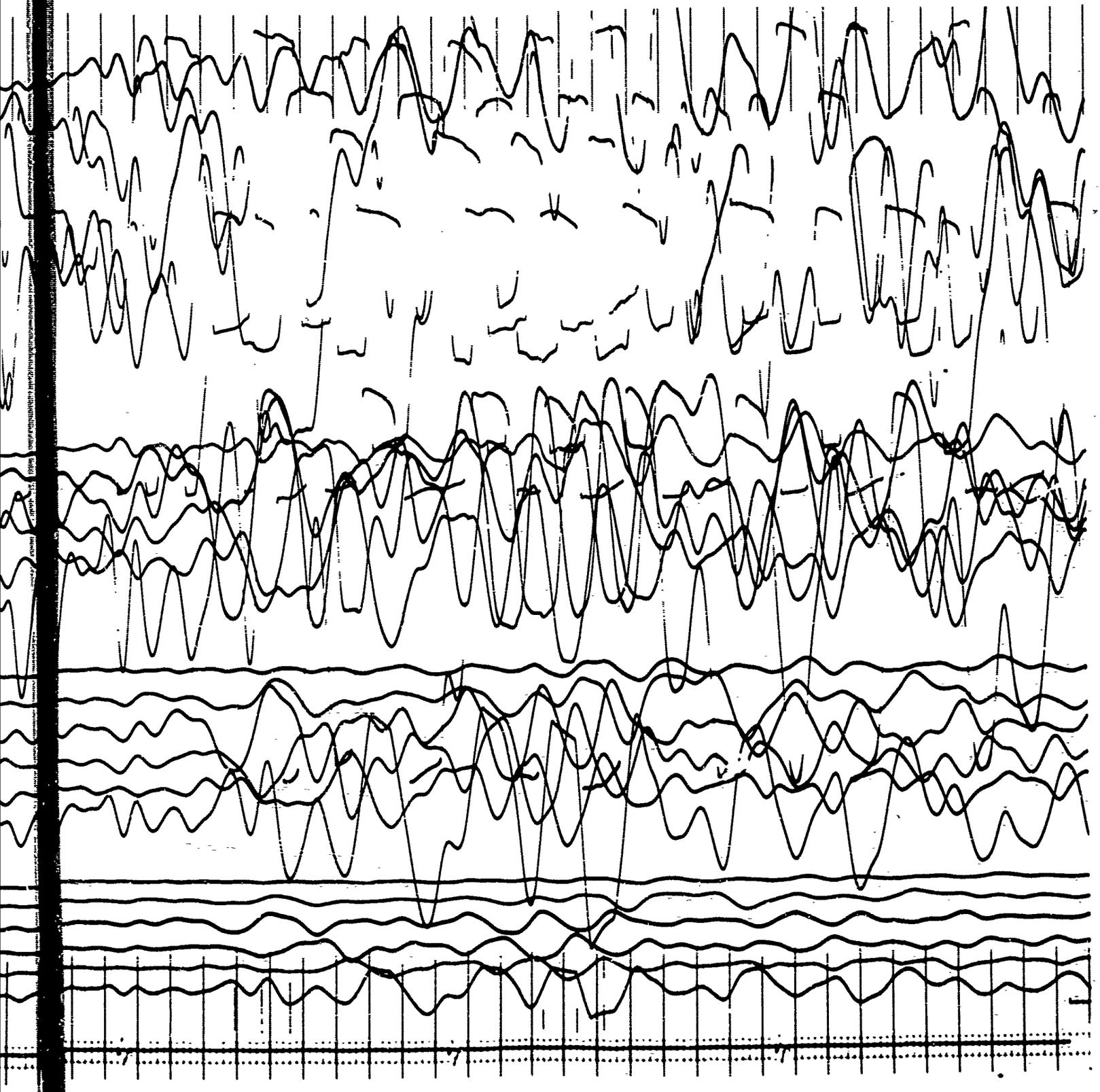

A-3

B

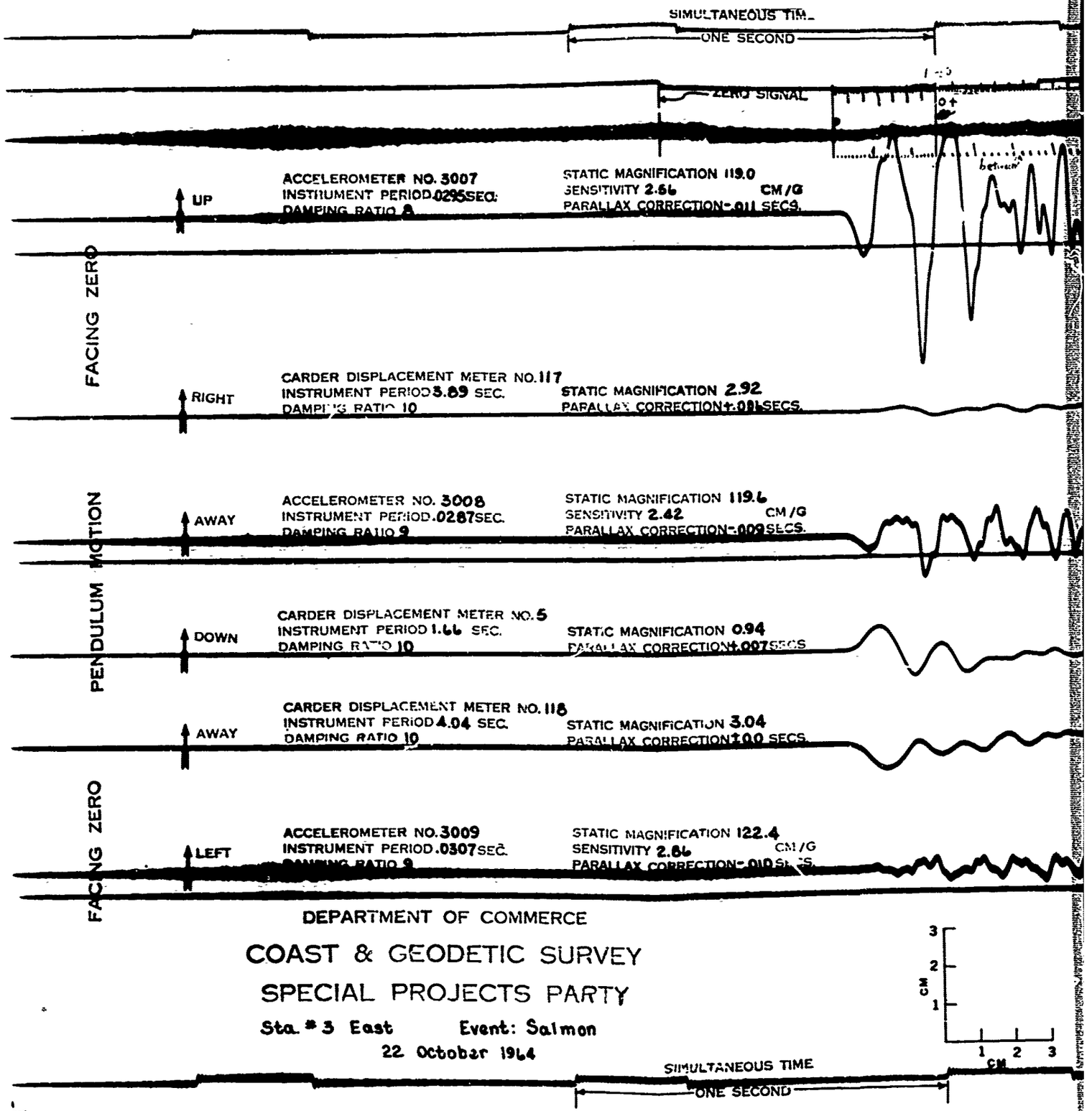
SIMULTANEOUS TIME
ONE SECOND
ZERO SIGNAL
FACING ZERO
UP
ACCELEROMETER NO. 3007
INSTRUMENT PERIOD .0295 SEC.
DAMPING RATIO .8
STATIC MAGNIFICATION 119.0
SENSITIVITY 2.56 CM/G
PARALLAX CORRECTION -.011 SECS.
RIGHT
CARDER DISPLACEMENT METER NO. 117
INSTRUMENT PERIOD 3.89 SEC.
DAMPING RATIO 10
STATIC MAGNIFICATION 2.92
PARALLAX CORRECTION +.001 SECS.
PENDULUM MOTION
AWAY
ACCELEROMETER NO. 3008
INSTRUMENT PERIOD .0287 SEC.
DAMPING RATIO .9
STATIC MAGNIFICATION 119.6
SENSITIVITY 2.42 CM/G
PARALLAX CORRECTION -.009 SECS.
DOWN
CARDER DISPLACEMENT METER NO. 5
INSTRUMENT PERIOD 1.66 SEC.
DAMPING RATIO 10
STATIC MAGNIFICATION 0.94
PARALLAX CORRECTION +.007 SECS.
AWAY
CARDER DISPLACEMENT METER NO. 118
INSTRUMENT PERIOD 4.04 SEC.
DAMPING RATIO 10
STATIC MAGNIFICATION 3.04
PARALLAX CORRECTION +.00 SECS.
FACING ZERO
LEFT
ACCELEROMETER NO. 3009
INSTRUMENT PERIOD .0307 SEC.
DAMPING RATIO .9
STATIC MAGNIFICATION 122.4
SENSITIVITY 2.86 CM/G
PARALLAX CORRECTION -.010 SECS.
DEPARTMENT OF COMMERCE
COAST & GEODETIC SURVEY
SPECIAL PROJECTS PARTY
Sta. #3 East Event: Salmon
22 October 1964
CM
3
2
1
1 2 3
CM
SIMULTANEOUS TIME
ONE SECOND

A

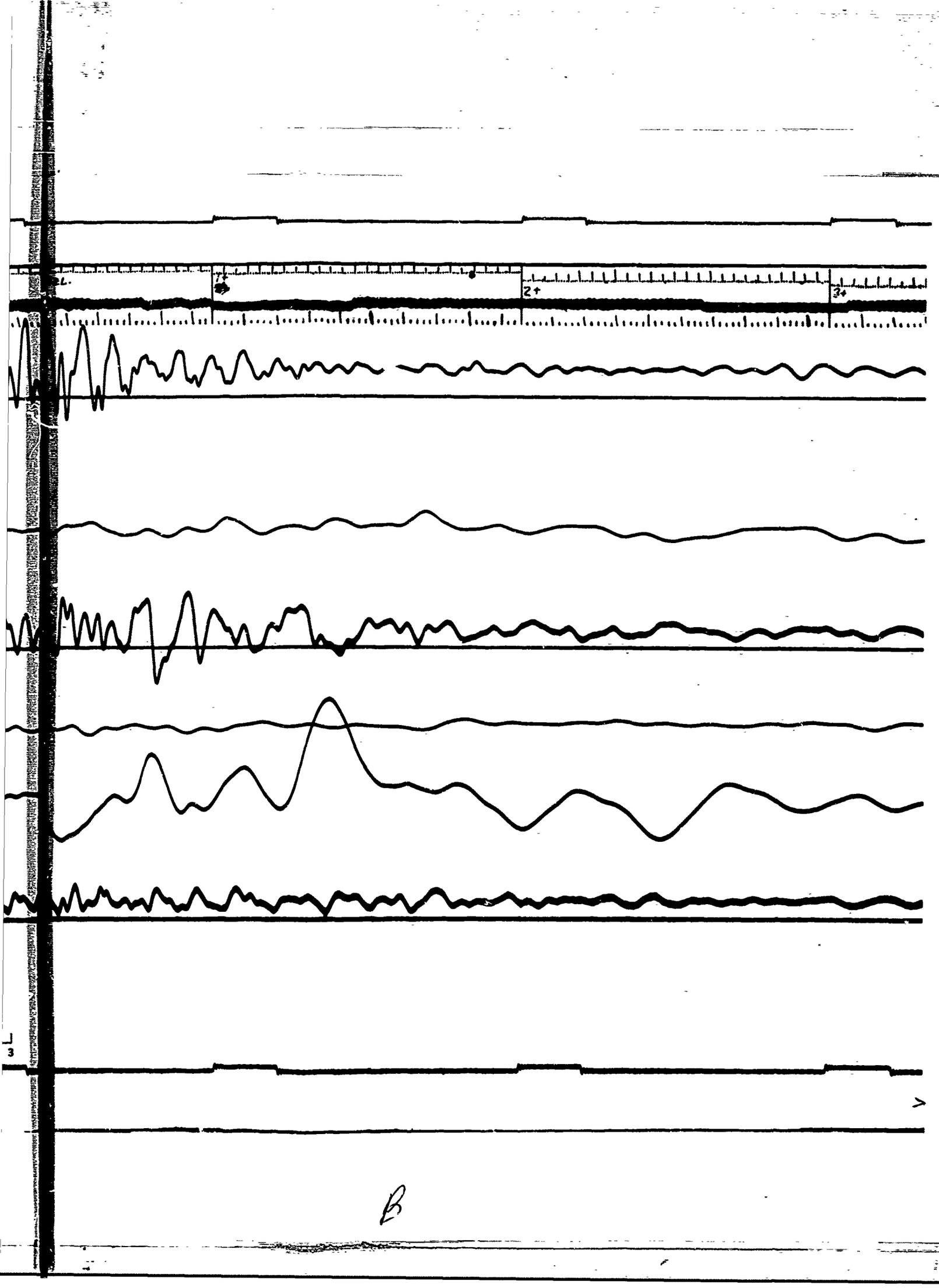

B

APPENDIX B

A STUDY OF THE LONG PERIOD MOTIONS OBSERVED AT HATTIESBURG AND COLUMBIA FROM EVENT SALMON

by

Thomas R. Shugart

The U.S. Coast and Geodetic Survey recorded ground vibrations from Event SALMON at the AEC Warehouse in Hattiesburg, Mississippi, and at the National Guard Armory in Columbia, Mississippi. The instruments used were C&GS Vibration Meters. The radial and transverse horizontal components of motion were recorded at both stations. The purpose of this report is to describe and to attempt to explain certain anomalous features of the seismograms from these stations.

INSTRUMENTATION

The C&GS Vibration Meter is a damped torsion pendulum whose magnification is achieved by means of an optical lever. The natural undamped periods were set near 4.5 seconds and the damping ratios were 10. The

frequency response is nearly flat for displacement at periods shorter than 4.5 seconds up to the highest frequencies seen on the records (about 10 cps). The response is nearly flat for acceleration for periods from 4.5 seconds to infinity. The sensitivity of the instrument to tilt (rotation about a horizontal axis) is about 3.2 mm of trace deflection per second of arc at periods from 4.5 seconds to infinity. The amplitude and phase response characteristic for small angles of tilt is identical to that for acceleration.

At both stations the instruments were installed on the floor of a one-story building. In both cases the floor was a concrete slab resting on the ground.

DESCRIPTION OF SEISMOGRAMS

The seismograms written at Hattiesburg and Columbia were of excellent quality and the amplitudes recorded were in good agreement with predictions. An anomalous long period motion was, however, observed on both components at Hattiesburg, and on the transverse component at Columbia. At Hattiesburg, the

seismograph traces moved away from their baselines in phase at about T+15 seconds (T being the time of detonation) to T+18 seconds, then gradually returned to their baselines leveling out at about T+26 seconds without overshoot. The magnitude of this drift on the traces was of the same order as the amplitude of the higher frequency vibrations which were superimposed.

In the case of the transverse component at Columbia the trace began to drift at the time of first motion (T+7.5 seconds) and reached its maximum displacement at T+13 seconds. It then returned to the baseline and overshot somewhat for about 5 seconds and then leveled out, vibrating about the original baseline after T+20 seconds. In the radial component at Columbia, the drift was so small that it was masked by the superimposed vibrations.

These instruments have been used to record from underground nuclear shots on many previous occasions, but the anomalous recordings described above have not been observed before.

ANALYSIS

The following possible explanations have been suggested to account for the anomalous seismograms:

1. A displacement (sliding or slumping) of the local ground surface at the station, triggered by the vibration from the shot.
2. Translational motion of a low frequency seismic wave originating at the source.
3. An instrument malfunction.
4. A tilting of the instrument base due to people moving around it or due to traffic outside the building in which it was housed.
5. A tilting of the ground surface due to local slumping.
6. A tilting of the ground surface due to a traveling seismic wave of some sort.

The first two possibilities would presume that the trace motion was produced by some horizontal

translation of the instrument frame, permanent or otherwise. These two possibilities may be ruled out at once, since it is easy to show that a simple pendulum with velocity damping will write only a trace which has equal areas above and below the baseline for any transient translation of its frame. (See Attachment B-1.) This condition was not met even approximately by the three anomalous traces.

Although the possibility of an instrument malfunction can never be ruled out with perfect certainty, no one has been able to suggest a cause or mechanism of malfunction which would account for the observed drifting motion of the anomalous traces. Also, the fact that the drifting motion occurred at or near the beginning of the vibration from the shot in both Hattiesburg and Columbia and terminated long before the vibration died away is difficult to reconcile with a malfunction. The record of ground vibration (excluding the drifting) appears to be normal in form and amplitude, which fact would also indicate no malfunction of the instrument.

The possibility of tilting due to people moving around the instrument has been practically eliminated.

The instrument at Columbia was attended by an experienced operator who remained motionless during the recording. At Hattiesburg, the instrument was unattended and was located in a light tight room. Any unauthorized person entering the room during the recording would presumably have caused the photographic recording paper to become fogged.

It is conceivable that a heavy vehicle could have passed slowly near the outside of the building causing the ground surface to tilt. But the probability that this could have happened nearly simultaneously in Hattiesburg and Columbia at just the time when seismic energy from the shot was beginning to arrive,and only at that time, would seem to be vanishingly small.

There is then a high probability that the seismograms actually recorded a shot-associated tilt of the ground surface at the stations and that the translational vibrations were superimposed. This being the case, an effort was made to isolate the tilting motion by filtering out the translation. It was arbitrarily

assumed that the tilting occurred at frequencies lower than 0.3 cps and that frequencies above 0.3 cps were due to translation. Each of the digitized seismograms was transformed by Fourier series analysis. The resulting amplitude and phase spectra were divided by the instrument transfer function appropriate to each instrument operating as an accelerometer or tiltmeter. All frequencies above 0.3 cps were arbitrarily eliminated, the remaining harmonics resynthesized and the resulting corrected and filtered seismograms were plotted. They exhibit the tilt and/or acceleration as a function of time for all frequencies below 0.3 cps. It should be mentioned that there is no way to distinguish between tilt and acceleration from the seismogram, except that the integrated acceleration must be zero (i.e., the areas above and below the baseline must be equal), but the integrated tilt need not. By this criterion, the corrected and filtered seismograms may be interpreted to exhibit a long period (10 to 20 seconds) tilting motion with superimposed accelerations

having a predominant period of 4 seconds $\pm$0.5 second. Even the Columbia radial record showed a small amount of tilt which had been masked by the high frequencies. This radial tilt was in phase with the transverse tilt. The corrected and filtered grams are very similar to the original seismograms in the long period motions.

The maximum tilt angles were scaled from the synthesized tilt-accelerograms and the direction and magnitude of the resultant tilt were calculated. At the Hattiesburg station the maximum was 14.0 arc sec tilt in the direction N86°W. At the Columbia station it was 3.5 arc sec in the approximate direction S37°W. The directions given are those in which the tilted surface had a downward slope.

The next question to be resolved was whether the tilt was associated with a wave which originated at the source, or was a purely local phenomenon. The direction of the tilting suggests the latter, while the fact that the ground surface returned to a level position on both components at both stations would

make local slumping seem an unlikely explanation. If the tilt was due to passage of a wave traveling from the source, it should have been observable at the Gulf Oil Refinery station located roughly halfway between the source and Hattiesburg. Here a three component seismograph of the Carder Vibration Meter type was used. The radial components had a tilt sensitivity of 0.042 cm/arc sec and the transverse had 0.046 cm/arc sec. The vertical component was not sensitive to tilt. All three components of the Gulf Oil Refinery seismogram were corrected and filtered as described above. The resynthesized grams were plotted to a scale such that as little as 3 arc sec of tilt would have been seen easily. No evidence of tilt was observed. The grams showed equal areas above and below the baseline as pure accelerograms should. Moreover, the accelerations of the tilt-insensitive vertical component were the same order of magnitudes and frequencies as those of the horizontal components. Thus, it is reasonable to conclude that the long period tilts

observed at Hattiesburg and Columbia were not produced by a wave radiating along the surface from the source.

LONG PERIOD ACCELERATIONS

The primary objective of the digital filtering described above was to isolate the rotational motion (tilt) as much as possible. However, on the filtered tilt-accelerograms it is possible to see and measure the translational accelerations for periods longer than 3.3 sec.

The largest accelerations below 0.3 cps observed at the refinery occurred at a time of T+26 seconds when the acceleration reached a peak value of 2.7×10^{-5} g. This was the peak motion of a wave train which began at T+20 seconds and persisted to T+40 seconds at a period of about 3.8 seconds. The particle motion was retrograde and nearly circular in the vertical-radial plane throughout this time interval. The corresponding peak particle displacement due to this wave was calculated to be 10^{-2} cm.

On the Hattiesburg radial tilt-accelerogram, the peak acceleration below 0.3 cps occurred at T+55 seconds in a similar wave train of the same period. Here the peak acceleration was 1.12×10^{-5} g, and the corresponding displacement was 3.9×10^{-3} cm. The wave train was observed to persist from T+48 seconds to T+72 seconds.

On the Columbia record, a similar wave train began at about T+40 seconds and persisted to T+58 seconds. The peak acceleration in this wave train was 4.6×10^{-6} g, and the displacement was 1.48×10^{-3} cm. Any wave propagation velocity from source to station between 460 meters/sec and 610 meters/sec would account for energy in this wave train at all three stations. On the Columbia radial component the largest peak acceleration occurred at T+31 seconds in a wave of 3.9 second period. The peak value was 1.03×10^{-5} g, and the displacement was 3.9×10^{-3} cm.

It is important to note that for the frequency range below 0.3 cps, waves may be present with larger displacements and longer periods than those reported

above. Such waves could not, however, have given rise to accelerations larger than those observed and reported.

SUMMARY AND CONCLUSION

Table 1 lists the maximum values of tilt and acceleration observed for frequencies below 0.2 cps on each component of the stations at Hattiesburg, Columbia, and Gulf Oil Refinery. These values are far below levels which would reasonably account for structural damage. The existence of tilting motion at Columbia and Hattiesburg and its absence at Gulf Oil Refinery have been established fairly conclusively, but a satisfactory explanation of the causal mechanism has not been suggested.

TABLE 1 MAXIMUM PEAK TILT AND ACCELERATION AT PERIODS LONGER THAN 3.3 SECONDS

		Tilt arc sec	Acceleration (parts of gravity)	Period (sec)
Hattiesburg	Radial	10.8	1.12×10^{-5}	3.8
	Transverse	8.9	1.44×10^{-5}	3.9
Columbia	Radial	0.6	1.03×10^{-5}	3.9
	Transverse	3.5	6.1×10^{-6}	4.2
Gulf Oil Refinery	Vertical	--	2.37×10^{-5}	3.8
	Radial	--	2.7×10^{-5}	3.8
	Transverse	--	1.32×10^{-5}	3.8

ATTACHMENT B-1

The purpose of this Attachment is to show that a simple velocity damped pendulum seismograph, when its frame is subjected to a transient translation, will write a seismogram which encloses equal areas above and below the rest position of the trace.

The motion of the recorded trace may be expressed by the familiar equation[1]:

$$y'' + ay' + by = cx'' \qquad (1)$$

where:

y	is the displacement of the recorded trace from its baseline as a function of time
x	is the displacement of the frame from its initial rest position as a continuous function of time
$'$ and $''$	are first and second time derivatives
a, b, and c	are instrumental constants

---

[1] See for example, Richter, C. F., Elementary Seismology, Freeman and Company, 1958, p. 215, Equation (10).

Since x is a transient function of time, it may be assumed that the earth particle velocity, x', is different from zero only during a finite time interval between $t_1 > 0$ and $t_2 < \infty$, and thus, it is zero at t=0 and at $t = \infty$.

This condition may be expressed

$$x'_\infty = x'_0 = 0 \qquad (2)$$

It is evident that the seismograph trace deflection and its first derivative are zero at t=0 and $t = \infty$,

$$y_0 = y'_0 = y_\infty = y'_\infty = 0 \qquad (3)$$

Integrating equation (1) with respect to time between the limits t=0 and $t = \infty$ gives

$$[y' + ay]_0^\infty + b \int_0^\infty y\,dt = c[x']_0^\infty \qquad (4)$$

but

$$[y' + ay]_0^\infty = 0 \quad \text{from equation (3)}$$

and

$$[x']_0^\infty = 0 \quad \text{from equation (2)}$$

therefore, equation (4) becomes

$$\int_0^\infty y\,dt = 0 \qquad (5)$$

Equation (5) expresses the fact that the total area under the curve $y=f(t)$ is zero as asserted. Except for equation (2) and continuity of x, no restriction has been placed on the form of x. Since x_0 need not equal x_∞, x may involve permanent displacement without invalidating the proof.

ATTACHMENT B-2

At the October 1965 meeting of the Eastern Section of the Seismological Society of America, S. Sacks of the Carnegie Institution of Washington presented a paper, "Distortion in Electrodynamic Seismometers." He cautioned against interpreting as tilt, unusual long period motions (unequal areas above and below the baseline) observed at short epicentral distances. As a case in point, he referred specifically to the paper, "Near Earthquakes Recorded with Long Period Seismographs"; H. Berckhemer and G. Schneider; BSSA, Vol 54, No. 3; June 1964.

The distortion which causes the apparent tilt is described as a "high Q violin string type vibration of restoring springs in vertical seismometers." Some characteristics of the phenomenon are as follows:

1. The period of the function initiating the distortion is short, compared to the natural period of the seismometer.
2. The seismometer, in effect, sees a burst of short period energy as a sort of impulse function.

3. The record shows a long period, drift-like response to the short period energy.
4. The amplitude of the low frequency distortion is very roughly equal to the amplitude of the forcing function.
5. The susceptibility of the instrument to this type of distortion may be reduced by oil damping of the spring's bowstring vibrations.

It appears that this type of distortion could have caused the extremely low-frequency motions on the Hattiesburg and Columbia vibration meter records for the SALMON Event. The instrument periods were much longer than the vibration periods (the questionable low frequencies excluded). The amplitudes of the distortion (?) corresponded roughly to the amplitudes of the signal, and there was an apparent relationship between the arrival of various short period waves and the behavior of the distortion (?).

Several vibration meter records of other underground explosions were examined to see if they contained any unusual low frequencies in the presence of normal

high frequency seismic motions. The records chosen were those most likely to contain high frequency energy, i.e., those with shot and/or station on rock, and short source to detector distance. No records from NTS events were found with any appreciable amplitudes at periods shorter than 0.5 sec. Vibration meters were not installed for the GNOME or HARDHAT Events, both of which had proportionately more high frequency energy than did NTS events in alluvium. Three vibration meter stations recorded the SHOAL Event in granite. One of the records showed almost no motion at periods shorter than 0.5 sec, and one had very small trace amplitudes. However, the seismogram from the Naval Air Station showed a 5 sec period wave early in the record. In this part of the record, there were some measurable amplitudes with periods shorter than 0.3 sec. The low-frequency motion is not nearly as striking as that recorded at Hattiesburg and Columbia for SALMON.

It is possible, of course, that the vibration meters for SALMON were not properly installed. The damping fluid could have been of too low viscosity or perhaps omitted entirely from one or both damping cups. It would be of interest to perform a simple experiment to try to produce a low frequency distortion in a vibration meter. Ideally, the recording station would be on rock and as close as possible to a shot in rock. The magnification of the vibration meters could be decreased somewhat by shortening the mirror focal lengths. One seismometer could be operated with proper damping of the bowstring vibration, the other with the bowstring vibration underdamped or undamped. Both instruments would record the same directional component of motion.

TECHNICAL AND SAFETY PROGRAM REPORTS SCHEDULED FOR ISSUANCE BY AGENCIES PARTICIPATING IN PROJECT DRIBBLE

SAFETY REPORTS

Agency	Report No.	Subject or Title
USWB	VUF-1020	Weather and Surface Radiation Prediction Activities
USPHS	VUF-1021	Final Report of Off-site Surveillance
USBM	VUF-1022	Pre and Post-Shot Safety Inspection of Oil and Gas Facilities Near Project Dribble
USGS	VUF-1023	Analysis of Geohydrology of Tatum Salt Dome
USGS	VUF-1024	Analysis of Aquifer Response
REECo	VUF-1025	On-Site Health and Safety Report
RFB, Inc.	VUF-1026	Analysis of Dribble Data on Ground Motion and Containment - Safety Program
H-NSC	VUF-1027	Ground-Water Safety
FAA	VUF-1028	Federal Aviation Agency Airspace Advisory
H&N	VUF-1029	Summary of Pre and Post-Shot Structural Survey Reports
JAB	VUF-1030	Structural Response of Residential-Type Test Structures in Close Proximity to an Underground Nuclear Detonation
JAB	VUF-1031	Structural Response of Tall Industrial and Residential Structures to an Underground Nuclear Detonation.

NOTE: The Seismic Safety data will be included in the USC&GS Technical Report VUF-3014

TECHNICAL REPORTS

Agency	Report No.	Subject or Title
SL	VUF-3012	Free-Field Particle Motions from a Nuclear Explosion in Salt - Part I
SRI	VUF-3013	Free-Field Particle Motions from a Nuclear Explosion in Salt - Part II
USC&GS	VUF-3014	Earth Vibration from a Nuclear Explosion in a Salt Dome
UED	VUF-3015	Compressional Velocity and Distance Measurements in a Salt Dome

LRL	VUF-3016	Vent-Gas Treatment Plant
LRL	PNE-3002 *	Response of Test Structures to Ground Motion from an Underground Nuclear Explosion
SRI	VUF-3017	Feasibility of Cavity Pressure and Temperature Measurements for a Decoupled Nuclear Explosion
LRL	VUF-3018	Background Engineering Data and Summary of Instrumentation for a Nuclear Test in Salt
WES	VUF-3019	Laboratory Design and Analyses and Field Control of Grouting Mixtures Employed at a Nuclear Test in Salt
LRL	VUF-3020	Geology and Physical and Chemical Properties of the Site for a Nuclear Explosion in Salt
EG&G	VUF-3021	Timing and Firing

* This report number was assigned by SAN

In addition to the reports listed above as scheduled for issuance by the Project DRIBBLE test organization, a number of papers covering interpretation of the SALMON data are to be submitted to the American Geophysical Union for publication. As of February 1, 1965, the list of these papers consists of the following:

Title	Author(s)	Agency(s)
Shock Wave Calculations of Salmon	L. A. Rogers	LRL
Nuclear Decoupling, Full and Partial	D. W. Patterson	LRL
Calculation of P-Wave Amplitudes for Salmon	D. L. Springer and W. D. Hurdlow	LRL
Travel Times and Amplitudes of Salmon Explosion	J. N. Jordan W. V. Mickey W. Helterbran	USC&GS AFTAC UED
Detection, Analysis and Interpretation of Teleseismic Signals from the Salmon Event	A. Archambeau and E. A. Flinn	SDC
Epicenter Locations of Salmon Event	E. Herrin and J. Taggart	SMU USC&GS
The Post-Explosion Environment Resulting from the Salmon Event	D. E. Rawson and S. M. Hansen	LRL
Measurements of the Crustal Structure in Mississippi	D. H. Warren J. H. Healy W. H. Jackson	USGS

All but the last paper in the above list will be read at the annual meeting of the American Geophysical Union in April 1965.

LIST OF ABBREVIATIONS FOR TECHNICAL AGENCIES

BR LTD	Barringer Research Limited Rexdale, Ontario, Canada
ERDL	Engineering Research Development Laboratory Fort Belvoir, Virginia
FAA	Federal Aviation Agency Los Angeles, California
GIMRADA	U. S. Army Geodesy, Intelligence and Mapping Research and Development Agency Fort Belvior, Virginia
H-NSC	Hazleton-Nuclear Science Corporation Palo Alto, California
H&N, INC	Holmes & Narver, Inc. Los Angeles, California Las Vegas, Nevada
II	Isotopes, Inc. Westwood, New Jersey
ITEK	Itek Corporation Palo Alto, California
JAB	John A. Blume & Associates Research Division San Francisco, California
LRL	Lawrence Radiation Laboratory Livermore, California
NRDL	U. S. Naval Radiological Defense Laboratory San Francisco, California
REECo	Reynolds Electrical & Engineering Co., Inc. Las Vegas, Nevada
RFB, INC.	R. F. Beers, Inc. Alexandria, Virginia
SDC	Seismic Data Center Alexandria, Virginia
EG&G	Edgerton, Germeshausen & Grier, Inc. Las Vegas, Nevada
SL	Sandia Laboratory Albuquerque, New Mexico
SMU	Southern Methodist University Dallas, Texas
SRI	Stanford Research Institute Menlo Park, California
TI	Texas Instruments, Inc. Dallas, Texas
UA	United Aircraft El Segundo, California
UED	United Electro Dynamics, Inc. Pasadena, California
USBM	U. S. Bureau of Mines Washington, 25, D. C.
USC&GS	U. S. Coast and Geodetic Survey Las Vegas, Nevada
USGS	U. S. Geologic Survey Denver, Colorado
USPHS	U. S. Public Health Service Las Vegas, Nevada
USWB	U. S. Weather Bureau Las Vegas, Nevada